PolyPublie
Polytechnique Montréal

POLYTECHNIQUE MONTRÉAL
UNIVERSITÉ D'INGÉNIERIE

Titre: Title:	Étude métabolique des cellules myéloïdes suppressives dans le contexte du phénomène d'immunosuppression
Auteur: Author:	Iness Hammami
Date:	2011
Type:	Mémoire ou thèse / Dissertation or Thesis
Référence: Citation:	Hammami, I. (2011). Étude métabolique des cellules myéloïdes suppressives dans le contexte du phénomène d'immunosuppression [Ph.D. thesis, École Polytechnique de Montréal]. PolyPublie. https://publications.polymtl.ca/584/

Document en libre accès dans PolyPublie
Open Access document in PolyPublie

URL de PolyPublie: PolyPublie URL:	https://publications.polymtl.ca/584/
Directeurs de recherche: Advisors:	Mario Jolicoeur, & Gregory De Crescenzo
Programme: Program:	Génie chimique

Ce fichier a été téléchargé à partir de PolyPublie, le dépôt institutionnel de Polytechnique Montréal
This file has been downloaded from PolyPublie, the institutional repository of Polytechnique Montréal

https://publications.polymtl.ca

UNIVERSITÉ DE MONTRÉAL

ÉTUDE MÉTABOLIQUE DES CELLULES MYÉLOÏDES SUPPRESSIVES DANS LE CONTEXTE DU PHÉNOMÈNE D'IMMUNOSUPPRESSION

INESS HAMMAMI

DÉPARTEMENT DE GÉNIE CHIMIQUE

ÉCOLE POLYTECHNIQUE DE MONTRÉAL

THÈSE PRÉSENTÉE EN VUE DE L'OBTENTION

DU DIPLÔME DE PHILOSOPHIAE DOCTOR (Ph.D)

(GÉNIE CHIMIQUE),

JUIN 2011

© Iness Hammami, 2011.

UNIVERSITÉ DE MONTRÉAL

ÉCOLE POLYTECHNIQUE DE MONTRÉAL

Cette thèse est intitulée :

ÉTUDE MÉTABOLIQUE DES CELLULES MYÉLOÏDES SUPPRESSIVES DANS LE CONTEXTE DU PHÉNOMÈNE D'IMMUNOSUPPRESSION

présentée par : HAMMAMI Iness

en vue de l'obtention du diplôme de : Philosophiae Doctor

a été dûment acceptée par le jury d'examen constitué de :

M. PERRIER Michel, Ph.D., président

M. JOLICOEUR Mario, Ph.D., membre et directeur de recherche

M. DE CRESCENZO Gregory, Ph.D., membre et codirecteur de recherche

M. HENRY Olivier, Ph.D., membre

Mme. KLAPA Maria, Ph.D., membre

DÉDICACE

À Leila, qui nous manque énormément…

REMERCIMENTS

Je souhaite tout d'abord remercier mon directeur de recherche, Pr. Mario Jolicoeur pour m'avoir accueillie dans son laboratoire, pour son encadrement et la liberté qu'il m'a accordée dans le cadre de ces travaux, mais par-dessus tout pour m'avoir formée à la recherche scientifique. Je lui suis également reconnaissante de l'opportunité qui m'a été donnée de participer à l'enseignement et à de multiples congrès internationaux.

Je voudrais également remercier mon co-directeur Gregory De Crescenzo pour son soutien, sa disponibilité, son aide et la latitude qu'il a pu me laisser dans la réalisation de ce projet.

Il en est également pour Dr Vincenzo Bronte qui m'a accueilli à deux reprises dans son laboratoire et qui m'a permis de côtoyer des chercheurs de formations différentes. Je, lui et son groupe de recherche, notamment Barbara, Wiaam et Ilaria, suis également reconnaissante pour m'avoir initié à l'immunologie et à la manipulation des animaux.

J'aimerai remercier particulièrement Jingkui Chen pour m'avoir soutenu pour la partie analytique de mes travaux. Bien d'autres m'ont été d'une aide précieuse tout au long de ces années : Monica pour le SEM, Mohamed pour la qRT-PCR et Anne pour le microscope de fluorescence.

Merci également à tous les collègues, étudiants, stagiaires, particulièrement Marie, associés de recherche, techniciens et secrétaires du département de génie chimique

et amis que j'ai côtoyé durant ma thèse. Vous êtres trop nombreux pour tous vous mentionner mais votre présence m'était importante, alors Merci!

Merci à ma famille, à papa qui m'a toujours encouragé d'aller au bout de mon rêve et à mère, que je sentais tout près de moi dans des moments difficiles pour m'aider à persévérer malgré son absence depuis des années.

Merci à mes amis tant en Tunisie qu'au Canada pour m'avoir écouté me plaindre des heures et des heures. Et enfin, Merci à Walid pour ses encouragements et pour avoir été là quand j'en avais besoin.

RÉSUMÉ

Le caractère invasif et les effets secondaires associés aux approches thérapeutiques anticancéreuses conventionnelles ont donné naissance à une nouvelle stratégie, appelée l'immunothérapie, qui consiste à rétablir la capacité du système immunitaire à reconnaître la tumeur et inhiber sa croissance. Toutefois, ce processus d'immunosurveillance devient rapidement dysfonctionnel dû à la maturation d'une population de cellules myéloïdes suppressives, les MDSC, et à son recrutement dans la rate, les organes lymphoïdes, le sang et la tumeur des personnes présentant un cancer. Ces cellules ont la particularité d'exprimer deux enzymes qui métabolisent l'acide aminé L-arginine (L-arg), soit la synthétase inductible d'oxyde nitrique (iNOS) et l'arginase 1 (ARG1). La faible concentration du L-arg dans le sang et l'accumulation des dérivés de l'oxyde nitrique (NO) inhibent les fonctions immunomodulatoires des cellules effectrices du système immunitaire ainsi que leur prolifération, et induisent leur mort. Jusqu'à présent, la majorité des approches thérapeutiques anti-MDSC cible des marqueurs de surface, des enzymes ou des voies signalisation spécifiques impliquées dans la maturation des MDSC ou au niveau du métabolisme du L-arg.

Les travaux présentés dans le cadre de cette thèse sont basés sur l'hypothèse que le phénomène d'immunosuppression est énergivore. En fait, la maturation des MDSC à partir de précurseurs myéloïdes implique plusieurs voies et facteurs de signalisation dont l'activation est directement ou indirectement dépendante de l'énergie. Nous avons également supposé que la compréhension des événements métaboliques ayant lieu durant la maturation des MDSC, le métabolisme du L-arg et l'interaction entre le NO et les

cellules effectrices du système immunitaire, peut mener à l'identification de nouvelles cibles de l'immunothérapie.

Dans un premier temps, la maturation des MDSC a été simulée en exposant des cellules de la moelle osseuse aux GM-CSF et IL-6. Cette combinaison de cytokines génère une population de MDSC similaire à celle qui infiltre la tumeur. Les résultats de ces travaux ont fait l'objet d'un premier article soumis à "Cancer Research". Il y est montré que la maturation des MDSC et l'activation subséquente des enzymes iNOS et ARG1 sont accompagnées par la stimulation du métabolisme central du carbone. Particulièrement, le glucose a été majoritairement métabolisé via la glycolyse avec une moindre quantité acheminée vers la voie des pentoses phosphates. Cependant, les MDSC diminuent leur respiration durant la maturation pour favoriser le mode anaérobique qui résulte en la production de lactate. Le faible rendement énergétique du métabolisme glycolytique est compensé par la stimulation de la glutaminolyse qui, à son tour, active la production de l'énergie par le cycle de l'urée. La L-glutamine (L-gln) s'est avérée également une source importante de pyruvate. En fait, l'enzyme malique convertit le malate en pyruvate tout en produisant la NADPH. De même, la régulation à la hausse du cycle de l'urée assure la synthèse endogène du L-arg.

Ensuite, afin de déterminer les besoins nutritionnels et énergétiques associés au métabolisme du L-arg, une lignée immortalisée de MDSC murines, MSC-1, a été utilisée. La ligne de base de l'énergétique des cellules MCS-1 a été tout d'abord établie pour servir de référence pour des études ultérieures. Deux états stationnaires correspondant aux phases exponentielle et stationnaire sont identifiés. Les cellules MSC-1 étaient actives durant la phase exponentielle, alors qu'une détérioration globale du métabolisme

est notée dans la phase stationnaire. Les résultats de ces travaux ont été publiés dans "Journal of Biotechnology" en 2011.

Dans un troisième papier soumis à "Cancer Immunology and Immunotherapy" en 2011, nous avons montré que l'activité de iNOS et la machinerie immunosuppressive qui y est associée requièrent la stimulation du métabolisme central du carbone, contrairement à l'ARG1 dont l'activité est indépendante de l'état métabolique des cellules. De plus, la glutaminolyse joue un rôle important dans le phénomène d'immunosuppression, particulièrement dans celui relié à l'enzyme iNOS, en assurant une forte activité du cycle de l'urée et subséquemment la production d'énergie et le recyclage du L-arg. Cependant, le glucose ne compense pas la régulation à la baisse de ces processus en absence de la L-gln. Ainsi, le contrôle des flux à travers la glutaminolyse, en inhibant le transporteur de la L-gln ou l'activité enzymatique de la glutaminase, pourrait constituer une cible de valeur pour le traitement des pathologies induites par le NO.

Enfin, pour caractériser l'effet des MDSC sur l'énergétique des cellules effectrices du système immunitaire, nous avons cultivé les cellules Jurkat, considérées comme modèle de cellules immunitaires stimulées (les cellules T), en présence d'un nouveau donneur de NO (AT38) conçu pour l'inhibition de la progression de la tumeur et l'accumulation des MDSC. Ces travaux, soumis à "Immunology and Cell Biology" en 2011, ont montré que ce donneur : i) inhibe irréversiblement la respiration cellulaire, ii) inhibe la prolifération des cellules, comme l'indiquait la diminution de la concentration en pyrimidines, iii) induit la mort des cellules Jurkat par apoptose jusqu'à une concentration "seuil" en glucose au-delà de laquelle les cellules mourraient par nécrose. Nous avons également démontré que le nitrite exerce les mêmes effets sur les cellules

Jurkat alors que le nitrate a un potentiel immunsouppressif dépendant de la concentration et du temps. Pour atténuer les effets nocifs des donneurs de NO sur le système immunitaire, une stratégie consistant à bloquer l'ouverture du pore de transition de perméabilité mitochondrial par la cyclosporine A est proposée. Cette approche permet de diminuer la capacité du NO à inhiber la prolifération des cellules Jurkat et à induire leur mort.

Nous avons donc réussi, lors de ces travaux, à caractériser le comportement nutritionnel des MDSC et particulièrement de mettre en évidence les événements métaboliques ayant lieu durant leur maturation. En conclusion, la régulation croisée entre le métabolisme du L-arg et le métabolisme central du carbone observée tant chez les MDSC que chez les cellules Jurkat a permis de suggérer le contrôle de l'état énergétique des cellules comme cible prometteuse pour l'immunothérapie.

ABSTRACT

The invasiveness and side effects of conventional anticancer therapeutic approaches gave rise to a new strategy, called immunotherapy, which consists on the recovery of the immune system ability to recognize tumours and inhibit their outgrowth. However, this immunosurveillance process rapidly becomes dysfunctional due to the maturation of a myeloid-derived suppressor cell (MDSC) population from bone marrow precursors and its recruitment in spleen, lymphoid organs, blood and tumour of cancer-bearing hosts. MDSCs have the particularity of expressing two enzymes that metabolize the amino acid L-arginine (L-arg): inducible nitric oxide synthase (iNOS) and arginase 1 (ARG1). The sparse availability of L-arg and the accumulation of nitric oxide (NO) derivatives then inhibit immunomodulatory functions of immune effector cells as well as their proliferation, and induce their death. Up to now, the majority of anti-MDSC therapeutic approaches are targeting surface markers, enzymes or specific signalling pathways implicated in MDSC maturation or L-arg metabolism.

The study presented herein is based on the hypothesis that the immunosuppression phenomenon is an energetically-costly process. In fact, the maturation of bone marrow precursors into MDSCs implies several signalling pathways and factors whose activation is directly or indirectly energy-dependent. We also propose that the comprehension of the metabolic events occurring during MDSC maturation, L-arg metabolism and interactions between NO and immune effector cells may lead to the identification of new targets for immunotherapy.

First, MDSC maturation was simulated by exposing bone marrow cells to GM-CSF and IL-6. This cytokine combination leads to the generation of a cell population similar to tumour-infiltrating MDSCs. Results of this work were the subject of a first article submitted to "Cancer Research". It was shown that MDSC maturation and the consequent activation of iNOS and ARG1 were accompanied by the enhancement of central carbon metabolism. Particularly, glucose was mostly metabolized through glycolysis with sparse quantity processed through the pentose phosphate pathway. However, MDSCs showed to down-regulate their respiration during the maturation process favouring an anaerobic metabolism that results in lactate production. The low energetic yield of glycolytic metabolism was compensated by the energy derived from the urea cycle whose activity was enhanced by the stimulation of glutaminolysis. Up-regulation of urea cycle activity ensures the endogenous synthesis of L-arg and so, the maintenance of MDSC immunosuppressive activity. Moreover, it turned out that L-glutamine (L-gln) is an important source of pyruvate. In fact, the malic enzyme converts malate into pyruvate and jointly ensures NADPH supply.

Thereafter, in order to identify the specific nutritional and energetic requirements that are related to L-arg metabolism, we used an immortalized cell line (MSC-1) derived from mouse MDSCs. The baseline of MSC-1 cell bioenergetic was first established to serve as a reference in subsequent study focussing on iNOS and/or ARG1 inhibition. Two steady-states corresponding to the exponential and stationary phases were identified. MSC-1 cells were active during the exponential phase, whereas a deterioration of global metabolic activity was noticed in the entry of the stationary phase. Results of this work were published in "Journal of Biotechnology" in 2011.

In a third paper submitted to "Cancer Immunology and Immunotherapy" in 2011, we have shown that iNOS-related immunosuppressive machinery requires the stimulation of central carbon metabolism whereas ARG1 activity showed to be independent of cell metabolic state. Moreover, glutaminolysis revealed playing an important role in the immunosuppression phenomenon particularly that related to iNOS, by ensuring an enhanced urea cycle activity which consequently produces energy and activates L-arg recycling pathway. However, glucose uptake did not compensate for the down-regulation of these processes in the absence of L-gln. Therefore, controlling fluxes through glutaminolysis, by inhibiting L-gln transporter or the enzymatic activity of glutaminase, may be a promising alternative to treat NO-induced pathologies.

Finally, to characterize MDSC effects on the energetic states of immune effector cells, we cultured Jurkat cells, considered as a model system of immune challenged cells (T cells), in the presence of a new NO donor (AT38) developed to inhibit tumour progression and MDSC accumulation. This work, submitted to "Immunology and Cell Biology" in 2011, showed that this donor: i) irreversibly inhibits cell respiration, ii) inhibits cell proliferation, as revealed by the decrease of pyrimidines' concentrations, iii) induces apoptosis until a glucose threshold concentration, above which cell death process was switched into necrosis. We also demonstrated that nitrite triggers similar effects on Jurkat cells, whereas nitrate has a time and concentration –dependent immunosuppressive potential. To attenuate harmful effects of NO on immune system, a strategy consisting on blocking the opening of the mitochondrial permeability transition pore by cyclosporine A was proposed. This approach has diminished NO ability to inhibit Jurkat cell proliferation and induce cell death.

We have thus characterized MDSC nutritional behaviour and particularly highlighted the metabolic events occurring during their maturation. In conclusion, cross-regulation between L-arg metabolism and the central carbon metabolism observed either in MDSCs or Jurkat cells is suggesting the control of cell energetic status as a promising target for immunotherapy.

TABLE DES MATIÈRES

LISTE DES TABLEAUX

LISTE DES FIGURES

LISTE DES ABBRÉVIATIONS

1400W : *N*-[3-(Aminomethyl)-benzyl]-acetamidine

α-KG: α-KetoGlutarate

ACoA : Acetyl COenzyme A

ADP : Adenosine DiPhosphate

AEC : Adenylate Energy Charge

AMP : Adenosine MonoPhosphate

AMPK: AMP Protein Kinase

APC : Antigen-Presenting Cell

ARG1: ARGinase 1

ASL : ArgininoSuccinate Lyase

ASS : ArgininoSuccinate Synthetase

ATP : Adenosine TriPhosphate

ATRA : All-*Trans*-Retinoic Acid

BEC : [(S)-(2-BoronoEthyl)-L-Cysteine]

BM : Bone Marrow

C/EBPβ : CCAAT/Enhancer Binding Protein β

CAT: Cationic Amino acid Transporter

CcOX : Cytochrome *c* OXidase

CHO : Chinese Hamster Ovary

ConA : CONcanavalin A

COX: Cyclo-OXygenase

CsA : CycloSporine A

CTL : Cytotoxic T-Lymphocyte

CTP : Cytidine TriPhosphate

DMHA : N,N-DiMethylHexylAnine

DMSO : DiMethylSulfOxide

DNA: DeoxyriboNucleic acid

DO : Dissolved Oxygen

EDTA : EthyleneDiamineTetraAcetic acid

EIF : Eykaryotic Initiation Factor

ERK : Extracellular signal-Regulated Kinase

G-CSF : Granulocyte-Colony Stimulating Factor

GCN 2 : General Control Non-depressible 2

GLUT: GLUcose Transporter

GM-CSF : Granulocyte Macrophage - Colony Stimulating Factor

GMP : Guanosine MonoPhosphate

GTP : Guanosine TriPhosphate

Hb: HemogloBin

HIF-1α : Hypoxia Induction Factor-1α

HNC : Head and Neck Cancer

HPLC : High Performance Liqui Chromatography

IL : InterLeukin

INF : INterFeron

iNOS : Inducible Nitric Oxide Synthase

JAK : JAnus Kinase

L-arg : L-ARGinine

L-gln : L-GlutamiNe

L-phe : L-phenylalanine

L-trp : L-tryptophane

LPS : LipoPolySaccharide

M-CSF : Macrophage-Colony Stimulating Factor

MAPK : Mitogen-Activated Protein Kinase

MDSCs : Myeloid-Derived Suppressor Cells

MHC : Major Histocompatibility Complex

MPTP : Mitochondrial Permeability Transition Pore

mRNA : Messenger RiboNucleic Acid

MS : Mass Spectroscopy

MSC-1 : Myeloid Suppressor Cells 1

MTOR : Mammalian Target Of Rapamycin

NADPH : Nicotinamide Adenine Dinucleotide PHosphate

NF-κB : Nuclear Factor-κB

NK : Natural Killer

NO : Nitric Oxide

NSAID : Non Steroidal Anti-Inflammatory Drug

NTP : Nucleoside TriPhosphate

OUR : Oxygen Uptake Rate

P-NMR : Phosphorus-Nuclear Magnteic Resonance

PFK : PhosphoFructoKinase

PBS : Phosphate Buffer Saline

PDE : PhosphoDiEsterase

PEP : PhosphoEnolPyruvate

PET : PolyEthyleneTerephthalate

PI3-K : PhosphoInositide 3-Kinase

PME : PhosphoMonoEster

PPP : Pentose Phosphate Pathway

RNOS : Reactive Nitric Oxide Species

SA : Salicylic Acid

STAT3 : Signal Transducer and Activator of Transcription

TAA : Tumor-Associated Antigen

TCA : TriCarboxylic Acid

TCR : T-Cell Receptor

TDSF: Tumor-Derived Soluble Factor

TGF : Transforming Growth Factor

TNF: Tumor Necrosis Factor

T_{reg}: T REGulatory

UDPG : Uridine DiPhosphoGlucose

UDPGal : Uridine DiPhosphoGalactose

UDPGalNAc : Uridine DiPhosphoGalactose-N-ACetyl

UDPGNAc : Uridine DiPhosphoGlucose-N-ACetyl

UPLC : Ultra Performance Liquid Chromatography

UTP : Uridine TriPhosphate

VEGF : Vascular Endothelial Growth Factor

INTRODUCTION

Selon le rapport “Statistiques canadiennes sur le cancer 2010”, publié par la “Société canadienne du cancer” (www.cancer.ca), on estime que 173 800 nouveaux cas de cancer et 76 200 décès causés par le cancer surviendront au Canada en 2010. Ceci représente des hausses respectives de 1.6% et 1.2% comparativement à 2009. La croissance démographique et le vieillissement de la population sont les principaux facteurs qui expliquent cette tendance à la hausse.

En 1998, le fardeau économique attribué au cancer sur la société canadienne se chiffrait à 14.2 milliards de dollars (selon Santé Canada, 2002), ce qui représente 9% des coûts totaux reliés au traitement de l'ensemble des maladies au Canada. Le cancer occupe la troisième place après les maladies cardiovasculaires (12%) et les maladies musculo-squelettiques (10%). La majorité de ces coûts (74%) sont des coûts directs reliés aux soins hospitaliers. Bien que de fortes baisses du taux de mortalité aient été observées ces 30 dernières années, les statistiques alarmantes sur le cancer ainsi que les coûts exorbitants qui y sont associés ont poussé les chercheurs à intensifier leurs efforts afin d'assurer une meilleure compréhension de la pathologie, en premier lieu, et d'identifier de nouvelles cibles et stratégies thérapeutiques.

Les traitements actuels et conventionnels pour la lutte contre le cancer sont la chirurgie, la chimiothérapie et la radiothérapie. Contrairement à la chirurgie qui consiste à extraire la tumeur pour alléger la tension sur l’organe et ainsi aider à prolonger la durée de vie du patient, la radiothérapie expose la tumeur à des doses spécifiques de radiations permettant l’altération du matériel génétique des cellules cancéreuses et le freinage de leurs capacités de croissance incontrôlée. Cette stratégie est utilisée dans les cas où la chirurgie est impossible due à

l'emplacement de la tumeur ou comme complément à la chirurgie afin de détruire les cellules tumorales résiduelles et soulager les symptômes associés à la maladie. Une méthode combinatoire, appelée radiochirurgie stéréostatique est également utilisée pour traiter spécifiquement des tumeurs de petites tailles (inférieures à 3,8 cm) et éviter l'exposition de cellules saines aux fortes doses de radiation.

Bien qu'elle soit connue pour ses multiples effets secondaires nocifs pour la qualité de vie du patient, la chimiothérapie est la stratégie thérapeutique anticancéreuse la plus utilisée. Elle est souvent prescrite comme adjuvant après la chirurgie ou la radiothérapie ou comme soin palliatif lorsque le cancer est à un stade de dissémination métastatique. Dans le cas des cancers de la prostate et du sein, l'hormonothérapie est utilisée pour diminuer le risque de réapparition locale ou distante des cellules tumorales.

D'autres stratégies thérapeutiques anticancéreuses moins invasives sont en cours de développement. Particulièrement, la thérapie génique gagne du terrain auprès des chercheurs. Cette stratégie utilise des systèmes de livraison de gènes non cytotoxiques capables de s'infiltrer dans les tissus atteints. Les inserts d'ADN livrés modifient ainsi la signature génétique des cellules tumorales afin de contrecarrer les erreurs génétiques induites chez les cellules cancéreuses et réparer leur cycle cellulaire altéré.

L'immunothérapie représente également une approche d'intérêt pour complémenter les stratégies thérapeutiques standards due à sa spécificité et à sa cytotoxicité limitée. En fait, le système immunitaire adaptif joue un rôle significatif dans la reconnaissance de la tumeur et le contrôle de sa progression. Cependant, les tumeurs développent de multiples mécanismes, d'ordres moléculaire ou métabolique, pour échapper au processus d'immunosurveillance. Plusieurs stratégies qui visent à corriger et à renforcer le système de défense naturel anti-tumoral, d'une façon non-toxique et non-invasive, sont en cours de développement.

Cette thèse est organisée en huit chapitres. Après l'introduction, une revue de littérature détaille les mécanismes d'immunosuppression, notamment celui assuré par les cellules myéloïdes suppressives ("Myeloid-Derived Suppressor Cell", MDSC) ainsi que les stratégies d'immunothérapie anti-MDSC. Le chapitre 2 décrit les hypothèses et les objectifs du projet ainsi que l'organisation du document. Les chapitres 3 à 6 présentent les articles publiés ou soumis dans le cadre de cette thèse. Finalement, les chapitres 7 et 8 présentent une discussion générale, la conclusion et les recommandations reliées à ce travail.

CHAPITRE 1. REVUE DE LITTÉRATURE

1.1. Préambule

La transplantation d'organe et le cancer sont deux situations cliniques où le rôle du système immunitaire retient l'attention. Dans le premier cas, le système immunitaire peut rejeter le nouvel organe et résulter en l'échec de la transplantation, d'où l'importance de supprimer cette réponse immunitaire. Par contre, en cancérologie, les cliniciens cherchent à renforcer la capacité du système immunitaire adaptatif à reconnaître et à détruire les cellules tumorales.

La première étape du mécanisme d'immunosurveillance est la reconnaissance des antigènes tumoraux (TAAs pour "Tumor-Associated Antigens") présents à la surface des cellules tumorales par les cellules présentatrices d'antigène (APCs pour "Antigen Presenting Cells") telles que les macrophages, les cellules dendritiques et les cellules B (Figure 1-1) (Abbas & Lichtman, 2006). Suite à la phagocytose des cellules tumorales, les APCs acheminent les TAAs aux organes lymphoïdes où ils seront transformés en peptides. Ces derniers sont ensuite présentés à la surface des APCs professionnelles aux cellules T $CD8^+$ et $CD4^+$ via les complexes majeurs d'histocompatibilité I et II (MHCs pour "Major Hiscompatibility Complexes"), respectivement. Une fois activées, les cellules T migrent vers le microenvironnement tumoral où se différentient les cellules $CD8^+$ en lymphocytes T cytotoxiques (CTLs pour "Cytotoxic T-Lymphocyte") qui sont capables de détruire les cellules tumorales.

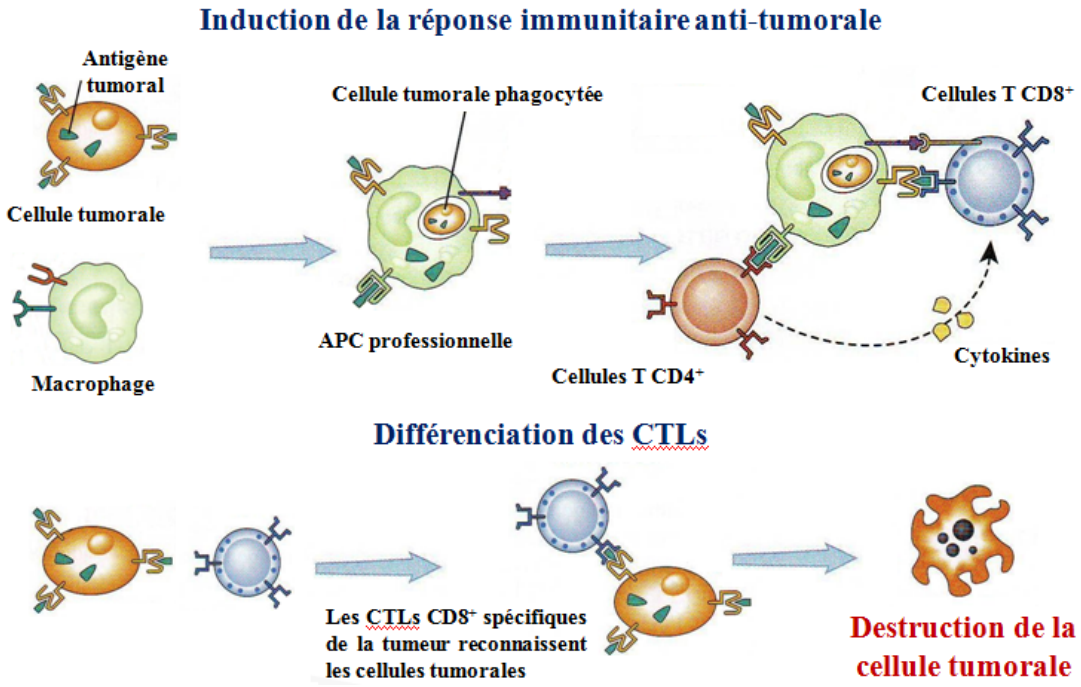

Figure 1-1 : Induction de la réponse immunitaires des cellules T CD8+ contre la tumeur (modifiée de Abbas et al., 2006).

1.2. Le phénomène d'immunosuppression

Le système immunitaire inné échoue souvent dans le contrôle de la progression de la tumeur, dû à des réponses immunitaires inefficaces ou aux multiples mécanismes que développent les tumeurs pour échapper au processus d'immunosurveillance.

La première stratégie de tolérance tumorale consiste à altérer la machinerie de traitement et de présentation des TAAs, soit en diminuant l'expression des MHCs de classe I ou en modifiant la séquence peptidique des TAAs, ce qui diminue leur compatibilité avec les récepteurs des CTLs (Restifo et al., 1993; Seliger et al., 1998). Les cellules tumorales peuvent également diminuer l'expression des co-stimulateurs requis pour l'activation des CTLs, tels que CD80,

CD86 and CD40 (Costello, Gastaut, & Olive, 1999). De plus, les cellules tumorales sécrètent des molécules immunosuppressives, telles que le facteur de croissance de la tumeur (TGF-β pour "Transforming Growth Factor-β"), les interleukines (ILs), les prostaglandines et le facteur de croissance de l'endothélium vasculaire (VEGF pour "Vascular Endothelial Growth Factor"), qui altèrent la fonction des APCs (Serafini, Borrello, & Bronte, 2006). Finalement, les tumeurs recrutent des cellules immunosuppressives, i.e. les cellules dendritiques tolérogéniques, les cellules T régulatrices (T_{reg} pour "T Regulatory") et les cellules myéloïdes suppressives (MDSC), dans la rate, les organes lymphoïdes, le sang et le microenvironnement tumoral pour contrôler la réponse immunitaire anti-tumorale. En fait, les cellules dendritiques sont considérées comme les meilleures APCs, et ce, dû à leurs fortes concentrations en MHCs et en co-stimulateurs ainsi qu'à leurs bonnes capacités de migration. Cependant, les cellules dendritiques tolérogéniques demeurent à l'état immature (i.e. faible expression de MHC et de co-stimulateurs et faible production de l'IL-12), ce qui facilite la tolérance immunitaire (D. Gabrilovich, 2004). Pour ce qui est des cellules T_{reg}, plusieurs mécanismes ont été proposés pour expliquer leurs rôles dans la suppression de la fonction anti-tumorale spécifique aux cellules T. Parmi d'autres, la sécrétion de cytokines inhibitrices, tels que TGF-β, IL-10, et IL-35, la sous-régulation de l'expression des co-stimulateurs et l'induction de la mort des APCs via la voie de perforine/granzyme sont les plus importants (Cao, 2010). Quant à elles, les MDSC peuvent induire le recrutement et l'expansion des cellules T_{reg} (P. Serafini, Mgebroff, Noonan, & Borrello, 2008) et réguler les fonctions immunomodulatoires des CTLs via le métabolisme du L-arginine (L-arg) (Kao et al., 2010).

1.3. Cellules myéloïdes suppressives

Les MDSC sont impliquées dans plusieurs situations pathologiques incluant les infections parasitiques et bactériennes, les inflammations chroniques et aigues, le stress traumatique et, en particulier, le cancer (Serafini, et al., 2006). L'accumulation des MDSC dans la tumeur, les organes lymphoïdes, la rate et le sang des patients atteints de cancer est souvent accompagnée par la dysfonction du processus d'immunosurveillance. Ceci a alors suscité l'intérêt des chercheurs à approfondir et à améliorer la compréhension du rôle des MDSC dans la progression de la tumeur (Paulo C. Rodriguez & Ochoa, 2006).

Les MDSC représentent une population hétérogène incluant des cellules dendritiques, des macrophages, des granulocytes et des cellules myéloïdes dans des phases précoces de différenciation (Serafini, et al., 2006). Chez la souris, les MDSC sont identifiées par l'expression des marqueurs de différenciation suivants : $CD11b^{+}$, $CD11c^{low}$, $CD31^{+}$, $Gr\text{-}1/Ly6\text{-}C^{+}$, $MHCII^{-/low}$, $ER\text{-}MP58^{+}$, $F4/80^{int}$ et $IL\text{-}4R\alpha^{+}$ (Dolcetti et al., 2008). Chez les souris saines, les cellules $CD11b^{+}/Gr\text{-}1^{+}$ sont présentes à des niveaux détectables dans la moelle osseuse mais à des proportions beaucoup plus faibles (< 4%) dans le sang et la rate (Serafini, et al., 2006). Les tests de cytotoxicité *in vitro* montrent que les MDSC extraites de souris saines ne sont pas immunosuppressives à moins de les utiliser dans des proportions très importantes par rapport aux cellules T dans la culture mixte.

L'absence d'un homologue du gène Gr-1 chez l'humain et la différence des marqueurs de différenciation selon le type de cancer entrave l'identification du phénotype des MDSC humaines (Peranzoni et al., 2010). Par exemple, chez les patients atteints du cancer de la tête et du cou (HNC pour "Head and Neck Cancer"), des cellules $CD34^{+}$ infiltrent la tumeur et suppriment les fonctions des CTLs. Par contre, une population de cellules $CD11b^{+}/CD14^{+}$ s'accumule dans le

sang des sujets présentant des mélanomes métastatiques et ces cellules inhibent la prolifération des cellules T (Marigo, Dolcetti, Serafini, Zanovello, & Bronte, 2008).

D'après le mécanisme de maturation et de recrutement des MDSC proposé par Bronte et ses collaborateurs (Serafini, et al., 2006), les tumeurs sécrètent une panoplie de facteurs solubles (TDSFs pour "Tumor-Derived Soluble Factors") qui recrutent les MDSC immatures de la moelle osseuse vers la rate et les organes lymphoïdes. Ces TDSFs stimulent ensuite la maturation des MDSC immunosuppressives et leur migration vers le microenvironnement tumoral. Dans la tumeur, les MDSC subissent une deuxième maturation les amenant à exprimer leurs phénotypes et fonctions immunosuppressives, et à supprimer la fonction immunitaire anti-tumorale via le métabolisme du L-arg (Figure 1-2).

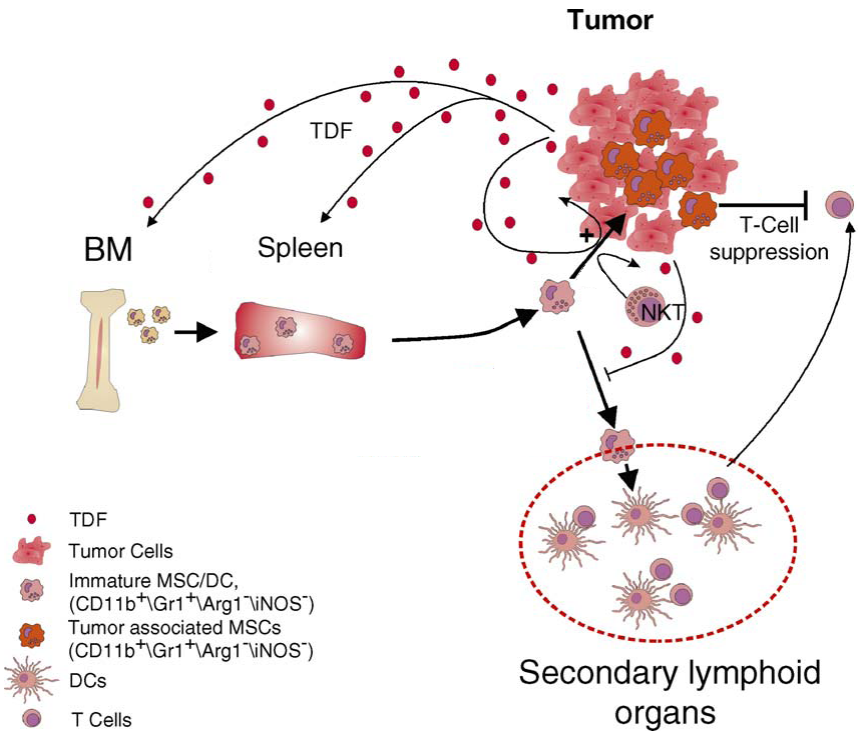

Figure 1-2 : Modèle hypothétique de recrutement/maturation des MDSC (d'après Serafini et al., 2006.

1.4. Facteurs solubles dérivés de la tumeur

La sécrétion des TDSFs représente la première étape de la suppression de la réponse immunitaire anti-tumorale puisque l'excision de la tumeur par chirurgie prévient l'accumulation des MDSC. Cependant, à ce jour, la génération du phénotype et de l'activité immunosuppressive des MDSC n'a pu être associée à un seul TDSF (Salvadori, Martinelli, & Zier, 2000; Sinha, Clements, & Ostrand-Rosenberg, 2005).

Parmi les TDSFs, le GM-CSF (pour "Granulocyte Macrophage- Colony Stimulating Factor") a été rapporté dans plusieurs types de cancers, tant chez la souris que chez l'humain, tels que le carcinome spinocellulaire, l'ostéosarcome et le cancer du poumon (Marigo, et al., 2008) et a reçu une attention particulière dû à ses effets paradoxaux. En fait, l'administration de faibles concentrations de GM-CSF (300 ng/jour) résulte en une immunisation anti-tumorale effective (P. Serafini et al., 2004). Par contre, en plus de leurs rôles dans la progression de la tumeur et la métastase (Obermueller, Vosseler, Fusenig, & Mueller, 2004), les fortes concentrations de GM-CSF ($\geq$ 1500 ng/jour) induisent la différenciation des cellules myéloïdes en monocytes/macrophages, cellules dendritiques, granulocytes et ostéoblastes et favorisent leur prolifération (Sebollela et al., 2005). Cependant, la culture *in vitro* des cellules de la moelle osseuse en présence de GM-CSF génère en une population dont le phénotype est partiellement similaire à celui des MDSC, soit $CD11c^{-}$, $Gr\text{-}1^{low}$, $CD11b^{+}$, $CD31^{+}$, $ER\text{-}MP58^{+}$, $asialoGM1^{+}$ et $F4/80^{+}$ (Rossner et al., 2005).

De même, le facteur M-CSF, qui est généralement associé à la progression de la tumeur et à un faible pronostic, a été rapporté dans plusieurs types de cancer dont la leucémie, le cancer du rein, celui de la vessie, etc. (Dolcetti, et al., 2008). Particulièrement, le traitement *in vitro* des précurseurs myéloïdes par la combinaison du M-CSF et de l'IL-6 inhibe la maturation des

cellules dendritiques et résulte en la génération d'un phénotype monocytique doté de caractéristiques immunosuppressives et présentant les marqueurs de surface suivants : $CD14^{+}$, $CD64^{+}$, $CD1a^{-}$, $CD86^{-}$, $CD80^{-}$, $HLA\text{-}DR^{low}$ (Menetrier-Caux et al., 1998). Par contre, même s'il n'existe pas de relation directe entre le G-CSF et la maturation des MDSC, le G-CSF joue un rôle important dans la progression de la tumeur en favorisant sa néovascularisation ainsi que la différenciation des cellules dendritiques tolérogéniques et des T_{reg} (Rutella, Zavala, Danese, Kared, & Leone, 2005).

D'autre part, le VEGF constitue le facteur de croissance le plus étudié dans le contexte du phénomène d'immunosuppression. En fait, de fortes concentrations de VEGF dans le sang environnant la tumeur inhibent la différenciation des cellules dendritiques via la voie de NF-κB (Johnson, Clay, Hobeika, Lyerly, & Morse, 2007; Melani, Chiodoni, Forni, & Colombo, 2003). En plus, il a été démontré que les MDSC peuvent réguler la biodisponibilité du VEGF et ainsi favoriser la progression de la tumeur et l'angiogenèse via l'expression de la métalloprotéinase 9 (Yang et al., 2004).

De même, les tumeurs sécrètent de grandes quantités de chimiokines inflammatoires et homéostatiques, telles que les chimiokines CCL2/CCR2, CXCL5/CXCR2 et SDF-1/CXCR4 qui induisent la migration des MDSC dans la rate et la tumeur, et ce dans différents types de cancer (Dolcetti, et al., 2008).

Le dernier groupe de facteurs dérivés de la tumeur est constitué de cytokines pro-inflammatoires, telles que IL-1, TNF, INF-α et INF-β et anti-inflammatoires, telles que IL-10 et TGF-β. Particulièrement, l'IL-6, qui est souvent associée à un faible pronostic chez les patients présentant une tumeur solide, est impliquée dans la différenciation des macrophages et des cellules dendritiques *in vivo* et *in vitro* (Park et al., 2004; Trikha, Corringham, Klein, & Rossi, 2003). Les récents travaux de Marigo et ses collaborateurs ont comparé les populations générées

in vitro par les combinaisons GM-CSF+G-CSF et GM-CSF+IL-6 (Marigo et al., 2010). Bien que les deux combinaisons activent les mêmes marqueurs de surface, soient le $CD11b^+$, le $Gr\text{-}1^+$ et l'$IL\text{-}4R\alpha^+$, le profilage génomique des MDSC générées par la combinaison du GM-CSF+IL-6 les associent aux MDSC infiltrant la tumeur, d'où leur potentiel immunosuppressif plus élevé par rapport à celui des MDSC générées par la combinaison du GM-CSF+G-CSF qui sont similaires aux MDSC présentes dans la rate. Il a été également démontré que la maturation des précurseurs myéloïdes en MDSC est dépendante du facteur de transcription C/EBPβ qui, en plus de promouvoir la métastase, régule la capacité des MDSC à métaboliser le L-arg.

1.5. Métabolisme du L-arginine

Le L-arg est un acide aminé semi-essentiel qui peut être dérivé de l'alimentation ou produit de manière endogène à partir d'autres acides aminés (i.e. glutamine, glutamate et proline) par les intestins et les reins. Il s'agit d'un composant intégral des protéines et fonctionne comme un intermédiaire du cycle de l'urée. Il est également un précurseur de la synthèse de biomolécules non-protéiques indirectement impliquées dans la vasodilatation, le relargage du calcium, la neurotransmission et principalement l'immunité (Peranzoni et al., 2007).

Comme chez la majorité des cellules animales, le transport de L-arg chez les cellules myéloïdes se fait par le transporteur d'acides aminés cationiques CAT-2B (Lind, 2004). Dans des conditions normales, les cellules myéloïdes ne consomment pas le L-arg et l'utilisation d'un régime alimentaire riche en L-arg s'est avérée inefficace dans la promotion de leurs potentiels immunosuppressifs (Popovic, Zeh, & Ochoa, 2007).

Le L-arg peut être catabolisé par 4 groupes d'enzymes : les synthétases d'oxyde nitrique (NOS pour "Nitric Oxide Synthase"), les arginases (ARG), les amidinotranférases arginine:glycine et les décarboxylases d'arginine (Figure 1-3) (S. M. Morris, Jr., 2004).

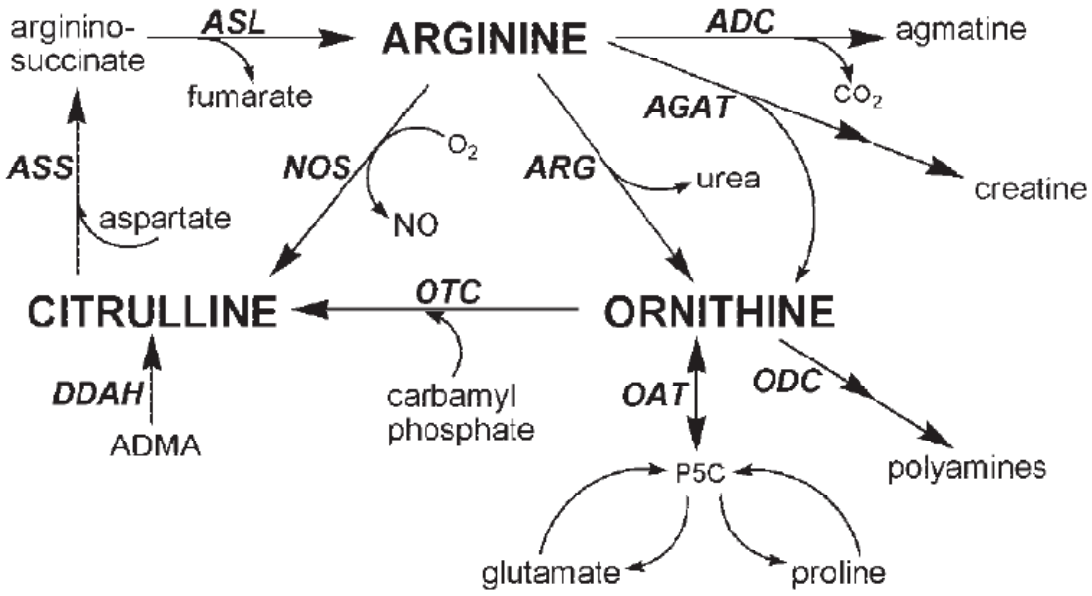

Figure 1-3 : Catabolisme et recyclage du L-arg, extrait de Morris, 2004.

Spécifiquement, les MDSC métabolisent le L-arg par l'isoforme inductible de l'enzyme NOS (iNOS) et l'arginase cytoplasmique (ARG1). En présence d'oxygène et de NADPH, l'enzyme iNOS oxyde le L-arg pour produire l'oxyde nitrique (NO pour "Nitric Oxide") et la L-citrulline; cependant, l'ARG1 convertit le L-arg en L-ornithine et urée sans l'intervention de cofacteurs. En présence de stress immunitaire, l'expression et l'activité du transporteur CAT-2B ainsi que celles des enzymes iNOS et ARG1 sont co-induites. Les activités enzymatiques de ARG1 et iNOS sont respectivement induites par les cytokines de type Th1 (les interférons- α, β et γ) et Th2 (IL- 4, 6, 10 et 13, TGF- β) (Munder, Eichmann, & Modolell, 1998), par contre

l'expression de CAT-2B peut être régulée par les deux types de cytokines (Hammermann et al., 2000; P. C. Rodriguez et al., 2003).

La constante de Michaelis (K_m) de l'ARG1 (~ 10 mM) est beaucoup plus élevée que celle de l'iNOS (~ 5 μM) ; alors que le taux maximal (V_{max}) de l'ARG1 est 10^3 - 10^4 fois celui de l'iNOS. Ainsi, le rapport V_{max}/K_m pour iNOS et ARG1 sont similaires et les deux enzymes sont alors en compétition pour L-arg à de faibles concentrations (Mori, 2007). En plus de leur compétition pour un substrat commun, les enzymes iNOS et ARG1 peuvent réguler leurs activités enzymatiques de façon croisée. En fait, la surexpression de l'ARG1 inhibe la traduction de l'ARNm de l'enzyme iNOS (El-Gayar, Thuring-Nahler, Pfeilschifter, Rollinghoff, & Bogdan, 2003; Lee, Ryu, Ferrante, Morris, & Ratan, 2003).

Tant chez les MDSC que chez les cellules T, le L-arg peut être synthétisé à partir de la L-citrulline par l'action séquentielle des enzymes cytosoliques : la synthétase et la lyase d'argininosuccinate (ASS et ASL pour "Arginosuccinate Synthetase" et "Lyase", respectivement) pour remédier à l'absence de L-arg dans le sang. La synthèse d'une molécule d'argininosuccinate requiert l'hydrolyse d'une molécule d'ATP en AMP; i.e. l'équivalent de 2 molécules d'ATP (S. M. Morris, Jr., 2004). De plus, la stimulation de l'activité de l'enzyme iNOS par la lipopolysaccharide (LPS) et l'INF-γ chez les macrophages stimule l'expression de l'ARNm de ASS ainsi que son activité enzymatique (Hattori, Campbell, & Gross, 1994). Ainsi, en plus de leurs rôles dans la maturation des MDSC, les facteurs solubles dérivés de la tumeur régulent les mécanismes d'internalisation du L-arg, son métabolisme et sa production endogène pour assurer la suppression permanente de la réponse immunitaire anti-tumorale.

1.6. Mécanismes de suppression des CTLs par les MDSC

Bien que les cellules T n'expriment pas d'enzymes qui métabolisent directement le L-arg, la diminution de la concentration de cet acide aminé dans le sang déclenche plusieurs processus qui altèrent les fonctions immunitaires des cellules T (Figure 1-4) (Bronte & Zanovello, 2005; Sica & Bronte, 2007).

Premièrement, l'absence de L-arg résulte en la perte de la chaîne CD3ζ du récepteur des cellules T (TCR pour "T-Cell Receptor") (Munder et al., 2006; P. C. Rodriguez, et al., 2003). Cette chaîne est une protéine transmembranaire indispensable pour la reconnaissance des antigènes ainsi que la transduction du signal. L'absence de la chaîne CD3ζ déstabilise l'expression du TCR, bloquant ainsi la prolifération des cellules T sans aucun effet sur leur viabilité (Munder, et al., 2006).

De même, le catabolisme du L-tryptophane (L-trp) et du L-phenyalanine (L-phe) par les MDSC via les activités enzymatiques de l'indoléamine 2,3- dioxygénase et de l'oxydase du L-phe, respectivement, résulte en la perte de la chaîne CD3ζ du TCR (Boulland et al., 2007; Fallarino et al., 2006). De plus, une limitation en L-arg, L-trp et en L-phe augmente la quantité d'ARNt non-chargé d'acides aminés, ce qui active le GCN2 ("General Control Non-depressible 2"). Le complexe GCN2/ARNt non-chargé phosphoryle la sous-unité α du facteur d'initiation de la traduction (EIF2α), ce qui altère la traduction de plusieurs ARNm (P. C. Rodriguez, Quiceno, & Ochoa, 2007).

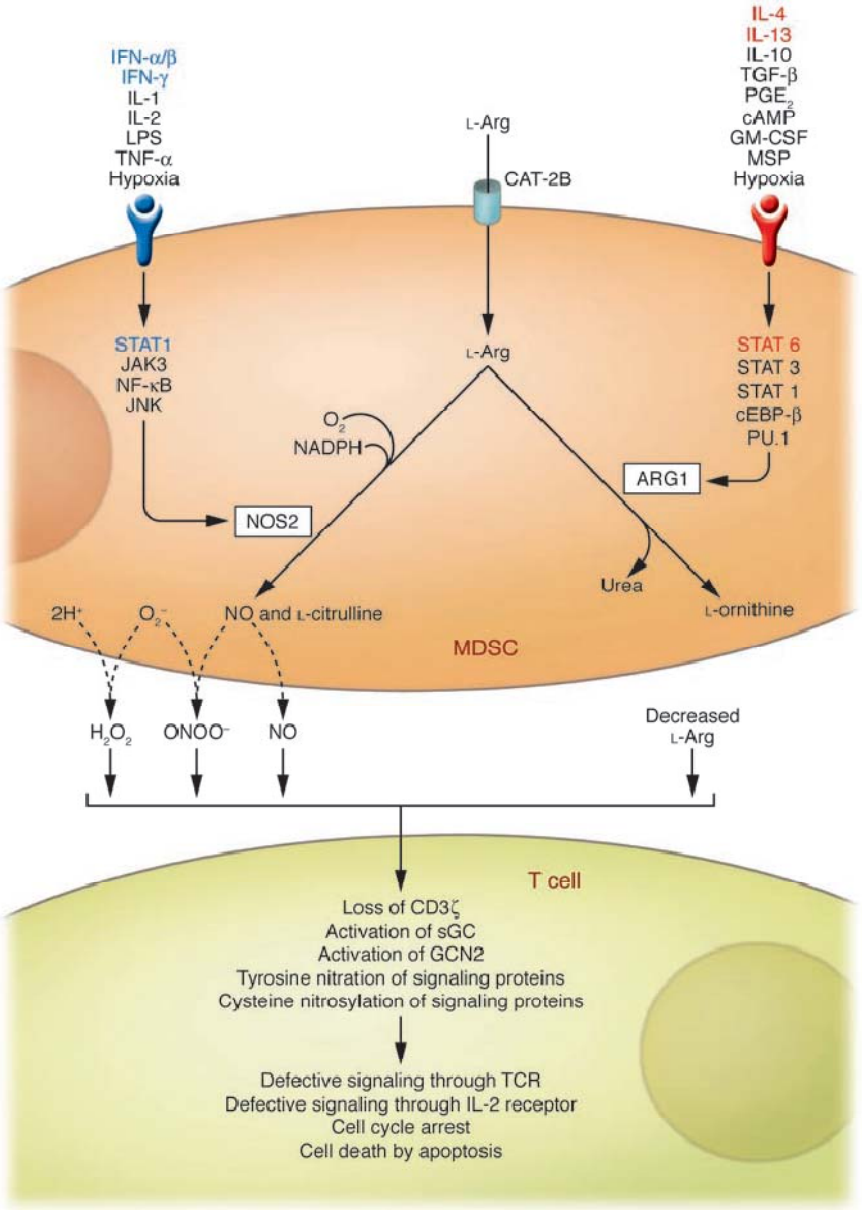

Figure 1-4 : Effets inhibiteurs des MDSC sur les CTLs (extrait de Sica et al, 2007).

En absence du L-arg, les cellules T n'expriment plus la cycline D3 ni la kinase 4 qui lui est associée, bloquant ainsi le cycle cellulaire à la phase G0/G1 (P. C. Rodriguez, et al., 2007). De plus, l'accumulation de l'urée active la voie mTOR (pour "Mammalian Target Of

Rapamycin") qui libère la rapamycine, un immunosuppresseur naturel qui inhibe également la prolifération des cellules T (Peng, Golub, & Sabatini, 2002).

1.7. Rôle du NO dans le phénomène d'immunosuppression

Le NO diffuse rapidement à travers la membrane cellulaire sans l'intermédiaire de transporteurs; il interagit avec des biomolécules tant dans les cellules qui le produisent que dans les cellules cibles pour générer des espèces oxygénées et/ou azotées réactives (RNOS pour "Reactive Nitrogen Oxide Species") hautement immunosuppressives (Kroncke, Fehsel, Suschek, & Kolb-Bachofen, 2001). L'exposition des cellules T à de fortes concentrations de RNOS cause des stress oxydatifs et nitrositifs qui affectent l'ADN, les protéines et les lipides et qui sont capables d'influencer les fonctions cellulaires, promouvoir des réactions inflammatoires, inhiber la respiration mitochondriale et induire l'apoptose (Figure 1-5) (Mocellin, Bronte, & Nitti, 2007).

Le peroxynitrite ($ONOO^{--}$), le RNOS primaire produit par la réaction du NO avec le superoxyde (O_2^-), est responsable de la peroxydation des lipides. Cette peroxydation détériore les propriétés biophysiques des membranes phospholipidiques, notamment leurs capacités de transport des ions et d'autres biomolécules, ce qui peut altérer les fonctions physiologiques et biochimiques des cellules (Nicolescu, Zavorin, Turro, Reynolds, & Thatcher, 2002). Le peroxynitrite interagit également avec l'ADN pour briser les liens entre ses deux brins (Losser & Payen, 1996) et nitrate les résidus tyrosines de certaines protéines qui deviennent des cibles pour la voie de dégradation protéolytique (Radi, 2004).

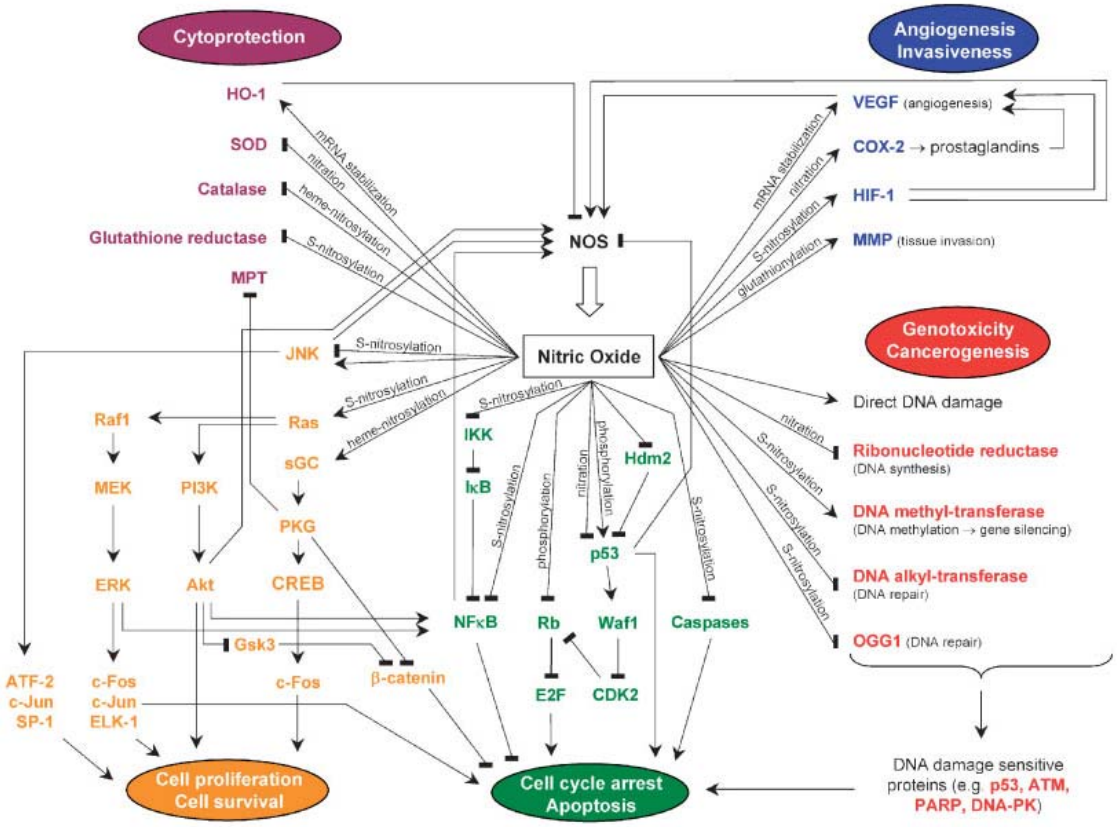

Figure 1-5 : Différentes cibles du NO dans la tumeur et les voies impliquées, extrait de Mocellin et al., 2007.

Plusieurs points de mutations de l'ADN sont causés par le trioxyde d'azote (N_2O_3). Ce dernier cède un groupement NO^+ aux nucléophiles, ce qui résulte en la désamination des bases d'ADN (la cytosine en uracile et la guanine en xanthine) (Marnett, Riggins, & West, 2003). Le N_2O_3 peut également réagir avec les amines secondaires pour former des N-nitrosamines carcinogéniques qui endommagent l'ADN par alkylation. Les dommages causés à l'ADN sont irréversibles puisque le NO inhibe des voies de réparation de l'ADN telles que celles impliquant la p53, la polymérase poly-ADP-ribose et les protéines kinase de l'ADN (Sancar, Lindsey-Boltz,

Unsal-Kacmaz, & Linn, 2004). De même, le NO nitrosyle des résidus cystéines cruciaux sur les enzymes de réparation de l'ADN, telles que l'alkyl transférase d'ADN (Jaiswal, LaRusso, Burgart, & Gores, 2000). Ainsi, les RNOS altèrent l'intégrité à la fois génétique et épigénétique des cellules T afin d'assurer leur dysfonctionnement et induire leur mort (Bernstein, Bernstein, Payne, & Garewal, 2002).

En plus, le NO affecte négativement les molécules de signalisation de manière directe en S-nitrosylant des résidus cystéines cruciaux, ou indirectement, en activant la guanylate cyclase soluble ou la protéine kinase dépendant de la cGMP (Bronte & Zanovello, 2005). En fait, en plus d'altérer la stabilité de l'ARNm de l'IL-2 (Macphail et al., 2003), le NO inhibe la phosphorylation, et donc l'activation, des protéines de signalisation (JAK1, JAK3, STAT5, ERK et AKT) impliquées dans la voie du récepteur de l'IL-2 (Bingisser, Tilbrook, Holt, & Kees, 1998; Mazzoni et al., 2002). Ceci empêche alors la prolifération des cellules T puisque la voie de signalisation du récepteur de l'IL-2 régule l'expression de la cycline D3 et la cdk4 (Engedal, Gjevik, Blomhoff, & Blomhoff, 2006).

Les RNOS sont également capables de nitrosyler certains résidus thiols de protéines spécifiques, menant ainsi à la perte de leur activité catalytique. Cette réaction est généralement réversible. Cependant, la S-nitrosylation des protéines qui contiennent du zinc, du cuivre ou du fer est irréversible à cause de la perte du groupement métallique, ce qui induit la dénaturation des protéines.

Particulièrement, l'exposition des cellules T aux RNOS S-nitrosyle le complexe IV (ou CcOX pour cytochrome *c* oxidase) de la chaîne respiratoire mitochondriale. En fait, cette enzyme contient deux groupes hème (a et a_3) et deux atomes de cuivre (Cu_A et Cu_B) dont le couple a_3 et Cu_B constitue le site de liaison de l'oxygène (Moncada & Erusalimsky, 2002). Dû à la ressemblance moléculaire entre l'O_2 et le NO, ce dernier se lie au site de liaison de l'oxygène et

inhibe la respiration cellulaire d'une manière réversible et transitoire. La nitrosylation de la CcOX cause une chute du flux d'électrons et conséquemment l'extrusion des protons. Afin de contrer la baisse du potentiel membranaire, la synthase d'ATP hydrolyse l'ATP cytoplasmique; la fuite de protons est ainsi restaurée. Cependant, l'exposition prolongée des cellules T au NO conduit à l'inhibition irréversible et permanente du complexe I ainsi qu'à l'ouverture du pore de transition mitochondrial et la libération du cytochrome *c* (Sarti et al., 2003).

Wang et ses collaborateurs ont proposé un mécanisme pour décrire l'initiation de l'apoptose par le cytochrome *c*. Brièvement, une fois dans le cytoplasme, le cytochrome *c* se lie à la protéine Apaf-1. La formation d'un complexe multimérique Apaf-1-cytochrome *c* stable (apoptosome) requiert l'hydrolyse du dATP/ATP attaché à Apaf-1 en dADP/ADP. La pro-caspase 9 est ensuite recrutée à l'apoptosome où elle sera clivée et activée pour déclencher une cascade de caspases impliquant notamment la caspase 3 (Li et al., 1997; Zou, Li, Liu, & Wang, 1999).

En plus de son rôle dans l'initiation de l'apoptose, il a été démontré que le NO promeut l'accumulation des protéines pro-apoptotiques p53 et Bax ainsi que la diminution de l'expression des facteurs anti-apoptotiques de la famille BCL-x_L (Messmer, Reed, & Brune, 1996).

1.8. Stratégies d'immunothérapie anti-MDSC

Comme souligné dans le chapitre INTRODUCTION de cette thèse, les tumeurs développent plusieurs mécanismes d'immunosuppression. Toutefois, la présente section se limitera aux approches thérapeutiques qui ciblent les MDSC. Ces stratégies d'immunothérapie anti-MDSC peuvent agir au niveau de : i) la différenciation des MDSC en cellules matures; ii) la

maturation des précurseurs myéloïdes en MDSC; iii) l'accumulation des MDSC dans les organes périphériques; et iv) la fonction des MDSC (Figure 1-6).

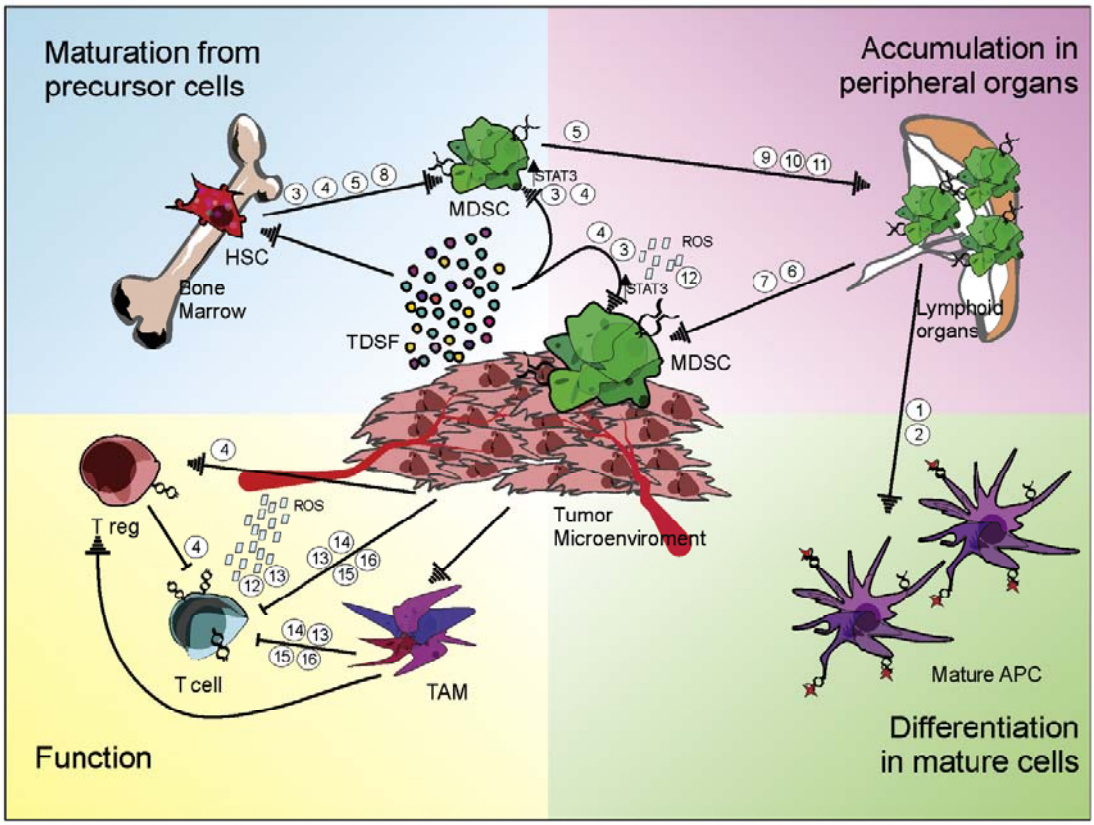

Figure 1-6 : Stratégies thérapeutiques ciblant les MDSC.

Différenciation : (1) ATRA, (2) Vitamine D_3. **Maturation** : (3) Inhibiteurs de STAT3, (4) Inhibiteurs de tyrosine kinase (Sunitinib), (5) Bevacizumab, (6) Anitcorps monoclonaux anti-BV8, (7) Amino-biphosphonates, (8) Inhibiteurs de MMP-9. **Accumulation** : (9) Gemcitabine, (10) 5-Fluoracil, (11) Antagonistes spécifiques des chimiokines CXCR2 et CXCR4. **Fonction** : (12) Désactivateurs de RNOS, Inhibiteurs de iNOS et ARG1 : (13) Nitroaspirine, (14) Inhibiteurs de phophodiesterase 5, (15) Inhibiteurs de cyclooxygenase 2, (16) Autres agents qui interfèrent avec la voie IL-13/IL-4Rα/STAT6. Extrait de Ugel et al, 2009.

1.8.1 Stratégies forçant la différenciation des MDSC en APCs

La différenciation des MDSC en cellules matures non-immunosuppressives représente une stratégie prometteuse puisque cette solution pourrait à la fois renforcer la réponse immunitaire anti-tumorale et augmenter l'efficacité des vaccins anti-tumoraux ou le transfert adoptif des CTLs spécifiques à la tumeur (Ugel et al., 2009).

Particulièrement, la vitamine A est connue pour son rôle dans la favorisation de la différenciation des progéniteurs myéloïdes en cellules dendritiques et macrophages. Une déficience en vitamine A résulte ainsi en l'accumulation des MDSC dans le sang et compromet les réponses immunitaires adaptatives dépendantes de la présentation des TAAs à la surface des cellules dendritiques. L'ATRA (pour "All-*Trans*-Retinoic Acid"), qui est un métabolite actif dérivé de la vitamine A, s'est avéré capable de différencier les MDSC en granulocytes matures (Kusmartsev et al., 2003; Nefedova et al., 2007). Des concentrations physiologiques d'ATRA (1 μM) combinées avec de faibles doses de GM-CSF (20 $ng.mL^{-1}$) induisent, *in vitro*, la différentiation des MDSC en cellules dendritiques présentant les deux marqueurs de surface CD11c et MHC de la classe II (D. I. Gabrilovich, Velders, Sotomayor, & Kast, 2001). *In vivo*, l'ATRA n'affecte pas directement la progression de la tumeur, mais force la différentiation des MDSC en cellules dendritiques, macrophages et granulocytes matures, ce qui augmente et prolonge significativement l'effet des vaccins anticancéreux (D. I. Gabrilovich, et al., 2001). Ces mêmes effets ont été rapportés chez des patients cancéreux traités avec des concentrations d'ATRA supérieures à 150 $ng.mL^{-1}$ (Mirza et al., 2006). Engedal et ses collaborateurs ont également démontré que l'ATRA stimule la prolifération des cellules T en modulant les cascades de signalisation déclenchées par la liaison de l'IL-2 à son récepteur (Engedal, et al., 2006). En fait, à de faibles concentrations (0.1 nM), l'ATRA augmente l'expression et l'activité de la

cycline D3 qui régule la progression de la phase G1/S du cycle cellulaire. Contrairement à l'ATRA qui agit directement sur les MDSC, le 1α25-dihydroxyvitamine D_3 a un effet indirect sur la différentiation des MDSC en APCS. En effet, l'administration de la vitamine D_3 chez des patients cancéreux réduit le nombre des cellules immunosuppressives $CD34^+$ et augmente la blastogenèse des cellules T, permettant ainsi le récupération des fonctions immunitaires anti-tumorales (Lathers, Clark, Achille, & Young, 2004).

1.8.2. Stratégies inhibant la maturation des MDSC

Bien qu'elle soit prometteuse, la stratégie de contrôle de la maturation des précurseurs hemapoïétiques en MDSC est compliquée compte tenu de la diversité des TDSFs secrétés par les cellules tumorales.

Certains TDSFs, tels que IL-6, VEGF et IL-10, activent chez les MDSC une voie de signalisation commune qui implique la famille des STAT (pour "Signal Transducer and Activator of Transcription") (Yu, Kortylewski, & Pardoll, 2007). Particulièrement, les MDSC sont caractérisées par l'activation permanente de STAT3; ceci résulte en de fortes concentrations d'espèces réactives oxygénées (D. I. Gabrilovich & Nagaraj, 2009) ainsi qu'en l'activation de plusieurs gènes dépendant de STAT3 tels que ceux des facteurs anti-apoptotiques BCL-x_L et des protéines pro-prolifératives (Cycline D1/D2) et pro-angiogéniques (MMP2/9, HIF1α) (Yu, et al., 2007). Étant donné que la suppression du gène codant pour STAT3 engendre des maladies auto-immunes diverses, l'inhibition de STAT3 devrait être intermittente.

Des inhibiteurs peptidomimétiques résistants aux protéases ont alors été développés pour se lier au terminal C de STAT3 afin de réduire son interaction avec ses récepteurs, et par conséquent bloquer la première étape de la voie de signalisation de STAT3 (Coleman et al.,

2005). De plus, le criblage, *in silico*, de larges librairies de molécules chimiques a permis l'identification de deux inhibiteurs de STAT3 nommés STA-21 et Nifuroxazide. Le STA-21 inhibe la capacité de STAT3 à se lier à l'ADN, ainsi que sa dimérisation et l'activité de la luciférase dépendante de STAT3 (Song, Wang, Wang, & Lin, 2005). Cependant, le Nifuroxazide inhibe la phosphorylation de STAT3 indirectement via l'inhibition des kinases Jak2 et Tyk2 (Nelson et al., 2008). Le STA-21 et le Nifuroxazide réduisent également la viabilité des cellules tumorales sans aucun effet sur les cellules normales. D'autre part, le JSI-124 (Curcubitacin I), un inhibiteur sélectif de la voie Jak2/STAT3, réduit le nombre des cellules $CD11b^{+}/Gr1^{+}$ en induisant leur apoptose ou en forçant leur différentiation en cellules matures (Nefedova et al., 2005). Le dernier groupe d'inhibiteurs de STAT3 sont les complexes platinés. Particulièrement, le CPA-7, qui est connu pour ses effets anticancéreux, réduit la phosphorylation et donc l'activation de STAT3 dans les cellules dendritiques et les lymphocytes tueurs naturels (NK pour "Natural Killer") qui s'infiltrent dans la tumeur et suppriment la fonction anti-tumorale des cellules T (Kortylewski et al., 2005).

De même, certains inhibiteurs de l'activité des tyrosines kinases sont également utilisés comme inhibiteurs de STAT3 et plusieurs molécules sont en cours d'approbation ou en phases d'essais cliniques. Parmi ces inhibiteurs, le rôle du Sunitinib dans la correction du processus d'immunosurveillance a été étudié dans plusieurs modèles de cancer. En plus d'inhiber la voie Src/STAT, le Sunitinib réduit le nombre des MDSC et des cellules T_{reg} en circulation et diminue l'expression des gènes angiogéniques dépendant de la STAT3. Le Sunitinib induit également l'expansion des cellules dendritiques $CD1c^{+}$ chez les patients présentant un cancer du rein métastatique et promeut les fonctions anti-tumorales des cellules T (Ugel, et al., 2009).

Le récepteur du VEGF (VEGFR pour "VEGF Receptor") représente la deuxième cible étudiée pour prévenir la maturation des MDSC. En fait, l'administration d'un anticorps

monoclonal anti-VEGFR à des patients présentant un cancer du rein diminue la proportion des cellules $CD11b^{+}VEGFR^{+}$ (Kusmartsev et al., 2008). De plus, étant donné que la MMP-9 peut réguler la biodisponibilité du VEGF, inhiber les métalloprotéinases matricielles par des amino-biphosphonates, tels que le Pamidronate et le Zoledronate, a représenté une approche immunothérapeutique de valeur. L'inhibition de l'expression de MMP-9 réduit également le support myéloïde dans le stroma tumoral, bloque la génération des MDSC et promeut la nécrose des cellules tumorales (Heissig et al., 2002; Melani, Sangaletti, Barazzetta, Werb, & Colombo, 2007).

1.8.3. Stratégies réduisant l'accumulation des MDSC

Les premières tentatives pour prévenir l'accumulation des MDSC dans la tumeur, la rate et les organes lymphoïdes ciblaient le marqueur de surface Gr-1. L'administration des anticorps monoclonaux anti-Gr-1 supprime la présence des MDSC $Gr1^{+}$ en plus de réduire la progression de la tumeur et prévenir sa réapparition (V. Bronte et al., 1999; Terabe et al., 2003). Cependant, le Gr-1 est fortement exprimé par les granulocytes et sa suppression non spécifique augmente le risque d'infections. De plus, la diminution de la concentration de l'anticorps anti-Gr-1 dans le sang peut résulter en l'accumulation rapide des MDSC.

D'autres travaux ont montré que la Gemcitabine, un agent utilisé en chimiothérapie, réduit le nombre de MDSC dans la rate sans aucun effet sur la fraction des cellules T $CD4^{+}$, $CD8^{+}$, NK, des macrophages et des cellules B (Suzuki, Kapoor, Jassar, Kaiser, & Albelda, 2005). Les mécanismes d'éradication des MDSC par la Gemcitabine ne sont pas encore connus. Toutefois, une augmentation du taux d'apoptose des splénocytes a été rapportée, *in vivo* et *in vitro*, suite au traitement à la Gemcitabine (Suzuki, et al., 2005). De même, l'utilisation de faibles doses du 5-

Fluorouracil inhibe la progression du cycle cellulaire des MDSC et induit leur apoptose en s'intercalant au niveau de l'ADN et de l'ARN (Cao et al., 1995).

Une autre stratégie pour prévenir l'accumulation des MDSC consiste à cibler les chimiokines responsables du recrutement des MDSC dans la tumeur. Particulièrement, le recrutement des cellules $CD11b^{+}/Gr1^{+}$ est assuré par les deux axes de chimiokines SDF-1/CXCR4 et CXCL//CXCR2. Des recherches récentes ont utilisé deux antagonistes spécifiques à la CXCR2 (S-265610) et CXCR4 (AMD3100) et ont montré leur capacité à réduire le nombre des MDSC dans la tumeur (Yang et al., 2008).

1.8.4. Stratégies inhibant les fonctions immunosuppressives des MDSC

Une dernière approche thérapeutique anti-MDSC agit directement au niveau de leurs voies immunorégulatrices; i.e. le métabolisme du L-arg par les enzymes iNOS et ARG1.

La première classe d'inhibiteurs de la fonction des MDSC sont les NO-NSAIDs (pour "NO-releasing Non-Steroidal Anti-Inflammatory Drugs"). Ces composés consistent en un groupement qui relâche un groupe NO, relié par un espaceur à une molécule de NSAID, telle que l'aspirine, l'acide salicylique, l'ibuprofène, etc., prévue pour réduire la toxicité gastro-intestinale de l'inhibiteur (Keeble & Moore, 2002). Le NO libéré par les NO-NSAIDs est nécessaire pour l'inhibition de l'activité enzymatique de iNOS; par contre, l'espaceur et la molécule de NSAID sont responsables de l'inhibition de l'activité de ARG1. Le mécanisme du relargage du NO par les NO-NSAIDs demeure ambigu, mais l'implication des estérases dans le catabolisme des NO-NSAIDs a été rapportée dans plusieurs travaux (Saavedra et al., 2000; Velazquez, Praveen Rao, & Knaus, 2005). De même, l'inhibition des voies de signalisation déclenchées par les cytokines Th2, particulièrement les IL-4 et IL-13, représente l'hypothèse la plus probable pour expliquer

l'inhibition du pouvoir immunosuppressif des MDSC par les NO-NSAIDs (Perez, Melo, Keegan, & Zamorano, 2002). Comme ils sont connus pour leur rôle dans l'inhibition de la progression de la tumeur, les NO-NSAIDs sont également utilisés comme additifs aux vaccins anticancéreux afin d'augmenter leur efficacité (Ugel, et al., 2009).

Les inhibiteurs de la phosphodiestèrase 5 (PDE5) ont également été utilisés pour corriger la réponse immunitaire anti-tumorale. L'administration du Sildenafil, un inhibiteur de la PDE5, utilisé cliniquement pour le traitement de l'hypertension pulmonaire, l'hypertrophie cardiaque, etc., retarde la croissance de la tumeur et inhibe les fonctions immunosuppressives des MDSC en diminuant les activités de iNOS et ARG1 (P. Serafini et al., 2006). En fait, les inhibiteurs de la PDE5 augmentent la concentration de la GMP cyclique, ce qui réduit la stabilité de l'ARNm de l'enzyme iNOS (Pilz & Casteel, 2003). De plus, l'accumulation de la GMP cyclique est associée à une faible teneur en calcium, qui, à son tour, diminue l'expression du récepteur de l'IL-4 et sous-régule l'activité de l'ARG1 (Rotella, 2002; Vellenga, Dokter, & Halie, 1993).

L'inhibition de la cyclo-oxygénase 2 (COX-2) a été également étudiée comme cible d'immunothérapie. En fait, la COX-2 est nécessaire pour la production de la prostaglandine E2 qui induit l'expression de l'ARG1 dans certains types de cancers (D. I. Gabrilovich & Nagaraj, 2009). Le Colecoxib, un inhibiteur sélectif de COX-2, réduit l'expression des enzymes iNOS et ARG1 ainsi que le nombre de cellules $CD11b^{+}Gr\text{-}1^{+}$ et stimule la fonction des cellules T $CD4^{+}$ présentes dans la rate (Talmadge et al., 2007).

Bien que les stratégies présentées ci-haut aient montré des bénéfices quant à la correction de la réponse immunitaire des CTLs et au freinage de la progression des tumeurs, ces approches thérapeutiques demeurent inefficaces, *in vivo*, devant le potentiel des cellules tumorales à changer leur signature génomique, protéomique et métabolomique pour échapper aux processus d'immunosurveillance.

CHAPITRE 2. OBJECTIFS ET ORGANISATION GÉNÉRALE DU DOCUMENT

Les cellules immunocompétentes requièrent de l'énergie pour maintenir leur intégrité cellulaire. La majorité de leurs fonctions, telles que la production de cytokines, la présentation d'antigène ainsi que leur migration, activation et cytotoxicité, sont directement ou indirectement dépendante de l'énergie (Buttgereit, Burmester, & Brand, 2000). Plusieurs stratégies immunothérapeutiques, consistant en la modulation de l'état énergétique des cellules immunitaires, sont actuellement utilisées afin de corriger les fonctions immunomodulatoires altérées dans le psoriasis, l'arythmie cardiaque et l'arthrite rhumatoïde, etc. Cependant, les stratégies thérapeutiques anti-MDSC proposées dans la littérature ciblent principalement des voies de signalisation, des marqueurs de surface, des enzymes clées, etc. Malgré les avancées accomplies dans la compréhension de la biologie des MDSC, les événements métaboliques qui régulent les différentes étapes du phénomène d'immunosuppression demeurent ambigus. Les travaux présentés dans cette thèse sont donc basés sur l'hypothèse que la suppression de la réponse immunitaire anti-tumorale est un processus énergivore. L'objectif principal a ainsi consisté à étudier le phénomène d'immunosuppression, tant au niveau des MDSC que celui des cellules T, d'un point de vue métabolique afin d'identifier de nouvelles cibles pour l'immunothérapie et optimiser les stratégies thérapeutiques en cours de développement. Spécifiquement, cette étude s'est concentrée sur trois étapes majeures du phénomène d'immunosuppression, soit i) la maturation des MDSC, ii) leurs fonctions, et iii) leurs interactions avec les cellules effectrices du système immunitaire.

Les travaux regroupés dans le premier article de cette thèse, soumis au journal *Cancer Research*, et présentés au troisième chapitre se sont attardés à la détermination des besoins énergétiques associés à la maturation des MDSC. Une combinaison des cytokines GM-CSF et IL-6 a été utilisée pour simuler, *in vitro*, la maturation des MDSC à partir de précurseurs myéloïdes fraîchement isolés de souris saines. Les MDSC générées *in vitro* expriment les deux enzymes iNOS et ARG1 et ont un profil génomique semblable à celui des MDSC qui infiltrent la tumeur (Marigo, et al., 2010). La maturation des MDSC est dépendante du facteur de transcription C/EBPβ et implique d'autres voies de signalisation telles que JAK/STAT3, MAPK et PI3-K (Fleetwood, Cook, & Hamilton, 2005). Ces travaux sont basés sur l'hypothèse que l'activation de ces cascades de signalisation et des processus biochimiques déclenchés en aval est dépendante de l'état énergétique des cellules. Il a ainsi pu être démontré que le processus de maturation des MDSC est dépendant de la stimulation du métabolisme central du carbone, et ce pour produire l'énergie et synthétiser les intermédiaires nécessaires à l'acquisition et le maintien du phénotype et de l'activité immunosuppressifs des MDSC qui en résultent.

Ensuite, pour étudier les besoins nutritionnels et énergétiques associés à la machinerie immunosuppressive des MDSC, une lignée cellulaire immortalisée dérivée de MDSC murines, MSC-1, a été utilisée comme système modèle pour l'étude de la biologie des MDSC (Apolloni et al., 2000). Le chapitre 4 s'attarde à la caractérisation de la ligne de base de l'état énergétique des cellules MSC-1 pour des études ultérieures portant sur la stimulation ou l'inhibition de ces cellules ou lors du processus de criblage d'agents thérapeutiques. Cet article est publié dans "*Journal of Biotechnology*" en 2011.

Le troisième article, soumis au journal "*Cancer Immunology and Immunotherapy*" et présenté dans le chapitre 5 vise à caractériser la régulation croisée entre le métabolisme du L-arg, le métabolisme central du carbone et la respiration cellulaire afin d'identifier les voies

métaboliques et les réactions biochimiques impliquées dans la suppression de la réponse immunitaire anti-tumorale.

Comme déjà mentionné dans le chapitre REVUE DE LITTERATURE, le NO, produit par les MDSC, a un rôle majeur dans la suppression des cellules T. L'utilisation des donneurs de NO, les NO-NSAIDs, pour des fins thérapeutiques est controversée, puisqu'en plus de leurs effets bénéfiques dans l'inhibition de la progression de la tumeur et l'altération des MDSC, le NO inhibe drastiquement la respiration des cellules T. L'objectif des travaux présentés dans le chapitre 6 et soumis au journal "*Immunology and Cell Biology*", a été d'étudier l'énergétique des cellules du système immunitaire en présence d'un nouveau donneur de NO, AT38, constitué d'une molécule d'acide salicylique liée à un groupement furoxane (article en soumission). Les cellules Jurkat, immortalisées de cellules T leucémiques, considérées comme modèle de cellules immunitaires stimulées et des concentrations spécifiques ont été utilisées pour simuler *in vitro* l'effet d'AT38 sur le système immunitaire. Il a été démontré que la présence d'AT38 détériore sévèrement l'état énergétique des cellules Jurkat menant au déclenchement des mécanismes de la mort cellulaire, qui se sont avérés régulés par la glycolyse. Cette étude a également permis de proposer une stratégie thérapeutique pour atténuer les effets néfastes d'AT38 ou autres NO-NSAIDs similaires sur le système immunitaire.

CHAPITRE 3. LA RÉPONSE DU MÉTABOLISME CENTRAL DU CARBONE ET LA BIOENERGETIQUE AU GM-CSF ET IL-6 DURANT LA MATURATION IN VITRO DES CELLULES MYÉLOIDES SUPPRESSIVES

3.1. Présentation de l'article

Cette section reprend l'article intitulé "**Central carbon metabolism and bioenergetics response to GM-CSF and IL-6 during myeloid-derived suppressor cell *in vitro* maturation**". L'article a été soumis dans la revue "Cancer Research" en 2011.

L'inhibition de la maturation des MDSC constitue une approche thérapeutique prometteuse pour le rétablissement du processus d'immunosurveillance et également la promotion de l'efficacité des thérapies anticancéreuses conventionnelles. Pour ce faire, l'étude des événements métaboliques ayant lieu lors de la maturation des MDSC s'avère indispensable pour comprendre ce processus et identifier les cibles qui pourraient éventuellement l'altérer. Dans ce chapitre, la maturation des MDSC a été alors simulée en exposant des précurseurs myéloïdes fraîchement isolés de souris saines à la combinaison de cytokines GM-CSF et IL-6 qui génère une population de MDSC similaire à celle qui infiltre la tumeur. Le profil nutritionnel et l'état énergétique des cellules ont été suivis tout au long de ce processus.

3.2. Central carbon metabolism and bioenergetics response to granulocyte macrophage – colony stimulating factor and interleukin-6 during myeloid-derived suppressor cell in vitro maturation

Ines Hammami[1], Jingkui Chen[1], Vincenzo Bronte[2], Gregory De Crescenzo[1], Mario Jolicoeur[1*]

[1]Department of Chemical Engineering. École Polytechnique de Montréal. Montreal, Quebec, Canada.

[2]Department of Pathology. Immunology Section. Verona University. Verona, Veneto, Italy.

* Corresponding author:

Mario Jolicoeur

PO 6079 Station Centre-Ville

Montreal, Qc, Canada H3C 3A7

Tel: +1 514 340 4711 ext. 4525

Fax: +1 514 340 4159

e-mail: mario.jolicoeur@polymtl.ca

3.2.1. Abstract

Tumour microenvironment contains a vast array of pro- and anti-inflammatory cytokines that alter myelopoesis and lead to the maturation of immunosuppressive cells known as myeloid-derived suppressor cells (MDSCs). Particularly, treating bone marrow (BM) precursors with the combination of Granulocyte Macrophage - Colony Stimulating Factor (GM-CSF) and Interleukin-6 (IL-6) was shown to generate a tumour-infiltrating MDSC-like population that has the ability to impair the anti-tumour specific T-cell function. We thus used this experimental approach to simulate, *in vitro*, the MDSC maturation process and monitored cells' metabolic response. Our results demonstrated that exposure of BM cells to GM-CSF and IL-6 activated L-arginine (L-Arg) metabolizing enzymes, which are responsible for MDSC immunosuppressive potential, within 24 h. The cells' central carbon metabolism, including glycolysis, TCA cycle, pentose-phosphate pathway and glutaminolysis, was also stimulated and led to the increase of the cell specific concentrations in ATP and NADPH. Interestingly, BM-derived MDSCs carried anaerobic glycolysis and exhibited high L-glutamine (L-Gln) uptake rate that resulted in lactate accumulation and supported the synthesis of intermediates of the L-Arg recycling pathway as well as the production of energy-rich shuttles. Exhaustive analysis of nucleotide-derived biomarkers revealed that BM-derived MDSCs were metabolically active during the maturation process, as indicated by a decreasing trend of the ATP-to-ADP ratio with time. Moreover, the AMP-to-ATP ratio, a marker of enhanced glycolysis, continuously increased in time, suggesting a role of the AMP protein kinase (AMPK) in the regulation of energy supply. Therefore, controlling fluxes through the glycolysis and the glutaminolysis may be a promising strategy to inhibit MDSC maturation and recover the anti-tumoral immune response.

3.2.2. Introduction

Tumour growth and progression are critically controlled by alterations in the microenvironment often caused by aberrant expression of tumour-derived soluble factors (TDSFs) (Obermueller, et al., 2004). In addition to their role in stimulating tumour cell proliferation, stromal activation and angiogenesis, TDSFs promote the maturation/recruitment of MDSC population that restrains the tumour-specific functions of $CD8^+$ and $CD4^+$ T lymphocytes (D. I. Gabrilovich et al., 2007). MDSCs have been characterized in tumour-bearing mice by the expression of the surface markers CD11b and Gr-1 (Serafini, et al., 2006). Their immunosuppressive functions are ensured by two enzymes: i) inducible nitric oxide synthase (iNOS) that converts L-Arg to nitric oxide (NO) and L-citrulline, and ii) arginase 1 (ARG1) that metabolizes L-Arg into urea and L-ornithine. The decreased availability of L-Arg and the accumulation of NO derivatives (NO_2^-, NO_3^-, N_2O_3, etc.) are known to trigger the inhibition of both T-cell functions and proliferation, and induce their death (Serafini, et al., 2006).

Several studies have highlighted the role of the hematopoietic factor GM-CSF in the accumulation of MDSCs at the tumor edge, and consequently the impairment of T-cell response to antigens (V. Bronte, et al., 1999; Dolcetti et al., 2010). However, attempts to generate fully competent MDSCs from BM precursors using GM-CSF were unsuccessful. Recently, the combination of GM-CSF and IL-6 was shown to generate a $CD11b^+/Gr\text{-}1^{low}$ population, the most tolerogenic and immunosuppressive sub-population among $CD11b^+/Gr\text{-}1^+$ cells (Dolcetti, et al., 2010). This cell population expressed both iNOS and ARG1, and its genetic signature was shown to be similar to that of tumour-infiltrating MDSCs. The maturation of BM-derived MDSCs is entirely dependent on the C/EBPβ transcription factor (Marigo, et al., 2010). However, to the best of our knowledge, no study has yet been conducted to elucidate the metabolic events that regulate

C/EBPβ activation. Indeed, despite the considerable progress accomplished in the comprehension of MDSC maturation, both *in vivo* and *in vitro*, understanding the immunosuppression phenomenon at the metabolomic level is lacking.

In fact, specific immune functions, including antigen processing and presentation, cytokenesis and activation, are known to be energetically-costly (Buttgereit, et al., 2000) and immune cells, such as lymphocytes and macrophages, modulate their metabolism and respiration to fulfill their energy requirements. The energetic metabolism was thus considered as potential target for immunotherapy. Drugs that affect cell bioenergetics are being used to reduce ATP production, for the treatment of psoriasis, rheumatoid arthritis, cardiac arrhythmia, etc., either by inhibiting reactions related to substrate oxidation or by increasing proton permeability through the mitochondria, in turn resulting in the uncoupling of oxidative phosphorylation (Buttgereit, et al., 2000). Moreover, we have previously shown that MSC-1 cells, an immortalized cell line derived from mouse MDSCs (Apolloni, et al., 2000), adapt their nutritional profile and their respiratory capacity to provide energy and substrates required by their immunosuppressive machinery (Hammami, Chen, Bronte, Decrescenzo, & Jolicoeur, 2011). These findings may thus suggest that these drugs can have indirect benefits on the recovery of the anti-tumor immune response. In the present study, we characterized the metabolic events occurring during the *in vitro* maturation of BM cells into MDSCs by the combination of GM-CSF and IL-6. We found that MDSC maturation is accompanied by an increase of central carbon metabolism and we emphasized the key role of AMPK in the maintenance of metabolically active cells.

3.2.3. Materials and Methods

3.2.3.1. Mice

Six- to eight-week-old male C57Bl/6 mice were purchased from Charles River (Quebec, Canada) and maintained under specific pathogen-free conditions in the animal facilities of the Université de Montréal. Experiments were performed according to state guidelines and approved by local ethics committee.

3.2.3.2. Cell culture

Single cell suspension was prepared from BM of normal mice and cultured in 100-mm Petri dishes (Becton Dickinson, Quebec, Canada) in RPMI1640 medium (Sigma, Ontario, Canada) supplemented with 10% (v/v) irradiated foetal bovine serum (Cedarlane, Ontario, Canada), 1mM Sodium Pyruvate (Sigma), 50 μM β-Mercaptoethanol (Sigma), 100 $U.mL^{-1}$ Penicillin, 150 $U.mL^{-1}$ Streptomycin (Cedarlane) and 2 mM L-glutamine (Cedarlane) , in a 5% CO_2 and 37ºC incubator. MDSCs were derived by treating BM cells with 40 $ng.mL^{-1}$ of GM-CSF and 40 $ng.mL^{-1}$ of IL-6 (both from Cedarlane) for 4 days as described by Marigo *et al* (Marigo, et al., 2010).

Prior to any analysis, cells were detached by a 2mM EDTA solution, rinsed with phosphate buffer saline and centrifuged for 6 min at 250 × *g* and 4°C.

3.2.3.3. Assays

Glucose, lactate, glutamate and glutamine concentrations in supernatants were measured using a dual-channel immobilized oxidase enzyme biochemistry analyzer (2700 SELECT, YSI Inc. Life Sciences, Yellow Springs, OH, USA), using calibration buffers provided by the manufacturer.

Nitric oxide concentrations were respectively assayed by a Nitrate/Nitrite Colorimetric Assay Kit (Cedarlane).

3.2.3.4. Determination of ARG 1 activity

Total BM cells and BM-derived MDSCs were lysed with 50 µL of a lysis buffer containing 0.1% Triton X-100 (Sigma) and 100 µg/mL of pepstatin, antipain and aprotinin (all from EMD BioSciences, San Diego, CA). After 30 minutes in a thermomixer at 37ºC, cells debris were removed by centrifugation at 15,000 × *g* for 20 min and cell lysates were kept in -80ºC prior to analysis. ARG1 activity was quantified in cell lysates by urea determination with α-isonitrosopropiophenone as previously described by Munder *et al* (Munder et al., 1999). One unit (U) of ARG1 activity is defined as the enzyme activity that catalyses the production of 1 mol urea/min.

3.2.3.5. Proliferation assay

The immunosuppressive activity of BM-derived MDSCs was assessed as their ability to inhibit Jurkat cell proliferation (leukemic T-cells, clone E6-1, Cedarlane). Jurkat cells were treated with 5 $\mu g.mL^{-1}$ of Concanavalin A (conA, Sigma) for 2 days prior to the test.

Experiments were performed in 24-well tissue culture plates (VWR, Ontario, Canada) in a final volume of 1 mL. ConA-activated Jurkat cells were inoculated (500 µL at 0.2×10^6 $cells.mL^{-1}$) in MILLICELL®PC 0.4 µm culture plate inserts (Millipore) and added to wells containing 500 µL of BM cell suspension (0.2×10^6 $cells.mL^{-1}$) cultured in the presence of GM-CSF and IL-6 (40 $ng.mL^{-1}$ each) for 0, 24, 48, 72 and 96 h.

Mixed cultures were kept in a 5% CO_2 and 37ºC incubator for 24 h. Jurkat cells were then counted and viability was determined by the Trypan Blue exclusion method.

3.2.3.6. Respirometry test

Respirometry assays were performed as described by Lamboursain *et al* (Lamboursain, St-Onge, & Jolicoeur, 2002). Briefly, 3 mL of a 15×10^6 of BM-derived $MDSCs.mL^{-1}$ suspension were inoculated in a 10-mL borosilicate glass syringe (Sigma) in which the plunger was substituted by an Ingold pO_2 probe (Mettler Toledo, Quebec, Canada). The respirometer was kept at 37°C and magnetically agitated (60 RPM) to ensure the homogeneity of cell suspension. Dissolved oxygen was recorded by an acquisition system (Centris, Longueuil, Canada).

3.2.3.7. Metabolite extraction

The extraction protocol was based on the method developed by Kimball *et al* (Kimball & Rabinowitz, 2006). Briefly, for each sample, 5×10^6 cells were extracted with 400 µL of 80% cold methanol in the presence of 0.2 g of Sand (Sigma). After 10 min on dry ice, the mixture was vortexed and then sonicated in ice and water for 5 min. The samples were then centrifuged for 7 min at 21,000 × *g* and 4ºC to collect supernatants. The pellets were extracted a second and third time as described above with 200 µL of 50% cold methanol and 200 µl of cold water, respectively. Supernatants were mixed and stored in -80 ºC prior to analysis. Extracts were filtered through 0.2 µm filters (Millipore, Ontario, Canada) before analysis.

3.2.3.8. Nucleotide concentrations

Nucleotide analysis was performed on a 1290 UPLC system coupled to a 6460 triple quadruple mass spectrometer (both from Agilent technologies, Quebec, Canada). Nucleotides were separated by a Symmetry C18 column (150*2.1 mm, 3.5 µm) (Waters) equipped with a Security C18 guard-column (Waters, 10*2.1 mm, 3.5 µm) by ion-pair method. DMHA (N,N-dimethylhexylanine, Sigma) was used as ion-pair reagent to improve the signal-to-noise ratio with positive ionization mode. Mobile phase consisted in Buffer A: 10 mM ammonium acetate, 15 mM DMHA at pH 7.0, and Buffer B: 50/50 % (v/v) acetonitrile/20 mM NH_4OAc at pH 7.0. mobile phase flow rate was set at 0.3 mL.min-1 with the following gradient: 0-10 min at 10% B, 10-20 min at linear gradient from 10 to 30% B, 20-21 min at linear gradient from 30 to 60% B, 21-26 min at 60% B, 26-27 min at linear gradient from 60 to 10% B and 27-35 min at 10% B.

3.2.3.9. Organic acid concentrations

Organic acids concentrations were assessed using the above-mentioned UPLC-MS/MS system using a Hypercarb column (100*2.1 mm, 5 µm) and a Hypercarb pre-column (2.1*10, 5 µm) (Thermo Fisher, Ontario, Canada).

Mobile phase consisted in Buffer A: 20 mM ammonium acetate at pH 7.5, and Buffer B: 10 % (v/v) methanol in water. Flow rate was set at 0.3 $mL.min^{-1}$ using the following gradient: 0-5 min at 10% A, 5-10 min at linear gradient from 10 to 20% A, 10-20 min at linear gradient from 20 to 100% A, 20-30 min at 100% A, 30-32 min at linear gradient from 100 to 10% A and 32-40 min at10% A.

3.2.4. Results

3.2.4.1. Effects of GM-CSF and IL-6 on BM-derived MDSC immunosuppressive activity

Although $CD11b^{+}/Gr\text{-}1^{+}$ cells can be detected at sizeable number in BM of healthy mice (Serafini, et al., 2006), BM cells did not show any immunosuppressive potential (Figure 3-1C and D). In fact, the enzymatic activities of both iNOS and ARG1 were extremely low in BM cells as revealed by constant concentration of nitrite and nitrate in the supernatant (62.86 ± 4.25 µM) and constant ARG1 activity at 124.93 ± 3.48 $nU.cell^{-1}$ throughout the culture (Figure 3-1A and B). Moreover, *in vitro* proliferation assays showed that BM cells did not affect Jurkat cell proliferation or viability (Figure 3-1C and D). In stark contrast, treating BM cells with GM-CSF and IL-6 resulted in a marked increase of ARG1 and iNOS activities after 16 h and 24h, respectively. In fact, nitrite and nitrate continuously accumulated at a rate of 6.64 ± 0.09

fmol.cell^{-1}.h^{-1} while ARG1 activity shifted from 122.17 ± 0.65 nU.cell^{-1} at the inoculation to 174.79 ± 3.58 nU.cell^{-1} (at 16 h) and continuously increased until a quasi-stable level of 304.30 ± 4.11 nU.cell^{-1} at 72 h. The accumulation of nitrite and nitrate suggested that L-Arg was permanently present in the medium; otherwise iNOS and ARG1 activities would have been down-regulated and a loss of BM-derived MDSC immunosuppressive activity should have been noticed.

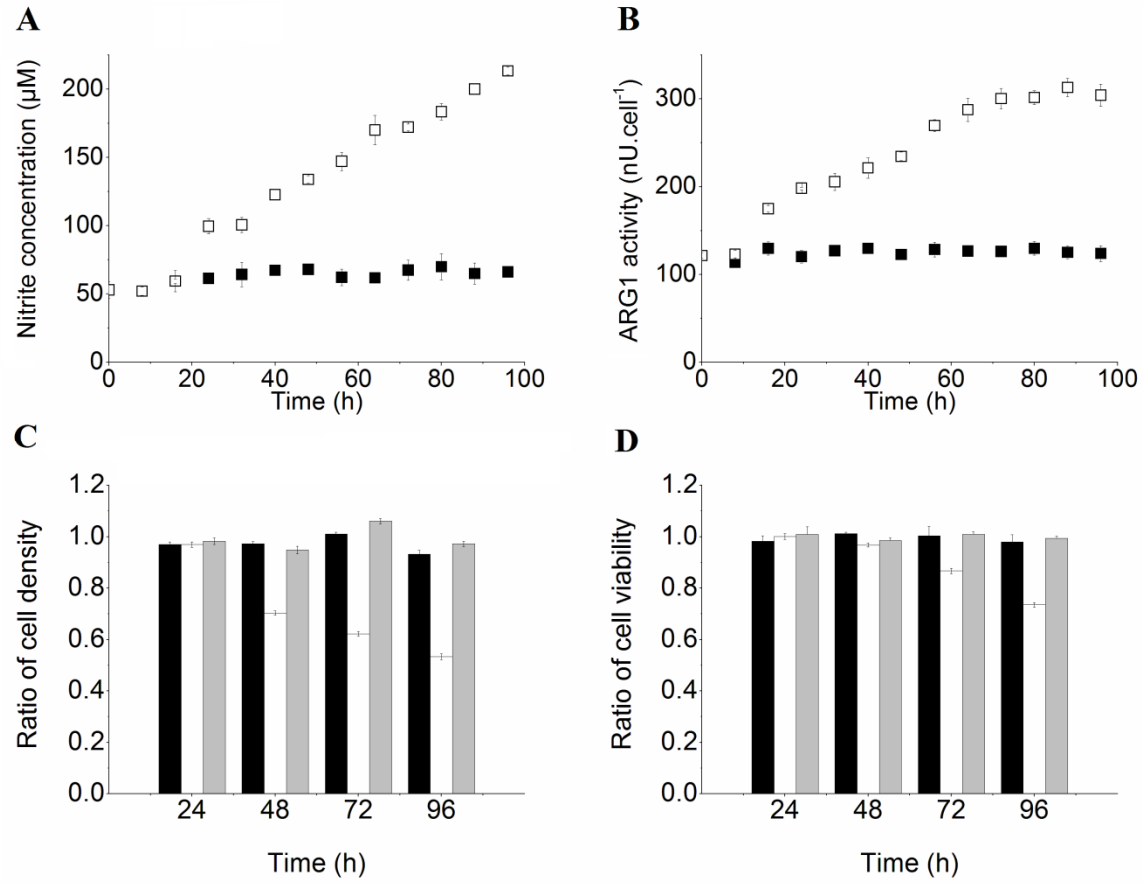

Figure 3-1 : Immunosuppressive activity of BM-derived MDSCs.

In all experiments, BM cells were extracted from 6 to 8-week-old C57Bl/6 mice and cultured for 4 days in the presence of GM-CSF and IL-6 (40 ng.mL^{-1} each, except for the control

cultures). A. Nitrite concentration based on the Griess reaction. B. ARG1 activity, one unit (U) of ARG1 activity is defined as the enzyme activity that catalyses the production of 1 µmol urea.min^{-1}. Filled and empty symbols correspond to BM cell and BM-derived MDSC cultures, respectively. The same nomenclature is used for all figures unless specified. C. and D. are, respectively, ratios (referred to the control culture) of Jurkat cell density and viability. ConA-activated Jurkat cells were cultured for 24 h in the presence of: (Black) untreated BM cells, (White) BM cells exposed to GM-CSF and IL-6 for 24, 48, 72 or 96 h and (Grey) cytokines.

The abilities of BM-derived MDSCs to inhibit Jurkat cell proliferation and to decrease their viability were respectively detected after 24 and 48 h of treatment (Figure 3-1C and D). This delay was most likely due to the increase of MDSC proportion in the cytokine-treated BM cell suspension since BM cells were not synchronized prior to GM-CSF and IL-6 addition. More specifically, after 96 h of treatment, BM-derived MDSCs decreased Jurkat cell density and viability by 46.6 ± 1.07 and 26.47 ± 0.89 %, respectively. Culturing Jurkat cells in the presence of GM-CSF and IL-6 did not affect cell proliferation nor viability (Figure 3-1C and D), suggesting that the effects observed in the treated-BM and Jurkat cell mixed culture were due to the maturation of BM-derived MDSCs and not to cytokine-related cytotoxic effects.

3.2.4.2. Nutritional profile of BM-derived MDSCs

BM-derived MDSCs exhibited a low specific growth rate of 0.13 ± 0.02 d^{-1} from 32 h, whereas no cell growth was detected in the untreated BM cell culture (control culture) although cells stayed viable throughout the culture. BM-derived MDSCs consumed glucose at a high rate of 0.243 ± 0.008 pmol.cell^{-1}.h^{-1} from 24 h whereas the control culture only scarcely consumed

glucose during the first 72 h and then started to consume it at a rate of 0.278 ± 0.013 pmol.cell^{-1}.h^{-1} (Figure 3-2A). The increase of glucose uptake was accompanied by the accumulation of glycolysis and PPP intermediates from 32 h. That is, the cell specific concentration in glucose-6-phosphate (G-6-P) and fructose-6-phosphate (F-6-P) increased, respectively, at rates of 5.173 ± 0.084 and 3.573 ± 0.005 10^{-3} fmol.cell^{-1}.h^{-1} (Figure 3-2B).

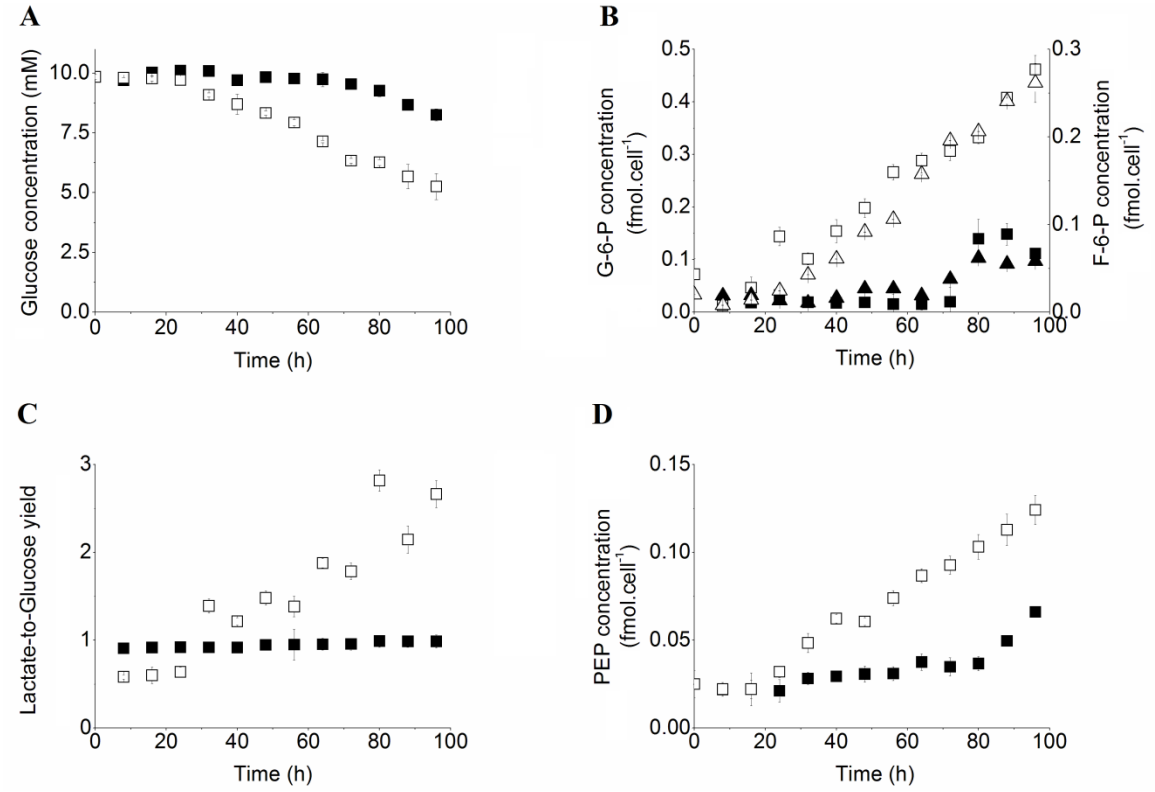

Figure 3-2 : GM-CSF and IL-6 modulate BM-derived MDSC glucose metabolism.

A. Glucose concentration in the supernatant. B. Cell specific concentrations in G-6-P (square) and F-6-P (triangle). C. Lactate-to-glucose yield. D. Cell specific PEP concentration. Cells were extracted using cold methanol and organic acids were analyzed using a UPLC-MS/MS system.

Also, the cell specific concentration in phosphoenolpyruvate (PEP), a PPP intermediate, was 3 to 5-fold lower than those of G-6-P and F-6-P and was accumulated at a lower rate (1.161 ± 0.073 10^{-3} fmol.cell^{-1}.h^{-1}) compared to that of G-6-P and F-6-P (Figure 3-2C). The increase of cell specific concentration in glycolysis and PPP intermediates, in the BM cell culture, coincided with the increase of glucose consumption rate (72 h) (Figure 3-2B and C).

Moreover, the enhanced glucose uptake was accompanied by a decrease of cell respiration. Indeed, the specific oxygen consumption rate decreased from 103.42 ± 6.14 fmol.cell^{-1}.h^{-1} at 24 h to 41.88 ± 3.62 fmol.cell^{-1}.h^{-1} at 96 h (data not shown), suggesting that BM cells switched from respiratory to glycolytic metabolism as MDSC maturation progressed. The lactate-to-glucose yield, in the GM-CSF and IL-6 -treated BM cell culture, was quasi-stable at 0.61 ± 0.02 for the first 24 h and then rapidly increased to 1.39 ± 0.04 at 32 h and reached values higher than 2 after 80 h (Figure 3-2D), suggesting that another source of carbon contributed to the accumulation of lactate. Conversely, the lactate-to-glucose yield of the BM cell culture was almost stable at 0.95 ± 0.02 (Figure 3-2D).

Furthermore, BM-derived MDSCs consumed L-Gln at a higher rate (0.040 ± 0.002 pmol.cell^{-1}.h^{-1}) than that reported in the control culture (0.021 ± 0.005 pmol.cell^{-1}.h^{-1}) (Figure 3-3A). The stimulation of glycolysis, PPP and glutaminolysis resulted in an increase of the cell content in TCA cycle intermediates (Figure 3-5). Particularly, α-ketoglutarate (α-KG), which can be derived from either isocitrate or L-Gln, was accumulated at a rate of 5.873 ± 0.005 10^{-3} fmol.cell^{-1}.h^{-1} (Figure 3-3B). Similarly, the cell specific concentration of fumarate, a by-product of the conversion of argininosuccinate into L-Arg, increased at a rate of 20.378 ± 0.005 10^{-3} fmol.cell^{-1}.h^{-1} after 24 h (Figure 3-3B), strongly suggesting that the maturation of BM cells into MDSCs was accompanied by the activation of L-Arg recycling pathways. Moreover, the examination of cell specific concentrations in both sources of pyruvate, i.e. malate, which is

derived from fumarate, and PEP, indicated that malate was 5-time more concentrated than PEP (Figure 3-2C and D).

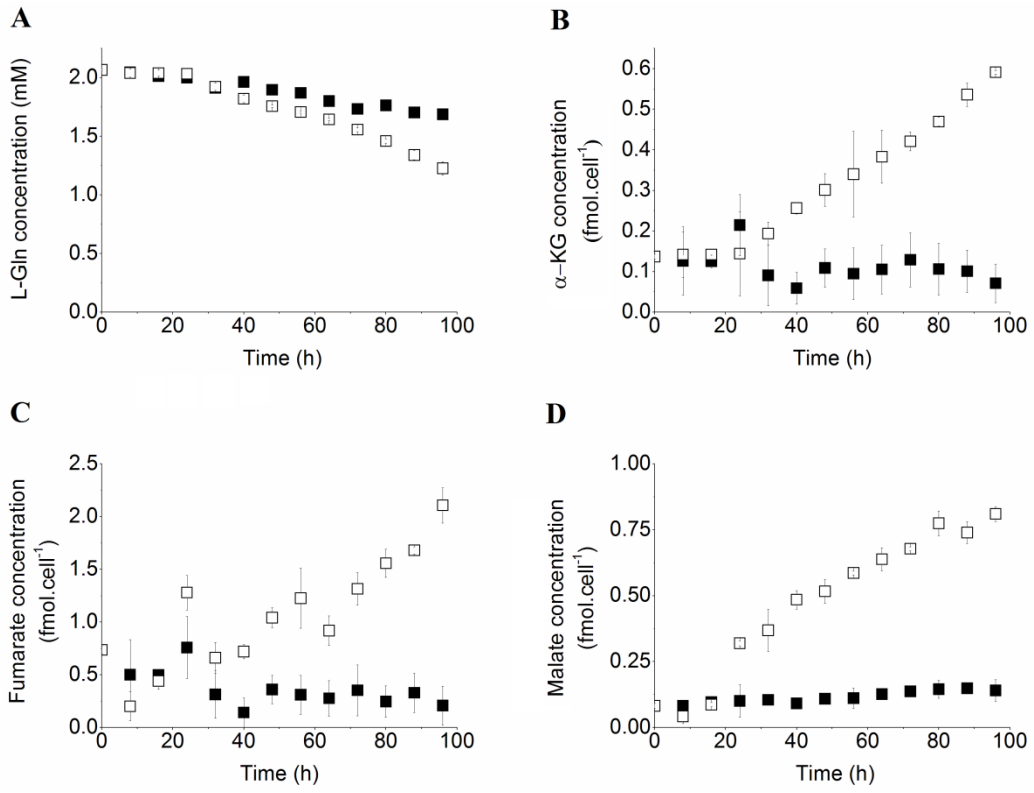

Figure 3-3 : Enhancement of glutaminolysis and TCA cycle during MDSC maturation process.

A. L-Gln concentration in supernatant. B., C. and D. correspond to cell specific concentration in α- KG, fumarate and malate, respectively.

3.2.4.3. Bioenergetics of BM-derived MDSCs

Consistent with the stimulation of the central carbon metabolism during the maturation process, BM-derived MDSC bioenergetic state was up-regulated. In fact, the intracellular pools in purines (GTP+ATP+ADP+AMP), which represent energy-related nucleotides, and pyrimidines (CTP+UTP+UDPGNAc), which are involved in various anabolic reactions and growth-related metabolic processes (Atkinson, 1977; McMurray-Beaulieu, Hisiger, Durand, Perrier, & Jolicoeur, 2009), increased at respective rates of 0.030 ± 0.007 and 0.014 ± 0.002 fmol.cell^{-1}.h^{-1} after 24 h of treatment (Figure 3-4A).

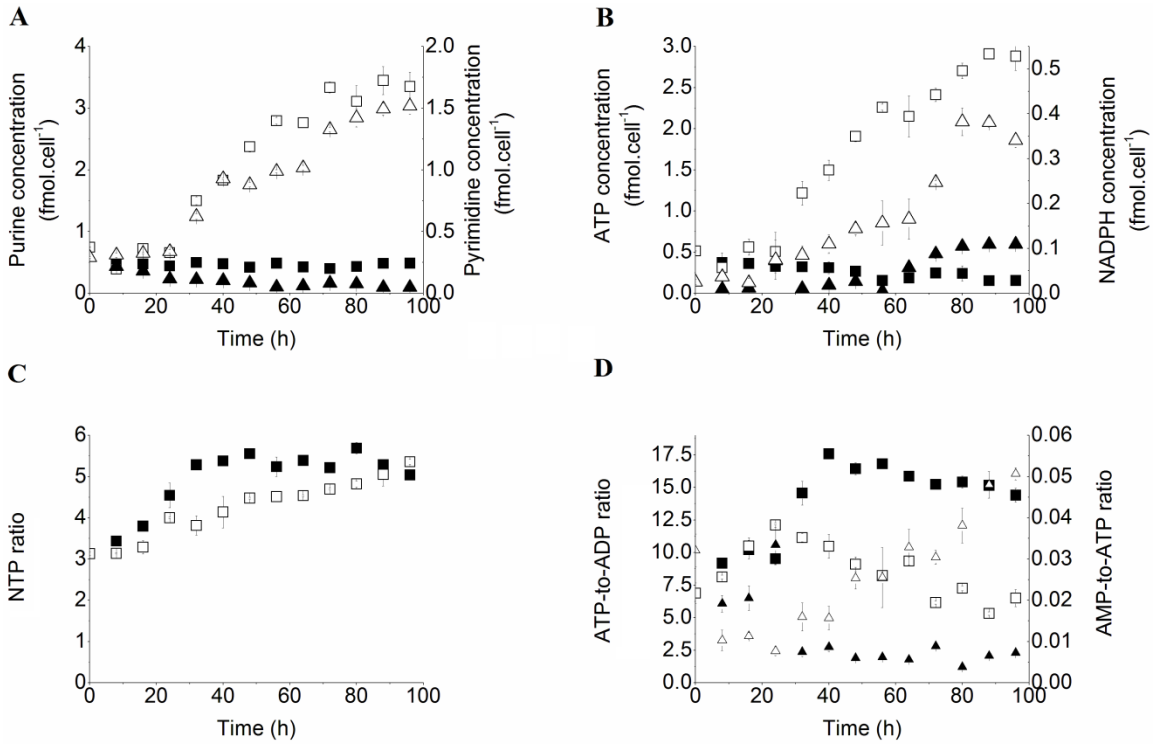

Figure 3-4 : Bioenergetic of BM-derived MDSCs.

A. Specific cell concentration in purines (GTP+ATP+ADP+AMP, square) and pyrimidines (CTP+UTP+UDPGNAc, triangle). B. Specific cell concentration in ATP (square) and NADPH (triangle). Nucleotide-derived behavioural markers: C. NTP ratio (ATP+GTP)/(UTP+CTP). D. ATP-to-ADP (square) and AMP-to-ATP (triangle) ratios.

The BM-derived MDSC energetic pool was mainly constituted of purines (60 to 70 %), an expected result at low specific growth rate. Conversely, the purine pool was quasi-stable at 0.46 ± 0.03 fmol.cell^{-1} in the control culture, and pyrimidines even showed a decreasing tendency due to cell quiescence (Figure 3-4A). Particularly, ATP was accumulated at a rate of 26.398 ± 2.789 10^{-3} fmol.cell^{-1}.h^{-1} from 24 h. The enhanced activity of the TCA cycle may thus have indirectly contributed to the production of ATP since the glycolytic metabolism has a low energy yield. Furthermore, the cell specific concentration in NADPH increased at a rate of 1.68 ± 0.04 10^{-3} fmol.cell^{-1}.h^{-1} between 24 and 64 h (Figure 3-4B). The rate of NADPH accumulation shifted rapidly to 9.72 ± 0.02 10^{-3} fmol.cell^{-1}.h^{-1} between 64 and 80 h. In addition to the role of the oxidative phase of PPP in the NADPH production, the malic enzyme produces considerable amounts of NADPH jointly with pyruvate. ATP and NADPH production rates were thus both higher than the demands of the maturation process and the resulting immunosuppressive machinery. The cell specific NADPH concentration slightly decreased from 0.382 ± 0.031 fmol.cell^{-1} at 80 h to 0.0341 ± 0.016 fmol.cell^{-1} at the end of the culture, suggesting either higher demand from NADPH-requiring processes or down-regulation of NADPH production.

Exhaustive study of nucleotide-derived biomarkers showed that cell metabolic activity increased as the MDSC maturation progressed. In fact, treating BM cells with GM-CSF and IL-6 increased the NTP ratio, defined as ([ATP]+[GTP])/([UTP]+[CTP]), which is the ratio of energetic nucleotides to anabolism-related nucleotides (McMurray-Beaulieu, et al., 2009), from

3.14 ± 0.07 (during the first 24 h) to 5.36 ± 0.06 at the end of the culture (96 h) (Figure 3-4C). An increase of the NTP ratio normally marks the deterioration of cell metabolic activity if the cell growth process was active. In our case, the rates of ATP (Figure 3-4B) and GTP (data not shown) accumulation were higher than those of CTP and UTP (data not shown), indicating that BM-derived MDSCs were catabolically active. Nevertheless, the NTP ratio of the control culture increased rapidly after cell inoculation and reached a plateau (5.34 ± 0.014) from 32 h. This increase is mostly due to the decrease of pyrimidines in cell pool.

Although the cell specific ATP concentration increased along the culture, ATP was continuously depleted from the intracellular pool during the maturation process as revealed by the decreasing trend of the ATP-to-ADP ratio, a marker of respiration and energy consumption (Reich & Sel'Kov, 1981) (Figure 3-4D). Indeed, the ATP-to-ADP ratio in the BM-derived MDSC culture was 2 to 3-times lower than that of the control culture, and decreased at a specific rate of 0.058 ± 0.002 h^{-1}. On the other hand, the AMP-to-ATP ratio, which is considered as a marker of glycolysis stimulation and regulator of the AMPK activity (Cidad, Almeida, & Bolanos, 2004), shifted after 24 h and was considerably higher than that of the control culture, indicating sustained ATP production.

3.2.5. Discussion

The tolerogenic and immunosuppressive environment created by tumors depends on the transcription factor C/EBPβ (Marigo, et al., 2010). Since tumor-infiltrating MDSCs have the highest immunosuppressive potential among the different MDSC sub-populations (Dolcetti, et al., 2010), we have simulated, *in vitro*, the maturation of BM precursors into MDSCs using a combination of GM-CSF and IL-6. The understanding of the immunosuppression phenomenon at

the metabolome level may have great outcomes on the identification of new immunotherapy targets. Complementary to work conducted by Marigo and colleagues, where the BM-derived MDSCs were harvested after 96 h of treatment for further analysis (Marigo, et al., 2010), we have continuously monitored (every 8 h) the progression of MDSC maturation.

Exposure of BM cells to GM-CSF and IL-6 triggered a continuous up-regulation of iNOS and ARG1 activities after 24 and 16 h, respectively (Figure 3-1A and B). This delayed effects can be attributed to cytokine internalization and to the activation of the C/EBPβ transcription factor (Marigo, et al., 2010) and other signalling pathways (JAK/STAT3, MAPK and PI3-K) that were shown to regulate expression and activation of L-Arg metabolizing enzymes (Fleetwood, et al., 2005). The immunosuppressive potential of BM-derived MDSCs increased, as revealed by the progressive decrease of Jurkat cell density and viability concomitantly with the duration of BM cell exposure to cytokines (Figure 3-1C and D).

The activation of iNOS and ARG1 was accompanied by the up-regulation of glucose uptake (Figure 3-2A) and glycolysis (Figure 3-5), as shown by the AMP-to-ATP ratio, which was up to 5-fold higher than that observed in the control culture (Figure 3-4D), and by the accumulation of G-6-P and F-6-P (Figure 3-2B). This accumulation may suggest that cells continue producing these intermediates without consuming them, a behavior that has previously been associated to the initiation of cell death (McMurray-Beaulieu, et al., 2009). However, cells were viable and grew throughout the culture. They also produced L-Arg and lactate, suggesting that cells consumed these intermediates to support both the catabolic processes and the sparse synthesis of anabolism-related macromolecules. Thus, the accumulation is due to a higher rate of production compared to that of consumption.

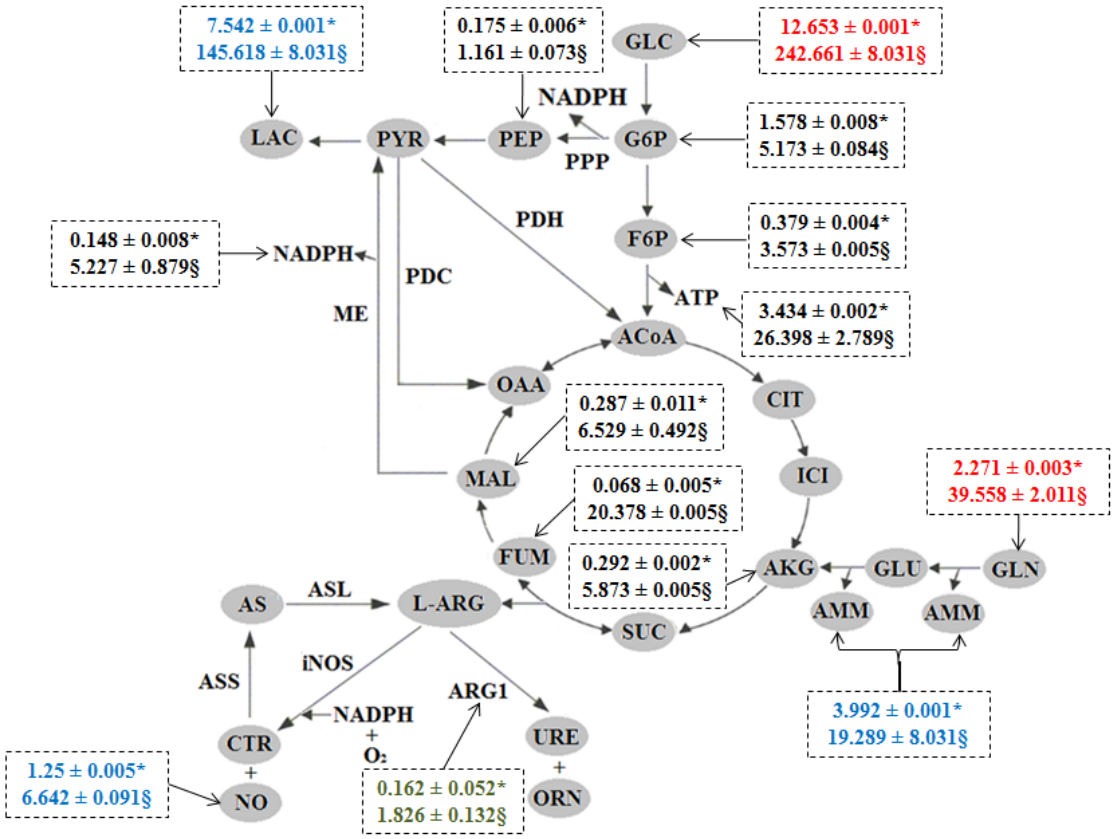

Figure 3-5 : Metabolic map of the BM-derived MDSCs.

Nutrient consumption rates (in mol.cell^{-1}.h^{-1}, red), metabolite production rates (in pmol.cell^{-1}.h^{-1} for lactate and ammonia and in fmol.cell^{-1}.h^{-1} for NO, blue), intracellular metabolite accumulation rates (in 10^{-3} fmol.cell^{-1}.h^{-1}, black) and increase rate of ARG1 activity in nU.cell^{-1}.h^{-1} (green). Values marked with * and § corresponds respectively to the following culture periods: from 0 to 24 h and from 32 to 96 h.

Concurrently, PPP was also stimulated, as revealed by the increase of cell specific PEP concentration (Figure 3-2D). Differences between cell specific concentrations in glycolysis and PPP intermediates suggest that glucose is mainly processed through glycolysis (Figure 3-2B and

D). This may be a consequence of the low specific growth rate exhibited by BM-derived MDSCs, which may have limited fluxes of the non-oxidative reactions of the PPP. These results are in agreement with previous work of Ando and colleagues where IL-6 was shown to enhance the expression of the glycolytic enzymes hexokinase 2 and 6-phosphofructo-2-kinase/fructose-2,6-biphosphatase-3 of mouse embryonic fibroblasts via the IL-6/STAT3 pathway (Ando et al., 2010). Similarly, GM-CSF has been reported to promote rapid glucose transport in *Xenopus oocytes* via the PI3-K pathway (Dhar-Mascareno, Chen, Zhang, Carcamo, & Golde, 2003). Moreover, we have recently shown that the inhibition of the L-Arg metabolizing enzymes, i.e. iNOS and ARG1, in MSC-1 cells is accompanied by the down-regulation of glucose uptake and overall glycolysis activity (Hammami, et al., 2011).

In addition to the stimulation of glycolysis and oxidative phase of PPP, L-Gln uptake was also increased in the presence of GM-CSF and IL-6 (Figure 3-3A). These pathways feed the TCA cycle with specific intermediates, thus ensuring the enhancement of its activity (Figure 3-3B, C and D and Figure 3-5). Particularly, accumulation of fumarate suggests that L-Arg is continuously synthesized and supports a permanent immunosuppressive activity (Figure 3-3C and Figure 3-1). Furthermore, the enhanced activity of the TCA cycle resulted in the accumulation of high levels of malate when compared to PEP (Figure 3-2D and Figure 3-3D), which are both precursors of pyruvate. This could suggest that the TCA cycle contributes to lactate accumulation since the lactate production -to- glucose consumption rates reached values higher than 2 (Figure 3-2D). In fact, BM-derived MDSCs carry anaerobic glycolysis despite non-limiting oxygen conditions, a typical behavior of tumor cells that produce lactate rather than high energy yield from respiration. This phenomenon results in the acidification of the tumoural microenvironment, a condition known to promote tumor progression and metastasis (Gatenby & Gillies, 2004). On that note, our results thus agree with recent findings showing that MDSCs

express the hypoxia-induction factor-1 α to adapt to quasi-hypoxic conditions encountered in tumors (Corzo et al., 2010). Similarly, previous work by Wada and coworkers has also revealed that GM-CSF triggers a rapid glucose-dependent extracellular acidification that is regulated by the protein kinase C and the sodium/proton antiporter (Wada et al., 1993). Moreover, iNOS activity has also been associated to an increased glucose consumption rate, increased glycolysis and PPP and the inhibition of oxidative phosphorylation in zymozan-treated macrophages (Albina & Mastrofrancesco, 1993).

Interestingly, although BM-derived MDSCs carry glycolytic metabolism, which is known for its low energy yield, the specific cell concentration in ATP was observed to increase gradually during the maturation process (Figure 3-4B). However, the decreasing trend of the ATP-to-ADP ratio suggests that ATP was continuously depleted from the intracellular pool (Figure 3-4D). This may be due to ATP consumption, and so ADP formation, or ADP production from AMP. Nevertheless, the production of ADP from AMP, via the enzymatic activity of adenylate kinase, requires ATP. Thus, the decrease of the ATP-to-ADP ratio is mainly due to ATP consumption. The enhanced AMPK activity, as deduced from the continuous increase of the AMP-to-ATP ratio (Figure 3-4D), is most likely responsible for the up-regulation of ATP-producing processes. Thus, BM-derived MDSCs may produce ATP at a higher rate than that required by the maturation process and other biochemical reactions. Indeed, AMPK is considered as an energy sensor in several metabolic disorders, such as cancer and diabetes, in which the enzyme switches cellular metabolism from anabolic to catabolic mode to react to cellular energy deficit (Hardie, 2011). In our case, anabolic processes were not considered to be highly active, according to the low specific growth rate observed in the BM-derived MDSC culture. The AMPK sensor may thus have been activated in response to the insufficient energy level associated to the anaerobic metabolism, and to ensure supplement energy supply required by the

maturation process and the immunosuppression machinery. Several studies have investigated the effect of IL-6 on cells' bioenergetics. In rat skeletal muscle cells, IL-6 was shown to up-regulate AMPK activity, and the IL-6-induced STAT3 was reported to be localized in mitochondria, resulting in an enhanced oxidative phosphorylation and consequently an increase of cell ATP level (Kelly, Gauthier, Saha, & Ruderman, 2009; Wegrzyn et al., 2009). However, we observed that BM-derived MDSC respiration decreased in the presence of GM-CSF and IL-6, although AMPK activity was stimulated. Therefore, conversely to muscle cells, our results suggest that AMPK in BM-derived MDSCs activates other energy-producing processes than respiration, probably via the TCA cycle. Further investigation is however required to verify whether AMPK inhibition may have beneficial effects on re-establishing the anti-tumour immunosurveillance response by altering the bioenergetic-related maturation process.

Moreover, the two principal NADPH producing pathways in mammalian cells, i.e. glutaminolysis and PPP, were stimulated in the presence of GM-CSF and IL-6. In fact, since the non-oxidative phase of PPP is devoted to anabolic processes and that BM-derived MDSCs exhibited a low growth rate, the conversion of glucose-6-phosphate into fructose-6-phosphate was probably preferred to the production of 6-phosphogluconolactone, the first PPP intermediate. However, NADPH was probably mostly derived from glutaminolysis, particularly via the malic enzyme, since fluxes through this pathway were considerably higher than those through the PPP (Figure 3-2D and Figure 3-3D), although the oxidative phase of the latter was shown to be stimulated. In fact, since BM-derived MDSCs exhibited low specific growth rate *in vitro*, the oxidative phase, which is responsible for NADPH production, was probably more active than the non-oxidative one, which is related to anabolic processes, resulting in the recycling of PPP intermediates into glycolysis. We have also observed in previous works that MSC-1 cells

cultured in the absence of L-Gln are characterized by a drastic decrease of cell specific NADPH concentration (75 % less) and of lactate level (50% less) (Hammami, et al., 2011).

Altogether, the present study suggests that the alteration of myelopoesis, and so MDSC maturation, may depend on an enhanced central carbon metabolism and the up-regulation of BM cell bioenergetic state (Figure 3-5). Furthermore, our results on nucleotide-derived behavioral biomarkers and on the distribution of TCA cycle intermediates unambiguously indicate that AMPK and malic enzyme are involved in the GM-CSF and IL-6 –induced stimulation of glycolysis and glutaminolysis, respectively. Moreover, mature MDSCs carry anaerobic glycolysis and partially oxidize L-Gln to ensure favorable conditions for tumor progression as do tumor cells. These results may thus have clinical relevance since the control of metabolic fluxes through glycolysis and glutaminolysis could potentially impair MDSC maturation, and indirectly help for recovering the anti-tumoral immune response.

3.2.6. References

1. Obermueller E, Vosseler S, Fusenig NE, Mueller MM. Cooperative autocrine and paracrine functions of granulocyte colony-stimulating factor and granulocyte-macrophage colony-stimulating factor in the progression of skin carcinoma cells. Cancer Res. 2004;64:7801-12.

2. Gabrilovich DI, Bronte V, Chen SH, Colombo MP, Ochoa A, Ostrand-Rosenberg S, et al. The terminology issue for myeloid-derived suppressor cells. Cancer Res. 2007;67:425; author reply 6.

3. Serafini, Borrello I, Bronte V. Myeloid suppressor cells in cancer: Recruitment, phenotype, properties, and mechanisms of immune suppression. Semin Cancer Biol. 2006;16:53-65.

4. Bronte V, Chappell DB, Apolloni E, Cabrelle A, Wang M, Hwu P, et al. Unopposed production of granulocyte-macrophage colony-stimulating factor by tumors inhibits CD8+ T cell responses by dysregulating antigen-presenting cell maturation. J Immunol. 1999;162:5728-37.

5. Dolcetti L, Peranzoni E, Ugel S, Marigo I, Fernandez Gomez A, Mesa C, et al. Hierarchy of immunosuppressive strength among myeloid-derived suppressor cell subsets is determined by GM-CSF. Eur J Immunol. 2010;40:22-35.

6. Marigo I, Bosio E, Solito S, Mesa C, Fernandez A, Dolcetti L, et al. Tumor-induced tolerance and immune suppression depend on the C/EBPbeta transcription factor. Immunity. 2010;32:790-802.

7. Buttgereit F, Burmester GR, Brand MD. Bioenergetics of immune functions: fundamental and therapeutic aspects. Immunol Today. 2000;21:192-9.

8. Apolloni E, Bronte V, Mazzoni A, Serafini P, Cabrelle A, Segal DM, et al. Immortalized myeloid suppressor cells trigger apoptosis in antigen-activated T lymphocytes. J of Immunol. 2000;165:6723-30.

9. Hammami I, Chen J, Bronte V, Decrescenzo G, Jolicoeur M. Immunosuppression mediated by myeloid-derived suppressor cells is energetically costly. Submitted Paper. 2011.

10. Munder M, Eichmann K, Moran JM, Centeno F, Soler G, Modolell M. Th1/Th2-regulated expression of arginase isoforms in murine macrophages and dendritic cells. J Immunol. 1999;163:3771-7.

11. Lamboursain L, St-Onge F, Jolicoeur M. A lab-respirometer forplant and animal cell culture. Biotechnol Progr. 2002;18:1377-86.

12. Kimball E, Rabinowitz JD. Identifying decomposition products in extracts of cellular metabolites. Anal Biochem. 2006;358:273-80.

13. Atkinson DE. Cellular Energy Metabolism and its Regulation. USA; 1977.

14. McMurray-Beaulieu V, Hisiger S, Durand C, Perrier M, Jolicoeur M. Na-butyrate sustains energetic states of metabolism and t-PA productivity of CHO cells. J Biosci Bioeng. 2009;108:160-7.

15. Reich JG, Sel'Kov EE. Energy metabolism of the cell - a theoritical treatise. London; 1981.

16. Cidad P, Almeida A, Bolanos JP. Inhibition of mitochondrial respiration by nitric oxide rapidly stimulates cytoprotective GLUT3-mediated glucose uptake through 5'-AMP-activated protein kinase. Biochem J. 2004;384:629-36.

17. Fleetwood AJ, Cook AD, Hamilton JA. Functions of granulocyte-macrophage colony-stimulating factor. Crit Rev Immunol. 2005;25:405-28.

18. Ando M, Uehara I, Kogure K, Asano Y, Nakajima W, Abe Y, et al. Interleukin 6 enhances glycolysis through expression of the glycolytic enzymes hexokinase 2 and 6-phosphofructo-2-kinase/fructose-2,6-bisphosphatase-3. J Nippon Med Sch. 2010;77:97-105.

19. Dhar-Mascareno M, Chen J, Zhang RH, Carcamo JM, Golde DW. Granulocyte-macrophage colony-stimulating factor signals for increased glucose transport via phosphatidylinositol 3-kinase- and hydrogen peroxide-dependent mechanisms. J Biol Chem. 2003;278:11107-14.

20. Gatenby RA, Gillies RJ. Why do cancers have high aerobic glycolysis? Nat Rev Cancer. 2004;4:891-9.

21. Corzo CA, Condamine T, Lu L, Cotter MJ, Youn JI, Cheng P, et al. HIF-1alpha regulates function and differentiation of myeloid-derived suppressor cells in the tumor microenvironment. J Exp Med. 2010;207:2439-53.

22. Wada HG, Indelicato SR, Meyer L, Kitamura T, Miyajima A, Kirk G, et al. GM-CSF triggers a rapid, glucose dependent extracellular acidification by TF-1 cells: evidence for sodium/proton antiporter and PKC mediated activation of acid production. J Cell Physiol. 1993;154:129-38.

23. Albina JE, Mastrofrancesco B. Modulation of glucose metabolism in macrophages by products of nitric oxide synthase. Am J Physiol. 1993;264:C1594-9.

24. Hardie DG. AMP-activated protein kinase: a cellular energy sensor with a key role in metabolic disorders and in cancer. Biochem Soc Trans. 2011;39:1-13.

25. Kelly M, Gauthier MS, Saha AK, Ruderman NB. Activation of AMP-activated protein kinase by interleukin-6 in rat skeletal muscle: association with changes in cAMP, energy state, and endogenous fuel mobilization. Diabetes. 2009;58:1953-60.

26. Wegrzyn J, Potla R, Chwae YJ, Sepuri NB, Zhang Q, Koeck T, et al. Function of mitochondrial Stat3 in cellular respiration. Science. 2009;323:793-7.

CHAPITRE 4. LES CELLULES MYÉLOIDES SUPPRESSIVES EXHIBENT DEUX ÉTATS BIOÉNERGÉTIQUES STATIONNAIRES *IN VITRO*

4.1. Présentation de l'article

Cette section reprend l'article intitulé "**Myeloid-derived suppressor cells exhibit two bioenergetic steady-states in vitro**". Ce travail a fait l'objet d'une publication dans "Journal of Biotechnology" en Janvier 2011 (Vol 152, No 1-2, p43-48).

Dans cet article, MSC-1, une lignée immortalisée dérivée de MDSC murine, a été utilisée comme système modèle pour caractériser leur ligne de base énergétique afin de différencier les effets de la progression de la croissance cellulaire de ceux des stimuli qui seront utilisés dans des travaux ultérieurs. Dans ce travail, un petit bioréacteur à perfusion a été adapté pour la culture des cellules mammifères afin de permettre le suivi en ligne du métabolisme énergétique par la résonance magnétique nucléaire ^{31}P (^{31}P-NMR). Pour ce faire, les cellules MSC-1 sont immobilisées sur un support de polyéthylène téréphtalate et le comportement des cellules adhérées à ce support a été comparé à celui des cellules cultivées en Petri. Le suivi en ligne du métabolisme des cellules MSC-1 viables par la ^{31}P-NMR ont été combinées à des mesures de concentrations de nucléotides dans des extraits acides pour décrire deux états énergétiques stationnaires correspondant aux phases de croissance exponentielle et stationnaire.

4.2. Myeloid-derived suppressor cells exhibit two bioenergetic steady-states in vitro

Ines Hammami[1], Jingkui Chen[1], Vincenzo Bronte[2], Gregory De Crescenzo[1], Mario Jolicoeur[1*]

[1]Department of Chemical Engineering. École Polytechnique de Montréal. Montreal, Quebec, Canada.

[2]Department of Pathology. Immunology Section. Verona University. Verona, Veneto, Italy.

* Corresponding author:

Mario Jolicoeur

PO 6079 Station Centre-Ville

Montreal, Qc, Canada H3C 3A7

Tel: +1 514 340 4711 ext. 4525

Fax: +1 514 340 4159

e-mail: mario.jolicoeur@polymtl.ca

4.2.1. Abstract

Growing tumours have acquired several mechanisms to resist to immune recognition. Among these strategies, myeloid-derived suppressor cells (MDSCs) contribute to tumour escape by suppressing T-cell specific anti-tumoural functions. The development of therapies that could specifically inhibit MDSC maturation, recruitment, accumulation and immunosuppressive functions is thus of great interest. This requires the identification of valuable biomarkers of MDSC behaviour *in vitro*. As for immune cells, whose energetic state is known as a biomarker of their functionality, we have characterized *in vitro* the metabolic and energetic behaviour of MSC-1 cells, an immortalized cell line derived from mouse MDSCs and used as model cell line.

Combined results from *in vitro* ^{31}P-NMR with living cells and HPLC-MS analyses from cell extracts allowed to identify two distinct bioenergetic steady-states that coincided with exponential and stationary growth phases. While the adenylate energy charge remained constant throughout the culture duration, both the percentage of total pyrimidines, the UTP-to-ATP and PME (phosphomonoesters)-to-NTP ratios were higher at the exponential growth phase compared to the plateau phase, suggesting metabolically active cells and the production of growth-related molecules. Conversely, the NTP ratio increased at the entry of the stationary phase revealing the deterioration of the global bioenergetic status and the arrest of anabolic processes.

4.2.2. Introduction

Tumors use various immunosuppressive strategies that down-regulate immune responses and thus limit the efficiency of anti-cancer therapies (Rabinovich, Gabrilovich, & Sotomayor, 2007). In this context, tumor-bearing hosts express a $CD11b^{+}/Gr\text{-}1^{+}$ heterogeneous cell population (including macrophages, granulocytes and dendritic cells) that has been named myeloid-derived suppressor cells (MDSCs) (D. I. Gabrilovich, et al., 2007). These cells metabolize L-arginine (L-arg) via the enzymatic activities of: i) the inducible nitric oxide synthase (iNOS) that leads to nitric oxide (NO) and L-citrulline production, and ii) arginase 1 (ARG1) that converts L-arg into urea and L-ornithine. The sparse availability of L-arg and the accumulation of NO derivatives are known to trigger the inhibition of both T-cell functions and proliferation, and induce their apoptosis (Serafini, et al., 2006). However, despite considerable progress accomplished in the comprehension of MDSC biology and functions, the metabolic events that occur in the tumor microenvironment during MDSC maturation and recruitment are still misunderstood.

Moreover, several studies have focused on the relationship between the energetic metabolism and the adaptive and innate immune systems (Buttgereit, et al., 2000). Particularly, the modulation of the bioenergetic status of immune effector cells in different situations of immune challenge (cancer, sepsis, etc.) has been extensively reported in the literature (Segerstrom, 2007). However, there is a lack of understanding on MDSC nutritional and energetic requirements that support the metabolism of L-arg and so the maintenance of their immunosuppressive potential. Indeed, the activity of iNOS and ARG1 and also enzymes responsible for the endogenous production of L-arg (argininosuccinate synthetase and lyase) are related to several other enzymes and pathways that can be directly or indirectly energy-requiring.

Therefore, it is of interest to elucidate how MDSCs regulate their nutritional and energetic behaviour to ensure the functionality of the immunosuppression-implicated machinery. We thus present an *in vitro* study on the characterization of the energetic behavior of MSC-1 cells, a MDSC-like immortalized cell line which constitutively expresses iNOS and ARG1 (Apolloni, et al., 2000). Briefly, two culture platforms were used: standard Petri dish and a small-scale perfusion bioreactor modified from Gmati et al (2004) to perform *in vivo* ^{31}P-NMR. For the latter, MSC-1 cells were immobilized on a biocompatible polyethylene terephthalate (PET) mesh (Ramires, Mirenghi, Romano, Palumbo, & Nicolardi, 2000; Rosch et al., 2003) to ensure their retention in the NMR probe reading zone.

The experimental platform used herein, i.e. HPLC-MS measurements on acidic extracts and ^{31}P-NMR monitoring of viable cells, allowed for the description, by means of behavioural biomarkers, of two distinct bioenergetic steady-states that coincided with the exponential and stationary growth phases. Considering the potential role of energetic metabolism in the MDSC immunomodulatory functions, these findings represent the baseline for further studies focussing on MSC-1 cell inhibition or stimulation with the ultimate aim of better understanding and control the immunosuppression phenomenon.

4.2.3. Methods

4.2.3.1. Cell culture and immobilization

MSC-1 cells were grown in RPMI1640 medium (Sigma-Aldrich, Ontario, Canada) supplemented with 2 mM L-glutamine (Cedarlane, Ontario, Canada), 1mM Sodium Pyruvate (Sigma), 100 $U.mL^{-1}$ Penicillin, 150 $U.mL^{-1}$ Streptomycin (Cedarlane) and 10 % (v/v) FBS (Cedarlane) in a 5 % CO_2 and 37 ºC incubator. Cells were immobilized on 1 cm^2 steam-sterilized PET meshes - thickness of 1 mm and a pore size of 175 µm (Texel. Inc., Quebec, Canada).

4.2.3.2. Cell density and viability

Density of immobilized cells was assessed by the Hoechst fluorescent DNA assay as previously described by Hoemann et al (Hoemann, Sun, Chrzanowski, & Buschmann, 2002).

Cell viability was determined using a LIVE/DEAD® Viability/Cytotoxicity Kit for mammalian cells (Molecular Probes, Eugene, OR, USA) according to manufacturer recommendations. Cells were observed with an inverted fluorescence microscope (Axiovert S100TV; Carl Zeiss Canada, Ontario, Canada) equipped with a mercury lamp and an adequate set of filters. Images were taken with a QICAM Fast 1394 camera (QImaging) and acquired with the NORTHERN ECLIPSE image acquisition software (Empix imaging).

4.2.3.3. Scanning Electron Microscopy

Cell morphology was studied using an Environmental Scanning Electron Microscope (Quanta 200 FEG, FEI Company Hillsboro, OR, USA) equipped with a secondary electron detector (Everhart-Thornley Detector) and working at a high vacuum mode. Specimens were fixed with 2% gluteraldehyde (Sigma), and sputter-coated with gold (Agar Manual Sputter Coater, Marivac Inc., Quebec, Canada) prior to observation. Cells dimensions were measured with XT DOCU software (FEI).

4.2.3.4. NO measurements

Nitric oxide concentrations were determined by the Griess enzymatic kit (Cedarlane) with respect to manufacturer technical instructions.

4.2.3.5. Determination of Arginase 1 activity

Total MSC-1 cells (inoculated on the plate or immobilized on the PET mesh) were lysed with 50 µl of a lysis buffer containing 0.1% Triton X-100 (Sigma) and 100 $\mu g.mL^{-1}$ of pepstatin, antipain and aprotinin (all from EMD BioSciences, San Diego, CA, USA). After 30 minutes in a thermomixer at 37ºC, cells debris were removed by centrifugation at 15000 × *g* for 20 seconds and cells lysates were kept in -80ºC prior to analysis. The determination of ARG1 activity was performed as previously described by Munder et al (Munder, et al., 1999).

4.2.3.6. Proliferation assay

The immunosuppressive activity was assessed as MSC-1 cell ability to inhibit T-cell proliferation. MSC-1 cells were cultured in the presence of Jurkat cells (Clone E6, Cedarlane) which were pre-treated with 5 $\mu g.mL^{-1}$ of Concanavalin A (ConA, Sigma) for 2 days. The test was performed in MILLICELL®PC 0.4 µm culture plate insert (Millipore, Ontario, Canada). Jurkat cells were counted every 3 h using a haemocytometer, and viability was determined by the Trypan Blue exclusion method.

4.2.3.7. Nucleotide extraction

Energetic nucleotides were extracted by perchloric acid (Ryll & Wagner, 1991) and measured by HPLC-MS (Waters, Milford, MA, USA). Briefly, 2 mL of 0.25% Trypsin – 1 mM EDTA (Invitrogen, Ontario, Canada) was added to the culture plate and incubated for 1 min at 37°C to activate the Trypsin enzyme. Conditioned medium was used to stop the enzyme activity and the detached cells were harvested by centrifugation at 200 × *g* for 6 min at 4°C. For the cells immobilized on the PET support, the mesh was centrifuged at 200 × *g* for 6 min at 4°C to remove the medium. Centrifugation did not lead to cell detachment. Cell pellets and cells on the PET support were rinsed by phosphate buffer saline (PBS) and centrifuged at 200 × *g* for 6 min at 4°C to remove the buffer.

Detached cells detached or those immobilized on the PET mesh were then extracted twice on ice, using 0.5 mL of a 0.5 M perchloric acid solution (Sigma). Cells extracts were centrifuged at 10 000 × *g* for 3 min at 4°C after each extraction and supernatants were collected. Ultimately, supernatants were neutralized by 0.3 mL of a 2 M $KHCO_3$ solution (Sigma). The precipitates

were removed by centrifugation at 15000 × *g* for 3 min at 4 °C. Supernatants were stored in liquid nitrogen prior to analysis.

Preliminary tests were performed to verify whether cell detachment may modify cell energetic state. Briefly, attached cells were extracted on plate after medium removal and PBS rinsing. Nucleotide concentrations were comparable to those reported in extracts of detached cells, suggesting that detaching cell do not lead to any significant change in cell bioenergetics.

4.2.3.8. Nucleotide measurements

Extracts were filtered through 0.2 µm filters (Millipore, Ontario, Canada). Nucleotides were separated on a Symmetry C_{18} column (150*2.1 mm, 3.5 µm) (Waters) and a Security C_{18} guard-column (Phenomenex, Torrance, CA, USA). Mobile phase consisted in Buffer A: 20 mM Ammonium acetate, 30 mM DMHA, pH 7.00 and Buffer B: 40 % (v/v) Acetonitrile in water. Flow rate was set at 0.3 $mL.min^{-1}$ using the following gradient: 0-12.5 min at 15% B, 12.5-13 min linear gradient from 15% B to 30% B, 13-38 min at 30% B, 38-43 min linear gradient from 30% B to 65% B, 43-48 min at 65% B, 48-49 min linear gradient from 65% B to 15% B and 49-55 min et 15% B.

4.2.3.9. Small-scale bioreactor

The small-scale perfusion bioreactor used in this study was modified from previous design (Gmati, Chen, & Jolicoeur, 2004). The system consisted of a 1-L glass erlenmeyer containing 600 mL of supplemented RPMI1640 culture medium with 10 % of Deuterium Oxide (Cambridge Isotope Laboratories, Quebec, Canada) oxygenated by surface aeration (200 $mL.min^{-}$

^{1}, 95 % air : 5 % CO_2). The oxygenated medium was continuously pumped into and out of the bioreactor by peristaltic pumps (Cole Parmer, Quebec, Canada) at a constant flow rate of 2.0 $mL.min^{-1}$. 100 million cells were immobilized on a cylinder of sterile PET mesh (4.7 mm OD, 25 mm length) and were allowed to adhere on the support for 16 h. The PET cylinder containing the immobilized cells and the culture medium were then carefully transferred in the small-scale bioreactor and the 1-L Erlenmeyer, respectively. Perfusion started immediately and cells were kept in the water bath for 1 h to recover from various stresses caused by cell manipulations and to reach stable metabolic activity as shown by Gmati et al, 2004.

4.2.3.10. In vivo ^{31}P-Nuclear Magnetic Resonance

In vivo ^{31}P-NMR spectra were recorded on a Varian Unity Inova 400 MHz spectrometer with a 10-mm Broad-Band probe. A 2 M solution of Methanephosphonic acid (Fisher scientific, Quebec, Canada) was used as phosphorous (^{31}P) concentration standard and chemical shift reference (30.60 ppm down shift from 85 % orthophosphonic acid). Intracellular pH was evaluated from inorganic phosphate chemical shift according to standard titration curve. 3000 scans/h were accumulated to generate spectra with adequate signal-to-noise ratio. Quantification of metabolites was accomplished by comparing their peaks areas to that of the reference.

4.2.4. Results and discussion

4.2.4.1. Behavior of MSC-1 cells immobilized on PET mesh

Since cell immobilization per se may affect their behavior (Continenza, Vicentini, Paradiso-Galatioto, Fileni, & Tchokogoue, 2003), a first series of experiments has confirmed that MSC-1 cell morphology, viability, growth, energetic and metabolic profiles, as well as their immunosuppressive activity were similar when cultured within a PET mesh as compared to standard Petri dish (control culture). Indeed, in both cultures, MSC-1 cells were initially round shaped (mean diameter of 8.9 ± 1.1 μm) at inoculation, and became flat and elongated (mean length of 21.4 ± 3.6 and a mean diameter of 7.6 ± 1.0 μm after 24 h) and grew in monolayer with similar intercellular connections (Figure 4-1A and B). Cells were viable throughout the culture (Figure 4-1C and D) and exhibited a similar specific growth rate (0.058 ± 0.001 h^{-1}, n = 12), as well as similar nutrient (glucose and glutamine) consumption and metabolite (lactate and ammonia) production rates (data not shown). Moreover, the intracellular pH, derived from the chemical shift of inorganic phosphate (Pi) monitored by ^{31}P-NMR, was stable at 6.9 ± 0.2 along MSC-1 cell culture (immobilized within the PET mesh) in the small-scale perfusion bioreactor. Taken together, these observations confirm that cells adhered to the PET fibers without exhibiting any noticeable stress.

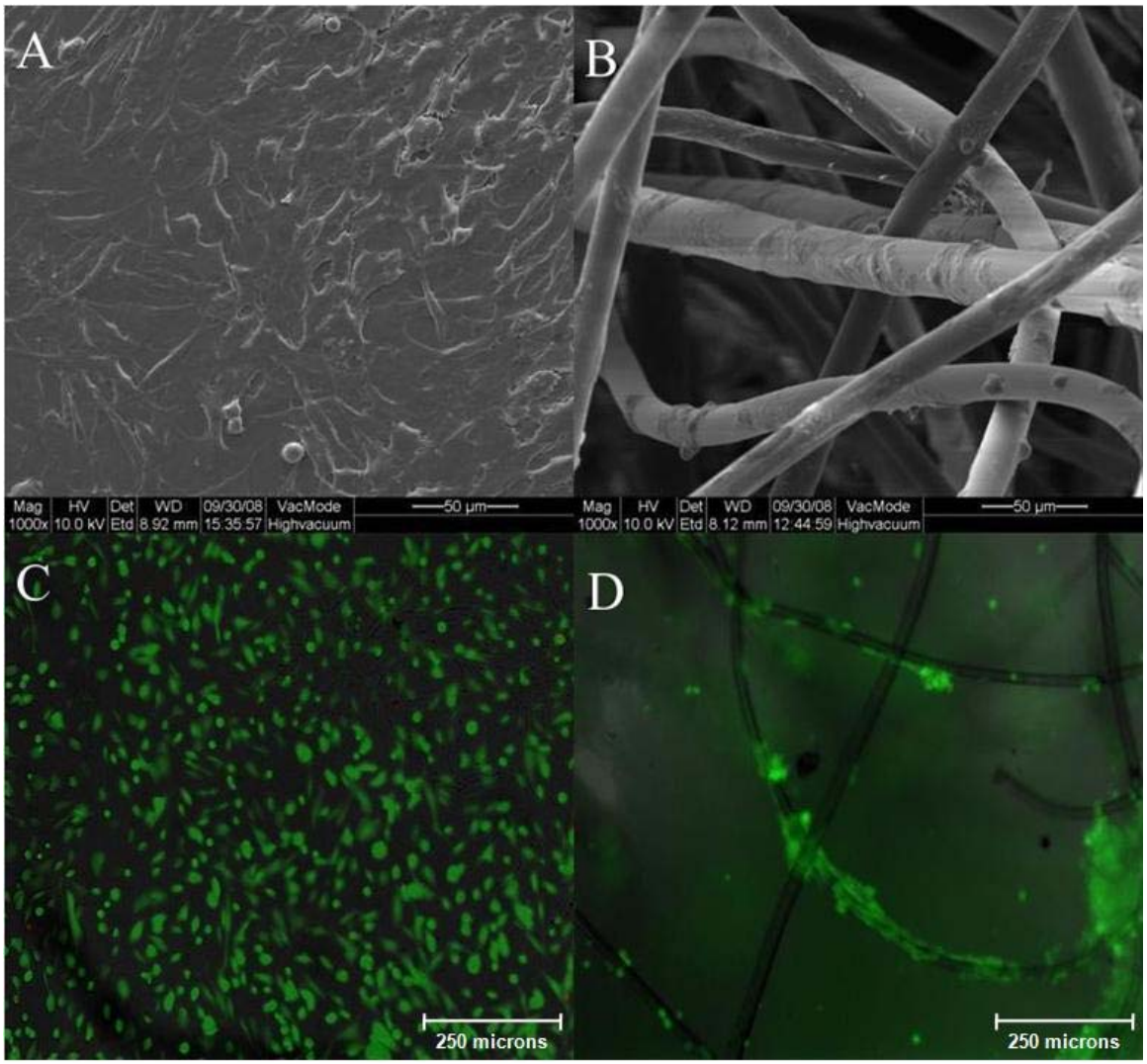

Figure 4-1 : Viable cells were uniformly distributed on the PET mesh and showed similar cytoskeletal rearrangements and dimensions in both cultures after 24 h.

A. and B. are respectively SEM images of MSC-1 cells grown on 1-cm2 of polystyrene (Petri) and PET mesh. Samples were fixed with 2% Gluteraldehyde and sputter-coated with gold prior to SEM imaging. C. and D. correspond to the respective fluorescence images of the aforementioned cultures. Samples were incubated for 30 min in a 0.5 µM of Calcein AM and 2 µM Ethidium Homodimer-1solution in a 37ºC/5% CO2 incubator.

In addition, the activities of both L-arg metabolizing enzymes (iNOS and ARG1) were assessed and an *in vitro* proliferation assay was performed in order to verify whether MSC-1 cell immunosuppressive activity was maintained further to their immobilization on the PET mesh. The iNOS activity, deduced from the concentration of both nitrite and nitrate (Figure 4-2A), and ARG1 activity (Figure 4-2B), were similar in Petri dish culture and within the PET mesh. More specifically, ARG1 activity, nitrite and nitrate concentration almost doubled from 30 h to the end of the culture, suggesting a higher L-arg consumption rate. The in vitro proliferation assay indicated that, after 48 h, Jurkat cell density (Figure 4-2C) and viability (Figure 4-2D) were reduced by 42% and 24 %, respectively, without any noticeable difference when cells were either cultured with or without PET mesh. Similar results were obtained when Jurkat cells were cultured in medium taken from MSC-1 cell culture performed in the small-scale perfusion bioreactor. These results imply that L-arg was metabolized at comparable rates and that, in all cultures, MSC-1 cells inhibited Jurkat cell proliferation and triggered their death.

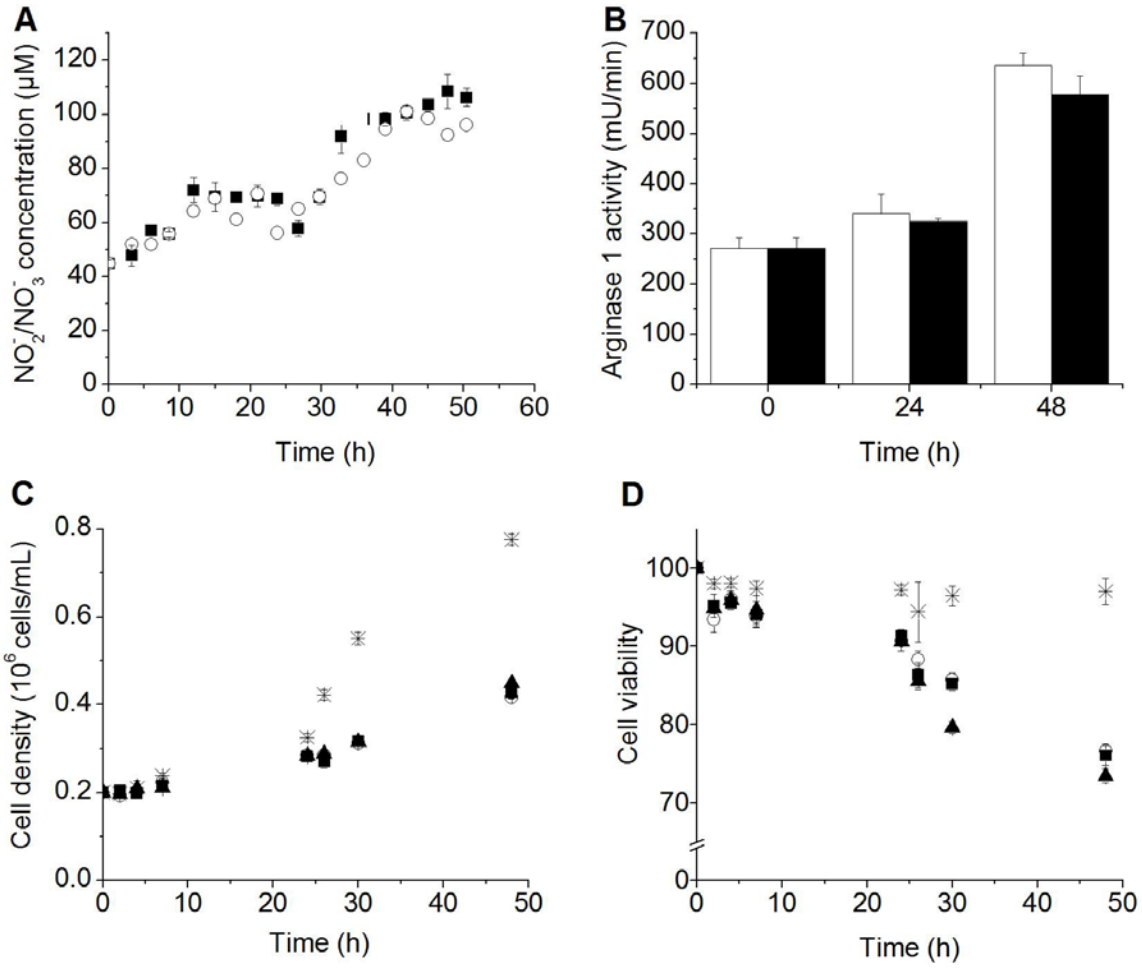

Figure 4-2 : MSC-1 cells immobilized on the PET mesh show similar iNOS and ARG1 activities when compared to control culture and are able to decrease T-cell proliferation and induce their apoptosis.

A. Sum of nitrate and nitrite concentrations in medium assessed by Griess reagents. B. Arginase 1 activity measurements in cell lysates. C. and D. Cell density and viability of ConA-activated Jurkat cells + MSC-1 cells grown on the insert (■); ConA-activated Jurkat cells + MSC-1 cells immobilized on the PET mesh (○); ConA-activated Jurkat cells cultured in conditioned medium used for culturing MSC-1 cells in the small-scale perfusion bioreactor for 24 h (▲); ConA-

activated Jurkat cells only (*). All data are presented as the mean ± standard error of the mean of triplicate experiments.

Furthermore, similar concentrations of intracellular energetic nucleotide, i.e., ATP (Figure 4-3A), ADP, AMP, CTP, GTP, UTP and β-NADPH and nucleoside diphosphate sugars (UDPGNAc) (data not shown) were recorded in both Petri dish and PET mesh cultures, thus suggesting similar energetic behavior with culture time. Moreover, the adenylate energy charge (AEC), defined as ([ATP]+0.5×[ADP])/([ATP]+[ADP]+[AMP]), which gives an insight of the energetic status of the cells (Atkinson, 1977), was constant at 0.74 ± 0.01 in all cultures (Figure 4-4A). Overall results indicated that MSC-1 cells were exposed to similar culture conditions in Petri dish and within the PET mesh.

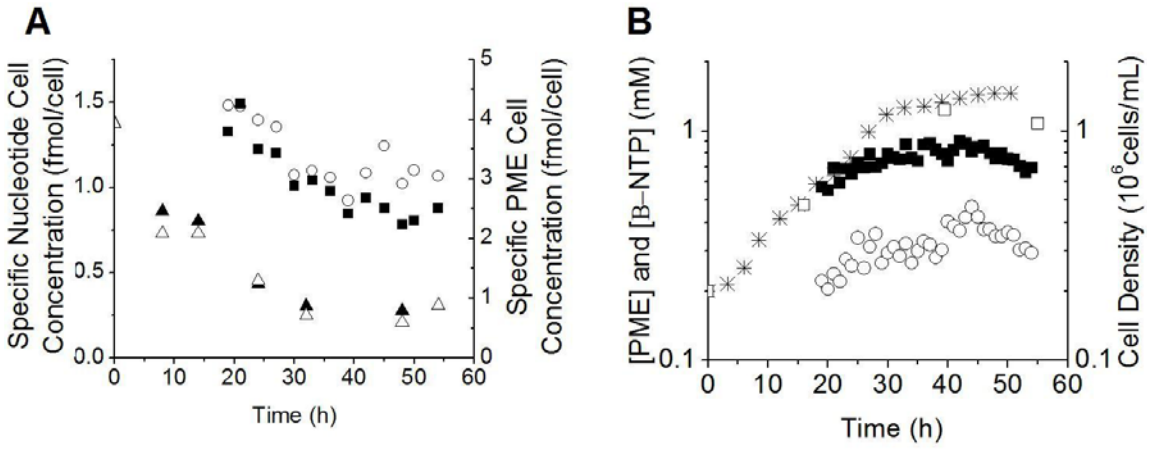

Figure 4-3 : MSC-1 cell bioenergetics and phospholipid metabolites measured by HPLC-MS and in vivo 31P-NMR.

A. Time-profiles of ATP (MSC-1 cells cultured in Petri dish (▲) and on the PET mesh (Δ)), PME (■) and β-NTP (○) specific cell concentration. B. PME (■) and β-NTP (○) correlated with cell growth on the PET mesh (*) and in the small-scale bioreactor (□).

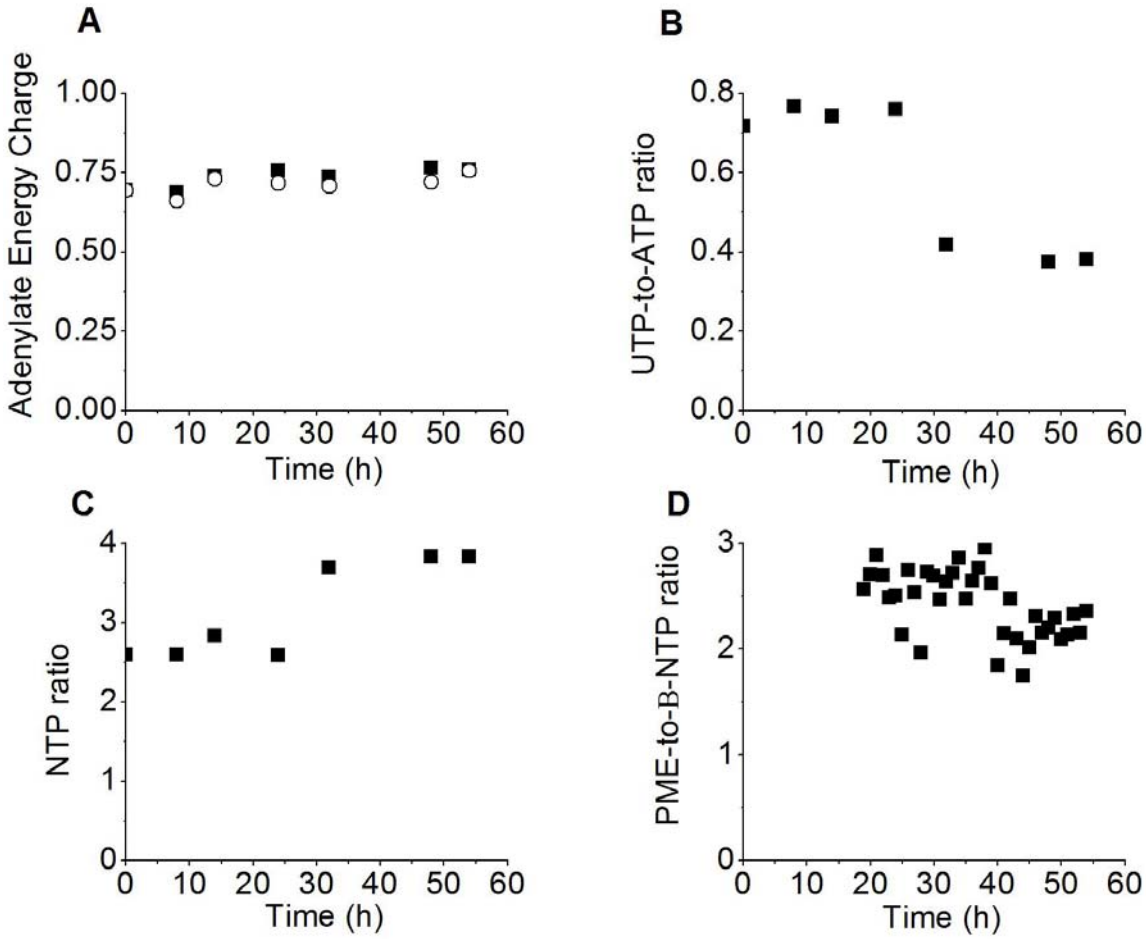

Figure 4-4 : Behavioural markers.

A. Adenylate Energy Charge, B. UTP-to-ATP ratio, C. NTP ratio and D. PME-to-β-NTP ratio were affected by the progress of growth process. Particularly, triphosphate nucleotides and the overall metabolic activity were decreased at the entry of the stationary phase.

4.2.4.2. Characterization of MSC-1 cell bioenergetics

Recent years have provided ample evidence on relationships between bioenergetics and immune responses and discussed strategies to modulate immune cell energetic metabolism in order to control their responses to immune challenges (Buttgereit, et al., 2000). However, there is a lack of understanding of the immunosuppression-related energy requirements. Indeed, literature reported that the co-induction of iNOS and ARG1 by lipopolysaccharide in macrophages modulate their central carbon metabolism and respiration (Costa Rosa, Curi, Murphy, & Newsholme, 1995; Murphy & Newsholme, 1998) , and so their energetic status.

The on-line monitoring of MSC-1 cell metabolism by ^{31}P-NMR showed that the phosphomonoester (PME) peak, which includes phospholipid-related metabolites, membrane lipids, phosphocholine, phosphoethanolamine, sugar phosphates (e.g. glucose- and fructose-6-phosphate) and other compounds related to cell growth (Daly, Lyon, Straka, & Cohen, 1988), increased during the exponential phase but gradually decreased during the decline phase (Figure 4-3B). However, the total concentration of PME increased at a lower specific rate (0.0167 ± 0.0008 h^{-1}) when compared to the maximal specific growth rate observed in Petri dish culture, hence suggesting a continuous decrease of PME cell content.

Moreover, the β-NTP peak, which accounts for triphosphate nucleotides, increased by a factor of 1.85 ± 0.35 after 19 h (MSC-1 cells doubling time) during the exponential phase, whereas the β-NTP cell specific concentration decreased from 1.427 ± 0.052 fmol.cell^{-1} in the exponential phase to 1.074 ± 0.051 fmol.cell^{-1} at the entry of the stationary phase (40 h) (Figure 4-3A). Similarly, nucleotide measurements by HPLC-MS showed that the cell specific concentrations in energy-rich nucleotides, i.e. ATP (Figure 4-3A), ADP, AMP, CTP, UTP, GTP and NADPH and UDPGNAc decreased continuously, at different rates, during the exponential

growth phase to reach stable levels at the entry of stationary phase (data not shown). However, GTP, UTP and CTP are partially used for the respective biosynthesis of proteins, polysaccharides and lipids of the cell membrane (Atkinson, 1977), and their synthesis was expected to increase during the exponential phase to support cell growth. Nevertheless, the observed demands of anabolic processes in these nucleotides seemed higher than the cell biosynthetic capacity. Both the intracellular pools in purines (GTP+ATP+ADP+AMP), which represent energy-related nucleotides, and pyrimidines (CTP+UTP+UDPGNAc), which are involved in different anabolic reactions and metabolic processes that are mostly growth-related (Atkinson, 1977), were depleted at the respective rates of 0.103 ± 0.006 fmol.cell^{-1}.h^{-1} and 0.030 ± 0.001 fmol.cell^{-1}.h^{-1} during the first 30 hours and reached steady-state from the entry of the plateau phase to the end of the culture announcing progressive switch of cell metabolism from metabolically active state during the exponential phase to a deteriorated state in the plateau phase.

More specifically, two distinct steady-states of specific nucleotide ratios can be distinguished at the exponential and the stationary growth phases. That is, the percentage of total pyrimidines, which was stable at 0.220 ± 0.004, decreased to a stable level of 0.164 ± 0.001 after 30 h (data not shown). Similarly, the UTP-to-ATP ratio, a biomarker of DNA and protein synthesis (Chou, Zeiger, & Rapaport, 1984), decreased from 0.75 ± 0.02 to 0.39 ± 0.02 after 30 h (Figure 4-4B). Conversely, the NTP ratio, which is the ratio of energetic nucleotides to anabolism-related nucleotides, increased from 2.65 ± 0.09, during the exponential growth phase, to 3.78 ± 0.06 after 30 h (Figure 4-4C). Furthermore, cell death coincided with a decrease of the PME-to-β-NTP ratio, a biomarker of the overall bioenergetic status and the respiration level, from 2.64 ± 0.09 at exponential growth to 2.23 ± 0.02 at the entry of the stationary phase (Figure 4-4D). As expected, the observed variations of cell specific nucleotide concentrations and energetic-derived biomarkers agreed with cell growth profile. In fact, part of the triphosphate

nucleotides is intended to cell growth-related processes during the exponential growth phase; these mechanisms were down-regulated at the early plateau phase where a global deterioration of the cell metabolic, and particularly anabolic, activity was noticed.

These results are in agreement with previous studies on CHO cells in which a decrease of the cell ATP content at late stationary phase and a similar nucleotide ratios variation with culture time were reported (Carvalhal, Marcelino, & Carrondo, 2003; McMurray-Beaulieu, et al., 2009). Indeed, the NTP ratio has been reported to increase at the end of the plateau phase; whereas the UTP-to-ATP ratio decreased at the entry of the stationary phase, thus suggesting the down-regulation of growth-related anabolic reactions and of global metabolic processes (McMurray-Beaulieu, et al., 2009).

To our knowledge, this is the first time that the bioenergetic behaviour of MSC-1 cells or other equivalent MDSC-like cells is described. Since the energy metabolism is an important part of the background machinery that ensures proper cell functions, the comprehension of the immunosuppression-related nutritional and energetic behaviour is required to better understand the metabolic traits that lead to the suppression of the anti-tumoural function. The bioassay platform used in this work, composed of a model cell line, MSC-1, and an experimental approach including HPLC-MS and in vivo ^{31}P-NMR, allowed for the characterization of MSC-1 cell bioenergetic baseline and particularly, the identification of distinct growth phases-related bioenergetic steady-states. Thus, nucleotide-derived physiologic biomarkers used herein will allow to highlight potential relationships between biochemical processes and metabolic behaviours in further studies focusing on cell inhibition or stimulation. Our results might thus have clinical relevance since the knowledge of MDSC physiology is an important prerequisite for the development of immunotherapy approaches and therapeutics.

4.2.5. Acknowledgements

We thank Drs A. Gigout and M. Nelea for their technical assistance for the SEM and fluorescence images acquisition. This project was funded by the Natural Sciences and Engineering Research Council of Canada (NSERC), the "Ministère du développement économique, innovation et exportation" (MDEIE) of the Government of Québec and the Québec-Italy Program.

4.2.6. References

Apolloni, E., Bronte, V., Mazzoni, A., Serafini, P., Cabrelle, A., Segal, D.M., Young, H.A., zanovello, P., (2000) Immortalized myeloid suppressor cells trigger apoptosis in antigen-activated T lymphocytes. The Journal of Immunology 165, 6723-6730.

Atkinson, D.E., (1977) Cellular Energy Metabolism and its Regulation, USA.

Buttgereit, F., Burmester, G.R., Brand, M.D., (2000) Bioenergetics of immune functions: fundamental and therapeutic aspects. Immunol Today 21, 192-199.

Carvalhal, A.V., Marcelino, I., Carrondo, M.J., (2003) Metabolic changes during cell growth inhibition by p27 overexpression. Appl Microbiol Biotechnol 63, 164-173.

Chou, I.N., Zeiger, J., Rapaport, E., (1984) Imbalance of total cellular nucleotide pools and mechanism of the colchicine-induced cell activation. Proc Natl Acad Sci U S A 81, 2401-2405.

Continenza, M.A., Vicentini, C., Paradiso-Galatioto, G., Fileni, A., Tchokogoue, E., (2003) In vitro study of Human Dermal Fibroblasts seeded on two kinds of surgical meshes: monofilamented Polypropylene and multifilamented Polyestere. Ital J Anat Embryol 108, 231-239.

Costa Rosa, L.F., Curi, R., Murphy, C., Newsholme, P., (1995) Effect of adrenaline and phorbol myristate acetate or bacterial lipopolysaccharide on stimulation of pathways of macrophage glucose, glutamine and O2 metabolism. Evidence for cyclic AMP-dependent protein kinase mediated inhibition of glucose-6-phosphate dehydrogenase and activation of NADP+-dependent 'malic' enzyme. Biochem J 310 (Pt 2), 709-714.

Daly, P.F., Lyon, R.C., Straka, E.J., Cohen, J.S., (1988) 31P-NMR spectroscopy of human cancer cells proliferating in a basement membrane gel. FASEB J 2, 2596-2604.

Gabrilovich, D.I., Bronte, V., Chen, S.H., Colombo, M.P., Ochoa, A., Ostrand-Rosenberg, S., Schreiber, H., (2007) The terminology issue for myeloid-derived suppressor cells. Cancer Res 67, 425; author reply 426.

Gmati, D., Chen, J., Jolicoeur, M., (2004) Development of a small-scale bioreactor: application to in vivo NMR measurement. Biotechnology and Bioengineering 89, 138-147.

Hoemann, C.D., Sun, J., Chrzanowski, V., Buschmann, M.D., (2002) A multivalent assay to detect glycosaminoglycan, protein, collagen, RNA, and DNA content in milligram samples of cartilage or hydrogel-based repair cartilage. Anal Biochem 300, 1-10.

McMurray-Beaulieu, V., Hisiger, S., Durand, C., Perrier, M., Jolicoeur, M., (2009) Na-butyrate sustains energetic states of metabolism and t-PA productivity of CHO cells. J Biosci Bioeng 108, 160-167.

Munder, M., Eichmann, K., Moran, J.M., Centeno, F., Soler, G., Modolell, M., (1999) Th1/Th2-regulated expression of arginase isoforms in murine macrophages and dendritic cells. Journal of Immunology 163, 3771-3777.

Murphy, C., Newsholme, P., (1998) Importance of glutamine metabolism in murine macrophages and human monocytes to L-arginine biosynthesis and rates of nitrite or urea production. Clin Sci (Lond) 95, 397-407.

Rabinovich, G.A., Gabrilovich, D., Sotomayor, E.M., (2007) Immunosuppressive strategies that are mediated by tumor cells. Annu Rev Immunol 25, 267-296.

Ramires, P.A., Mirenghi, L., Romano, A.R., Palumbo, F., Nicolardi, G., (2000) Plasma-treated PET surfaces improve the biocompatibility of human endothelial cells. J Biomed Mater Res 51, 535-539.

Rosch, R., Junge, K., Schachtrupp, A., Klinge, U., Klosterhalfen, B., Schumpelick, V., (2003) Mesh implants in hernia repair. Inflammatory cell response in a rat model. Eur Surg Res 35, 161-166.

Ryll, T., Wagner, R., (1991) Improved ion-pair high-performance liquid chromatographic method for the quantification of a wide variety of nucleotides and sugar-nucleotides in animal cells. J Chromatogr 570, 77-88.

Segerstrom, S.C., (2007) Stress, Energy, and Immunity: An Ecological View. Curr Dir Psychol Sci 16, 326-330.

Serafini, Borrello, I., Bronte, V., (2006) Myeloid suppressor cells in cancer: Recruitment, phenotype, properties, and mechanisms of immune suppression. Seminars in Cancer Biology 16, 53-65.

CHAPITRE 5. L'IMMUNOSUPPRESSION ASSURÉE PAR LES CELLULES MYÉLOIDES SUPPRESSIVES EST ÉNERGIVORE

5.1. Présentation de l'article

Cette section reprend l'article intitulé "**Immunosuppression mediated by myeloid-derived suppressor cells is energetically costly**". L'article a été soumis dans la revue "Cancer Immunology, Immunotherapy" en Novembre 2010.

La compréhension des besoins énergétiques et nutritionnels associés à la machinerie immunosuppressive spécifique au métabolisme du L-arg pourrait mener à l'identification de nouvelles pistes permettant l'altération de la fonction immunosuppressive des cellules MSC-1. Dans cette optique, les activités enzymatiques de iNOS et/ou ARG1 ont été inhibées par des inhibiteurs spécifiques et leur profil nutritionnel et leur comportement énergétique ont été suivis. De même, le rôle de la L-glutamine dans le phénomène d'immunosuppression a été conjointement investigué afin de mieux comprendre la régulation croisée entre le métabolisme du L-arg et le métabolisme central du carbone.

5.2. Immunosuppression mediated by myeloid-derived suppressor cells is energetically costly

Ines Hammami[1], Jingkui Chen[1], Vincenzo Bronte[2], Gregory De Crescenzo[1], Mario Jolicoeur[1*]

[1]Department of Chemical Engineering. École Polytechnique de Montréal. Montreal, Quebec, Canada.

[2]Department of Pathology. Immunology Section. Verona University. Verona, Veneto, Italy.

* Corresponding author:

Mario Jolicoeur

PO 6079 Station Centre-Ville

Montreal, Qc, Canada H3C 3A7

Tel: +1 514 340 4711 ext. 4525

Fax: +1 514 340 4159

e-mail: mario.jolicoeur@polymtl.ca

5.2.1. Abstract

Suppression of tumour-specific T-cell functions is a dominant mechanism of tumour escape. Myeloid-derived suppressor cells (MDSCs) metabolize L-arginine (L-Arg) via the enzymatic activities of the inducible nitric oxide synthase (iNOS) and arginase 1 (ARG1). In this work, MSC-1, an immortalized cell line derived from mouse MDSCs, was used as an *in vitro* model system of MDSCs. Characterization of MSC-1 cell nutritional profile revealed an anaerobic glycolysis with lactate accumulation, which is typical for primary MDSCs and tumour cells. Particularly, iNOS activity correlated with an enhanced central carbon metabolism and high bioenergetic states, whereas ARG1 activity did not exhibit specific nutritional or energetic trends. The inhibition of iNOS and ARG1 activities resulted in the down-regulation of MSC-1 cell immunosuppressive activity, and in the decrease of glucose and L-glutamine (L-Gln) uptake rates. In parallel, the cell content in energy-rich nucleotides and TCA cycle intermediates was decreased, which may has lead to the down-regulation of L-Arg endogenous biosynthesis. In addition, ARG1 activity was not affected under L-Gln limiting condition, whereas iNOS activity was inhibited from 18h. This result can be attributed to an observed decreased of cell content in NADPH, a co-factor of iNOS, as well as to the inhibition of the L-Gln-to-L-Arg conversion pathway, which has been revealed by the depletion of cell content in fumarate and malate. Taken altogether, our results suggest that the control of the fluxes related to glutaminolysis may represent a new target for immunotherapy.

5.2.2. Introduction

Complex interactions between tumours and the immune system are known to significantly affect the efficiency of anti-cancer treatments. While the adaptive immune system has the potential to recognize and prevent tumour outgrowth, molecules secreted by immune effector cells and growing tumours can act synergistically to promote the maturation of a $CD11b^{+}/Gr1^{+}$ cell population named "myeloid-derived suppressor cells" (D. I. Gabrilovich, et al., 2007). The accumulation of these cells has been reported under several pathological conditions, including bacterial and parasitic infections, acute and chronic inflammations and traumatic stresses. Special attention has been paid to the role of MDSCs in the suppression of tumour-specific T-cell function since they have been found in several cancer types such as prostate, breast, lung, and head and neck cancers (Serafini, et al., 2006). MDSCs represent a heterogeneous population, including macrophages, granulocytes, dendritic cells and myeloid cells at earlier stages of differentiation, which can be recruited in the tumour, spleen, blood and lymphoid organs of tumour-bearing hosts. MDSCs have been shown to impair the anti-tumoral immune response by metabolizing the semi-essential amino acid L-arginine. The latter can be derived from the diet, endogenous synthesis (by the kidneys, liver, intestine, etc.) and protein turnover (S. M. Morris, 2007). L-Arg is the substrate for two principal enzymes expressed by MDSCs: (i) iNOS that oxidizes L-Arg to generate nitric oxide (NO) and L-citrulline; and (ii) ARG1 that converts L-Arg into urea and L-ornithine. The Michaelis constant (K_M) of ARG1 (~ 10 mM) is much higher than that of iNOS (~ 5 μM); whereas the maximal rate (V_{max}) of ARG1 was reported to be 10^3 - 10^4 times higher than that of iNOS. Thus, the V_{max}/K_M values of ARG1 and iNOS are similar and so both enzymes are expected to compete for L-Arg at low substrate concentration (Mori, 2007).

The sparse concentration of L-Arg in the blood and the production of NO have been demonstrated to result in a gradual loss of the CD3ζ chain of the T-cell receptor and cause a significant decrease of T-cell proliferation due to cell cycle arrest in G_0/G_1 phase (P. C. Rodriguez & Ochoa, 2008). NO can also act at the level of the Interleukin-2 receptor signalling pathway by S-nitrosylating crucial cysteine residues on key proteins and by blocking phosphorylation reactions leading to the inactivation of several signalling molecules. Furthermore, NO rapidly reacts with oxygen, superoxide (O_2^-), water, hydrogen peroxide and various other compounds to generate reactive nitrogen oxide species, which can in turn result in T-cell dysfunction and death (Vincenzo Bronte, Serafini, Mazzoni, Segal, & Zanovello, 2003).

Up to now, various promising strategies have been suggested to overcome MDSC-mediated immunosuppression, but several clinical problems and side effects were reported (P. C. Rodriguez & Ochoa, 2008; Serafini, et al., 2006). Indeed, despite the considerable progress accomplished in the field of immune escape, the metabolic events that favour the maturation of MDSCs and enable their functions are still misunderstood. Therefore, a better understanding of the immunosuppression-related nutritional and energetic requirements of MDSCs is required in order to improve the efficiency of immunotherapy strategies.

As for well-known energetically demanding biological processes (e.g. thermoregulation, cell growth, etc.), the immune system requires energy to maintain its function (Demas, Chefer, Talan, & Nelson, 1997). The energy metabolism of immune cells is known to be subject to drastic changes while mounting a stress-response (e.g. inflammation, antibody administration, cytokine release, cell activation by antigens, etc.) (Fiorucci et al., 2004). Immune challenge redirects resources that could be otherwise allocated to other biological functions to support the increase of cell energetic demands (Demas, et al., 1997). Moreover, exposing T-cell subsets to different cytokines has shown trade-offs in the energetic and nutritional resources that produce a

cross-regulatory effect on immune system subcomponents (Fiorucci, et al., 2004; Long & Nanthakumar, 2004). Therefore, the enzymes responsible for metabolizing and recycling L-Arg may affect various enzymes and pathways that are directly or indirectly energy-requiring.

In this work, we used an immortalized cell line (MSC-1) derived from mouse MDSCs, a cell population that has previously been identified to be responsible for immunosuppression *in vivo*, but which retain their suppressive activity *in vitro* (Apolloni, et al., 2000; Mazzoni, et al., 2002). Being phenotypically similar to primary MDSCs, MSC-1 cell line represents a reliable model system, since these cells constitutively express iNOS and ARG1 and inhibit antigen-specific proliferative and functional cytotoxic T-lymphocyte response. To study possible regulation between MSC-1 cell nutritional and energetic demands and their immunosuppression-implicated machinery, iNOS and ARG1 activities were respectively inhibited by *N*-[3-(Aminomethyl)-benzyl]-acetamidine (1400W) and [(S)-(2-Boronoethyl)-L-cysteine] (BEC). 1400W has been selected because it is a tight-binding and highly selective inhibitor of iNOS and exhibits the highest potency among all previously reported iNOS inhibitors (Garvey et al., 1997), and BEC is a potent slow-binding competitive and selective inhibitor of ARG1 (Berkowitz et al., 2003). Both 1400W and BEC inhibitors are known to act on the enzymatic activity only without any reported effect on mRNA or protein levels of the enzyme (Berkowitz, et al., 2003; Garvey, et al., 1997). We have thus characterized the metabolic profile of iNOS or both iNOS and ARG1-inhibited MSC-1 cells. In addition, MSC-1 cells were cultured in the absence of L-Gln to elucidate its implication in the immunosuppression phenomenon. We report here that L-Arg metabolism by iNOS and ARG1 as well as its recycling modulate glucose, L-Gln and oxygen metabolisms to support MSC-1 cell immunosuppressive activity, particularly that ensured by iNOS.

5.2.3. Materials and Methods

5.2.3.1. Cell culture

The generation, culture, and phenotypes of MSC-1 immortalized cell line have been described previously (Apolloni, et al., 2000). MSC-1 cells express both L-Arg metabolizing enzymes (iNOS and ARG1) and are able to inhibit T-lymphocyte activation.

MSC-1 cells were grown in 75 cm^2 T-flasks (VWR, Ontario, Canada) in RPMI1640 medium (Sigma) supplemented with 10% (v/v) irradiated FBS (Cedarlane, Burlington, Ontario, Canada), 1mM Sodium Pyruvate (Sigma), 100 units/mL Penicillin, 150 units/mL Streptomycin (Cedarlane) and 2 mM L-glutamine (Cedarlane) when required, in a 5% CO_2 and 37ºC incubator. Cultures were inoculated at a cell density of 0.2×10^6 cells/mL and cells were passaged when they reached 80% of confluence.

When required, iNOS and ARG1 activities were inhibited with 100 μM of 1400W and 5 μM of BEC (both from Cedarlane), respectively.

5.2.3.2. Assays

Glucose, lactate, glutamate and glutamine concentrations in supernatants were measured using a 2700 SELECT biochemistry analyser (YSI Inc, Ohio).

Ammonia and nitric oxide concentrations were respectively assayed by the following enzymatic kits with respect to manufacturer technical instructions: Ammonia Assay Kit (Sigma) and Nitrate/Nitrite Colorimetric Assay Kit (Cedarlane).

Consumption and production specific rates (q_s, pmol.cells^{-1}.h^{-1}) were calculated using an average method based on the inverted biomass yield (pmol.cell^{-1}) multiplied by the maximal specific growth rate (μ_{max}, h^{-1}) (Görgens, Van Zyl, & Knoetze, 2005).

5.2.3.3. Determination of Arginase 1 activity

Total MSC-1 cells were lysed with 50 µL of a lysis buffer containing 0.1% Triton X-100 (Sigma) and 100 µg/mL of pepstatin, antipain and aprotinin (all from EMD BioSciences, San Diego, CA). After 30 minutes in a thermomixer at 37ºC, cells debris were removed by centrifugation at 15000 × *g* for 20 s and cells lysates were kept in -80ºC prior to analysis. The determination of ARG1 activity was performed as previously described by Munder and colleagues (Munder, et al., 1999).

5.2.3.4. Proliferation assay

The immunosuppressive activity of MSC-1 cells was assessed as their ability to inhibit Jurkat cell (leukemic T-cells, clone E6-1, Cedarlane) proliferation and induce their death. Jurkat cells were used as a model of immune challenged cells (Fiorucci, et al., 2004; Leist et al., 1999a). Jurkat cells were treated with 5µg/mL of Concanavalin A (conA, Sigma) for 2 days prior to the test.

Experiments were performed in 24-well tissue culture plates (VWR) in a final volume of 1 mL. First, MSC-1 cells were cultured in the presence of iNOS and/or ARG1 inhibitors (at concentrations indicated above) for 16 h (500 µL at 0.2×10^6cells/mL). ConA-activated Jurkat

cells were then inoculated (500 µL at 0.2×10^6cells/mL) in MILLICELL®PC 0.4 µm culture plate inserts (Millipore) and added to each well.

Mixed cultures were kept in a 5% CO_2 and 37ºC incubator for 32 h only to prevent the arrest of cell growth or the induction of cell death associated to nutrient limitation or toxic metabolite accumulation. Jurkat cells were then counted and viability was determined by the Trypan Blue exclusion method.

5.2.3.5. Respirometry test

Respirometry assays were performed as described by Lamboursain and colleagues (Lamboursain, et al., 2002). Briefly, MSC-1 cells were cultured for 48 h in the presence of 1400W and/or BEC or in the absence of L-Gln. 3 mL of a 5×10^6 cells/mL suspension were then inoculated in a 10-mL borosilicate glass syringe (Sigma) in which the plunger was substituted by a Ingold pO_2 probe (Mettler Toledo, Quebec, Canada). The respirometer was kept at 37°C and magnetically agitated (60 RPM) to ensure the homogeneity of cell suspension. Dissolved oxygen was recorded by an acquisition system (Virgo, Longueuil, Canada).

5.2.3.6. Metabolite extraction

The extraction protocol was based on the method developed by Kimball and colleagues (Kimball & Rabinowitz, 2006). Briefly, for each sample, 5×10^6 cells were washed with cold PBS and extracted with 400 µL of 80% cold methanol in the presence of 0.2 g of Sand (Sigma). After 10 min on dry ice, the mixture was vortexed and then sonicated in ice and water for 5 min. The samples were then centrifuged for 7 min at 21000 × *g* and 4ºC to collect supernatants. The pellets

were extracted a second and third time as described above with 200 µL of 50% cold methanol and 200 µl of cold water. Supernatants were mixed and stored in -80 ºC prior to analysis.

5.2.3.7. Nucleotide concentrations

Extracts were filtered through 0.2 µm filters (Millipore, Ontario, Canada) before analysis. Nucleotide concentrations were determined by ion-pairing liquid chromatography-electrospray ionization mass spectrometry (positive mode) using a HPLC-MS system (Waters, Milford, MA) equipped with a Symmetry C18 column (150*2.1 mm, 3.5 µm) (Waters) and a Security C18 guard-column (Waters, 10*2.1 mm, 3.5 µm).

DMHA was used as ion-pair reagent to improve the signal-to-noise ratio with positive ionization mode. Mobile phase consisted in Buffer A: 10 mM ammonium acetate, 15 mM DMHA at pH 7.0, and Buffer B: 40 % (v/v) acetonitrile in water. Flow rate was set at 0.3 mL $min.L^{-1}$ using the following gradient: 0-10 min at 15% B, 10-12 min at linear gradient from 15 to 40% B, 12-30 min at linear gradient from 40 to 70% B, 30-35 min at 70% B, 35-37 min at linear gradient from 70 to 15% B and 37-45 min at 15% B.

5.2.3.8. Organic acid concentrations

Extracts were filtered through 0.2 µm filters (Millipore, Ontario, Canada) before UPLC-MS/MS (Agilent, Quebec, Canada) analysis equipped with a Hypercarb column (100*2.1 mm, 5 µm) and a Hypercarb pre-column (2.1*10, 5 µm) (Thermo Fisher, Ontario, Canada).

Mobile phase consisted in Buffer A: 20mM ammonium acetate at pH 7.5, and Buffer B: 10 % (v/v) methanol in water. Flow rate was set at 0.3 $mL.min^{-1}$ using the following gradient: 0-5

min at 10% A, 5-10 min at linear gradient from 10 to 20% A, 10-20 min at linear gradient from 20 to 100% A, 20-30 min at 100% A, 30-32 min at linear gradient from 100 to 10% A and 32-40 min at10% A.

5.2.3.9. Statistical analysis

Data are shown as mean ± SEM (standard error of mean) of $n = 3$ independent experiments from 3 distinct MSC-1 cell cultures. Differences between mean values were calculated by a 2-tailed Student *t*-test for independent samples; $p < 0.05$ was accepted as significant.

5.2.4. Results

5.2.4.1. Effects of 1400W, BEC and L-Gln starvation on MSC-1 cell immunosuppressive activity

Although the half maximal effective concentration (EC_{50}) of 1400W is 0.8 ± 0.3 μM (Garvey, et al., 1997) and the K_I value of BEC is ranging from 0.4 to 0.6 μM (Kim et al., 2001), higher concentrations (i.e. 100 μM for 1400W and 5 μM for BEC) were used to guarantee the inhibition of iNOS and ARG1 activities in newly divided MSC-1 cells. In fact, these concentrations did not trigger any loss of cell viability (data not shown) or growth inhibition, and similar specific growth rates were observed for the control culture and cells treated with 1400W and both 1400W and BEC (Table 5-1). High concentrations of 1400W and BEC are commonly

used without any noticeable cytotoxic effect on several cell types (Cavicchi & Whittle, 1999; Colleluori & Ash, 2001; Farley, Wang, Law, & Mehta, 2008; Toque et al., 2010).

	Control culture: MSC-1 cells	MSC-1 cells + 1400W	MSC-1 cells + 1400W + BEC	MSC-1 – L-Gln
μ	0.047 ± 0.001	0.044 ± 0.001*	0.046 ± 0.003	0.009 ± 0.002*
q_{O_2}	66.03 ± 4.52	147.94 ± 2.24*	108.74 ± 1.27*	82.86 ± 12.23
q_s, glucose	292.49 ± 18.22	183.32 ± 1.79*	152.63 ± 8.11*	119.78 ± 18.93*
q_s, glutamine	85.83 ± 4.36	50.93 ± 3.74*	52.15 ± 0.61*	4.00 ± 1.08*
q_s, lactate	510.75 ± 28.09	255.96 ± 2.37*	291.53 ± 20.53*	225.56 ± 33.97*
q_s, ammonia	144.73 ± 10.78	64.11 ± 0.09*	105.41 ± 7.20*	5.26 ± 2.80*

Table 5-1: Specific growth rate (μmax, h-1), specific oxygen consumption rate (qO2, fmol.cell-1.h-1) and rates (qs, fmol.cell-1.h-1) of nutrient (glucose and glutamine) consumption and metabolite (lactate and ammonia) production.

i) MSC-1 cells grown in complemented culture medium (control culture); ii) MSC-1 cells grown in the presence of 100 μM of 1400W; iii) MSC-1 cells grown in the presence of 100 μM of 1400W and 5 μM of BEC; iv) MSC-1 cells grown in the absence of L-Gln. Experiments were performed in triplicate and errors are standard error of the mean, * $p<0.05$ when mean value is compared to that of the control culture.

Culturing MSC-1 cells in the presence of 1400W and BEC triggered rapid inhibition of iNOS activity since the concentration of nitrite and nitrate, used as a marker of iNOS activity, remained constant at 50.03 ± 4.57 μM, whereas nitrite and nitrate were accumulated at a rate of

2.33 ± 0.09 $\mu M.h^{-1}$ in the control culture (Figure 5-1A). However, the inhibition of ARG1 activity occurred at different rates (Figure 5-1B). In fact, ARG1 activity was decreased by 50% during the first 12 h of treatment, and then decreased from 45.78 ± 9.78 $nU.cell^{-1}.h^{-1}$ at 12 h to 9.42 ± 0.64 $nU.cell^{-1}.h^{-1}$ at 36 h, and remained quasi-stable until the end of the culture (48 h). *In vitro* proliferation assay showed that co-culturing Jurkat and MSC-1 cells pre-treated with 1400W and BEC reduced the immunosuppressive potential of MSC-1 cells. Indeed, Jurkat cell density (Figure 5-1C) and viability (Figure 5-1D) were similar to those measured in the control culture (Jurkat cells only). In stark contrast, in the presence of untreated MSC-1 cells, Jurkat cell density and viability after 32 h were respectively decreased by 37.08 ± 5.03 and 25.25 ± 2.32 % when compared to the control culture ($p<0.05$).

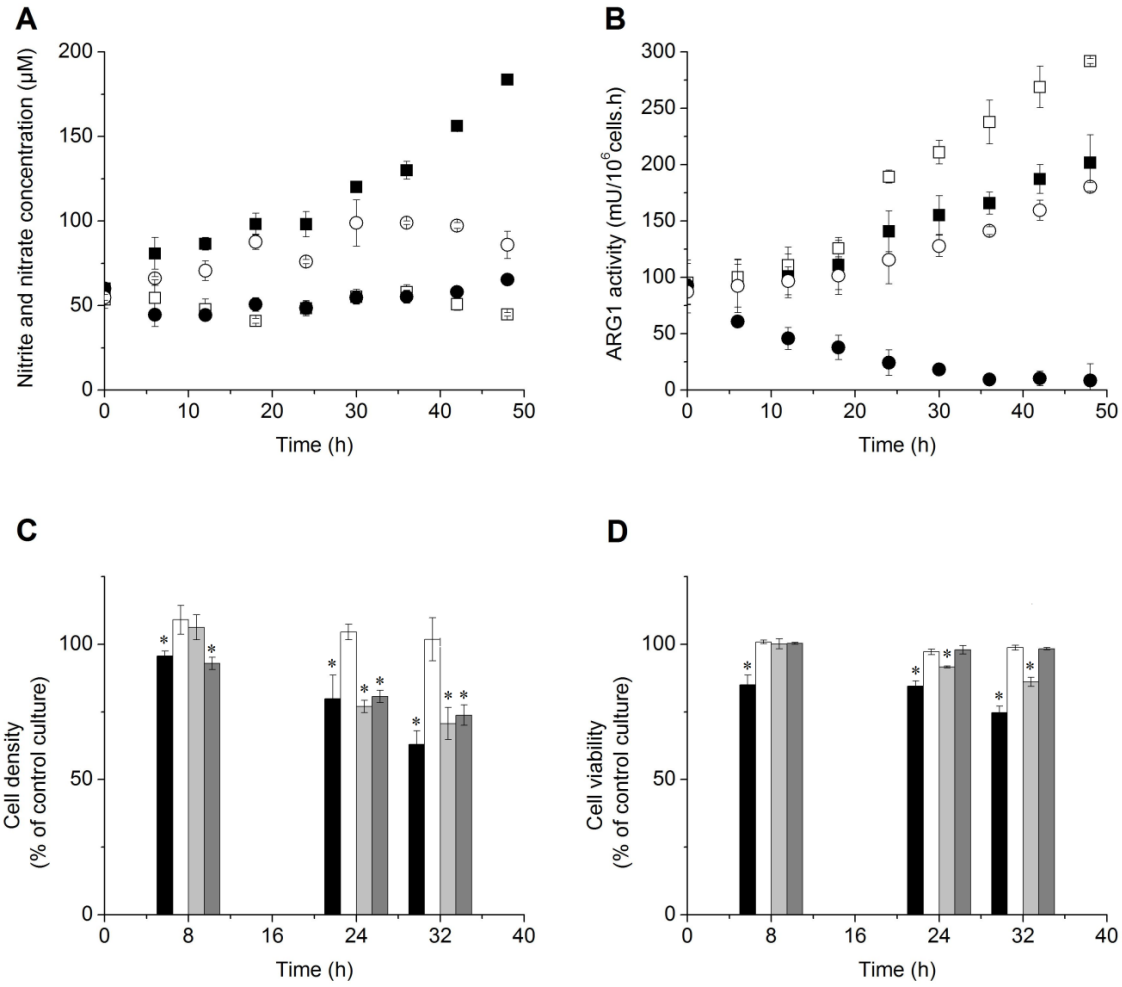

Figure 5-1: Effect of 1400W (100 µM) and BEC (5 µM) on iNOS and ARG1 activities and MSC-1 cell immunosuppressive activity.

All data are presented as the mean of different experiments (n = 3) ± standard error of the mean. A. Concentrations of nitrite and nitrate, marker of iNOS activity. B. ARG1 activity. (■) Control culture: MSC-1 cells only, (□) MSC-1 cells cultured in the presence of 1400W (100 µM), (●) MSC-1 cells cultured in the presence of 1400W (100 µM) and BEC (5 µM), and (○) MSC-1 cells cultured in the absence of L-Gln. Percentage of cell density (C) and viability (D) referred to the control culture (MSC-1 cells only). Jurkat cells were pre-cultured for 48 h in the presence of 5µg.mL^{-1} and then inoculated in the presence of: i) MSC-1 cells (black bar); ii) MSC-1 cells pre-cultured for 12 h in the presence of 1400W (100 µM) and BEC (5 µM) (white bar); iii) MSC-1

cells pre-cultured for 12 h in the presence of 1400W (100 μM) (light grey bar); iv) conditioned medium recuperated after 12 h of MSC-1 cell culture performed in the absence L-Gln. Then, 2 mM of L-Gln were added to the culture to complemet the medium (dark grey bar). * Significant difference to the 1400W and BEC-treated culture, $p<0.05$.

Interestingly, culturing MSC-1 cells in the presence of 1400W only resulted in an increase of ARG1 activity by 35 to 45% (compared to the control culture) after 24 h. This phenomenon was not observed for the L-Gln deprived culture where the accumulation of nitrite and nitrate ceased at around 18 h without any significant effect on ARG1 activity. In fact, conversely to the use of 1400W and BEC that did not affect MSC-1 cell growth, the absence of L-Gln decreased the specific growth rate from 0.047 ± 0.001 h^{-1} (control culture) to 0.009 ± 0.002 h^{-1} without any significant effect on cell viability (data not shown), and so the arrest of NO-derivative production is not related to the progress of growth process. In both cases, i.e. inhibition of iNOS and in the absence of L-Gln, MSC-1 cells were still able to inhibit Jurkat cell proliferation. However, MSC-1 cells cultured in L-gln depleted medium did not affect Jurkat cell viability. In the other hand, exposure of Jurkat cells to 1400W and BEC in the absence of MSC-1 cells did not affect their proliferation or viability compared to an untreated Jurkat cell culture (data not shown).

5.2.4.2. MSC-1 cell nutritional profile

The inhibition of iNOS or both iNOS and ARG1 activities was accompanied by a decrease of the specific glucose consumption rate from 292.50 ± 18.22 $fmol.cell^{-1}.h^{-1}$ (control culture) to 183.32 ± 1.79 and 152.63 ± 8.11 $fmol.cell^{-1}.h^{-1}$, respectively (Table 5-1). In agreement with lower glucose uptake rate, lactate production rate was also reduced from 510.75 ± 28.09

fmol.cell^{-1}.h^{-1} (control culture) to 255.96 ± 2.37 fmol.cell^{-1}.h^{-1} in the presence of 1400W and to 291.53 ± 20.53 fmol.cell^{-1}.h^{-1} when iNOS and ARG1 were inhibited. Interestingly, the lactate-to-glucose yield in the iNOS-inhibited culture (1.40 ± 0.03) was lower than those reported for the control culture (1.78 ± 0.18, $p<0.05$) and the 1400W and BEC -treated one (1.92 ± 0.24, $p<0.05$). In fact, culturing MSC-1 cells in the absence of L-Gln decreased the lactate production rate by 55.34 ± 9.11% when compared to the control culture indicating that L-Gln highly contribute to lactate accumulation. However, the specific glutamine consumption rate was decreased from 85.83 ± 4.36 fmol.cell^{-1}.h^{-1} (control culture) to substantially similar rates of 50.93 ± 3.74 fmol.cell^{-1}.h^{-1} when iNOS was inhibited, and to 52.15 ± 0.61 fmol.cell^{-1}.h^{-1} in the presence of both 1400W and BEC ($p<0.05$). Thus, the relative low lactate-to-glucose yield in the 1400W-treated culture may suggest that the nutrients were metabolized in a different way when only ARG1 was active. Moreover, the down-regulation of glucose uptake in the 1400W alone and both 1400W and BEC -treated cultures was accompanied by the increase of cell specific oxygen consumption rate from 66.03 ± 4.52 fmol.cell^{-1}.h^{-1} (control culture) to 147.94 ± 2.24 and 108 ± 1.27 fmol.cell^{-1}.h^{-1}, respectively. This effect cannot be attributed to glucose limitation since the same initial culture medium was used in all cultures. However, further investigation is required to verify whether the inhibitors used herein affect the affinity of glucose transporters or glycolytic enzyme activity levels. Moreover, the ratio of the consumption rates of oxygen-to-glucose increased from 0.23 ± 0.03 in the control culture to 0.81 ± 0.02 and 0.72 ± 0.5 in, respectively, the 1400W and both 1400W and BEC -treated cultures suggesting that uncoupling of glycolysis and respiration may have occurred and the mitochondrial respiratory chain may have primarily led to ATP production with minimal supply with TCA cycle substrates.

Furthermore, although similar L-Gln consumption rates were observed either in the presence of 1400W as with both 1400W and BEC, ammonia has accumulated at a higher rate

(105.41 ± 7.20 fmol.cell^{-1}.h^{-1}) with an ammonia-to-L-Gln yield of 1.27 ± 0.09 when both iNOS and ARG1 activities were inhibited compared to the 1400W -treated culture where the ammonia production rate was 64.11 ± 0.09 fmol.cell^{-1}.h^{-1} but a higher ammonia-to-L-Gln yield of 2.02 ± 0.16 was noticed (Table 5-1). This suggests that ARG1 activity is probably linked to amino acid deamination reactions.

Inhibiting iNOS and both iNOS and ARG1 activities resulted also in a decrease of the specific cell concentrations in TCA cycle substrates, particularly, fumarate, malate and α-ketoglutarate (Figure 5-2).

On the one hand, the decreased glucose and L-Gln uptake rates have resulted in a decrease of the production rates of acetyl coenzyme A, α-ketoglutarate and pyruvate, and so reduced TCA cycle supply with precursors and down-regulated conversion of pyruvate into acetyl coenzyme A or oxaloacetate. On the other hand, since cell growth was not affected in the presence of iNOS and ARG1 inhibitors and cell specific growth rate were substantially similar in the presence of 1400W and both 1400W and BEC (Table 5-1), a similar part of the TCA cycle substrates may have been devoted to synthesize anabolism-related macromolecules in parallel to energy production. Therefore, the decrease of cell specific concentration in TCA cycle substrates in the treated cultures is mostly due to the down-regulation of production capacity.

Nevertheless, culturing MSC-1 cells in L-Gln deprived medium slightly increased the oxygen consumption rate (82.86 ± 12.23 fmol O_2.cell^{-1}.h^{-1}) and resulted in the decrease of glucose uptake and lactate accumulation rates (Table 5-1), whereas the lactate-to-glucose ratio remained high (1.88 ± 0.01) suggesting that MSC-1 cells maintained a glycolytic metabolism and that sparse quantity of glucose derivatives entered the TCA cycle, as revealed by the decrease of TCA cycle substrate in the absence of L-Gln (Figure 5-2). In all cases, one can expect a decrease

of the endogenous production of L-Arg and so a consequent inhibition of the residual immunosuppressive activity.

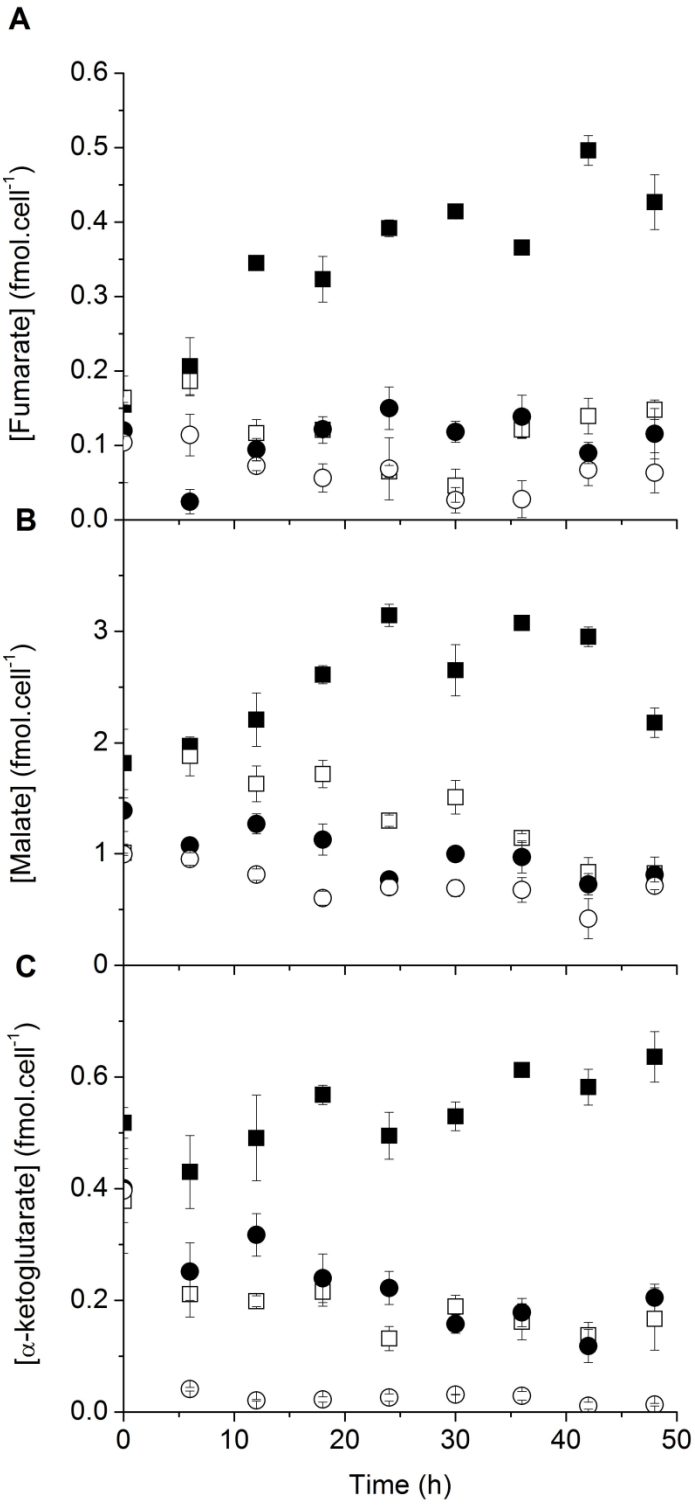

Figure 5-2: Inhibiting iNOS and/or ARG1 as well as culturing MSC-1 cells in the absence of L-Gln reduced the cell content in TCA cycle substrates.

A. Fumarate which is a by-product of the L-Arg production reaction reduced in the studied conditions. B. The specific concentration of malate was also decreased in the presence of 1400W and BEC suggesting the down-regulation of TCA cycle -derived lactate production. C. The absence of L-Gln has depleted the intracellular α-ketoglutarate and so decreased TCA cycle intermediates. Similar effects were noticed when iNOS and/or ARG1 were inhibited. Same symbols as in Figure 5-1.

5.2.4.3. Effect of 1400W, BEC and L-Gln deprivation on MSC-1 cell energetic profile

The inhibition of iNOS and/or ARG1 activities was shown to modulate MSC-1 cell nutritional profile and the distribution of TCA cycle intermediates. This observation suggested that these inhibitors may thus affect the MSC-1 cell bioenergetic state; we have then investigated their potential effects on immunosuppression-associated energetic requirements.

Inhibition of iNOS and ARG1 activities was accompanied by the decrease of cell specific ATP concentration. In fact, ATP decreased from 5.16 ± 0.20 fmol.cell^{-1} (at inoculation) to 2.49 ± 0.25 fmol.cell^{-1} after 24 h, and then increased at a rate of 0.046 ± 0.007 fmol.cell^{-1}.h^{-1} until the end of the culture (Figure 5-3A). However, in the control culture, ATP continuously accumulated at a rate of 0.033 ± 0.002 fmol.cell^{-1}.h^{-1} to a maximal value of 7.33 ± 0.12 fmol.cell^{-1}.h^{-1} at 48 h. The reduction of glucose uptake rate has negatively affected the glycolytic ATP production rate, as revealed by the marker of AMPK activity, the AMP-to-ATP ratio (Cidad, et al., 2004), which was 2 to 5 folds lower than that of the control culture (Figure 5-3D). Similarly, the down-

regulation of TCA cycle activity, either because of a reduced supply in TCA cycle substrates or their consumption by anabolic processes, decreased the production of TCA cycle-derived energy.

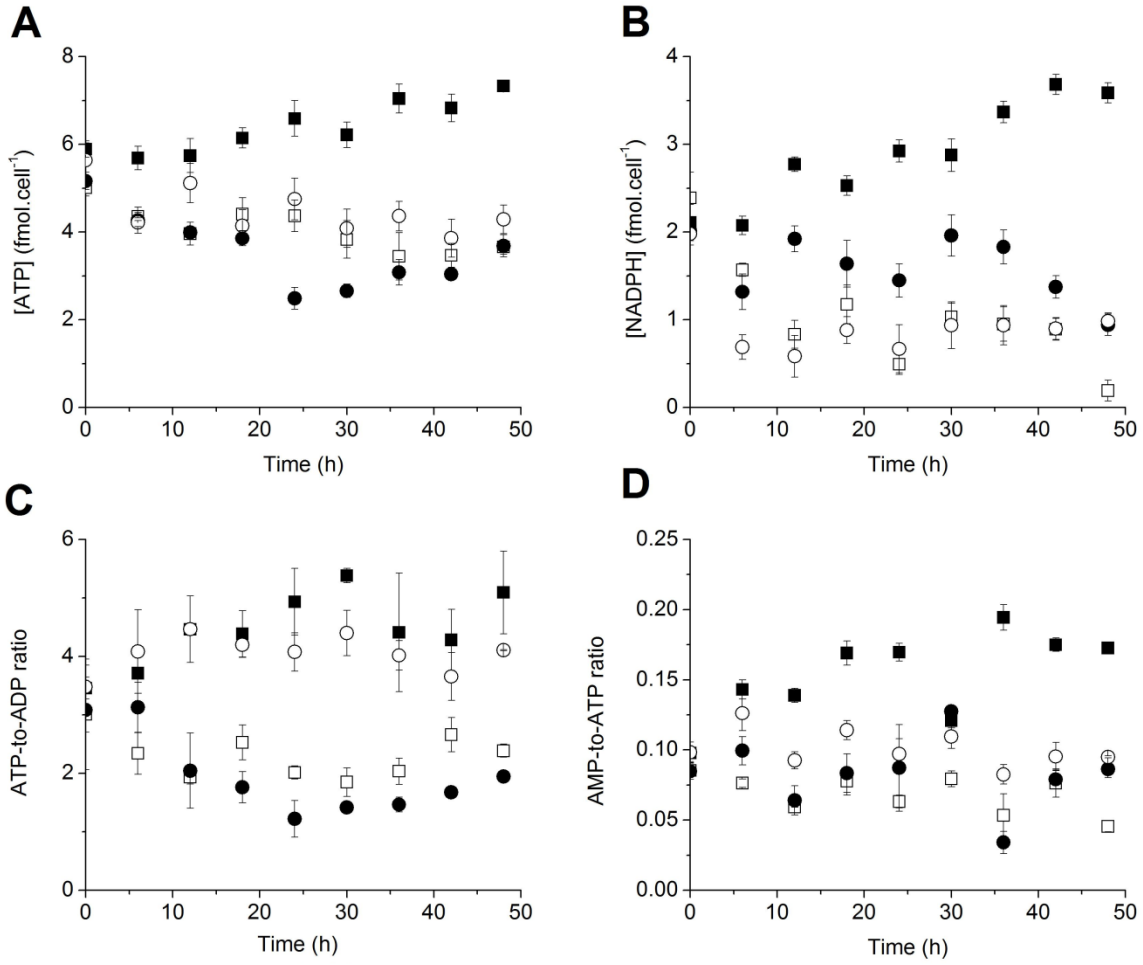

Figure 5-3: The inhibitors 1400W and BEC and the absence of L-Gln deteriorate MSC-1 cell energetic states.

The specific concentrations of ATP (A) and NADPH (B) decreased in the presence of iNOS and/or ARG1 inhibitors or in the absence of L-Gln. C. The ATP-to-ADP ratio, a biomarker of energy consumption, decreased when iNOS and/or ARG1 are inhibited. D. The behavioural marker, AMP-to-ATP ratio, indicates the down-regulation of glycolysis further to iNOS and/or ARG1 inhibition and in L-Gln deprived conditions. Same symbols as in Figure 5-1.

Moreover, although specific oxygen consumption rate was 2 to 3-times higher in the presence of 1400W and BEC when compared to the control culture, the ATP-to-ADP ratio, which is known as a marker of respiration and energy consumption (Reich & Sel'Kov, 1981), decreased from 3.08 ± 0.38 (inoculation) to 1.22 ± 0.31 after 24 h, with a slight increase thereafter (Figure 5-3C). Conversely, this ratio continuously increased from 3.46 ± 0.19 (inoculation) to a plateau value of 4.82 ± 0.38 at 30 h in the control culture. This may suggest that the rate of ATP consumption was higher than that of ATP production either by respiration or TCA cycle. ATP may have been consumed to support cell growth and to maintain cell integrity.

Similarly, MSC-1 cell specific NADPH concentration was almost stable at 1.60 ± 0.03 $fmol.cell^{-1}$ in the presence of 1400W and BEC; whereas, it has progressively accumulated at a rate of 0.034 ± 0.009 $fmol.cell^{-1}.h^{-1}$ in the control culture. In fact, NADPH is generated through the oxidative phase of the pentose-phosphate pathway from reactions catalyzed by glucose-6-phosphate dehydrogenase and phosphogluconate dehydrogenase (Newsholme, Costa Rosa, Newsholme, & Curi, 1996). Culturing MSC-1 cells in the absence of L-Gln has decreased the specific NADPH concentration from 1.98 ± 0.13 $fmol.cell^{-1}$ (inoculation) to a quasi-stable concentration of 0.82 ± 0.13 $fmol.cell^{-1}$ from 6 h (Figure 5-3B), demonstrating the important role of L-Gln in NADPH supply. Particularly, L-Gln derived NADPH was probably produced by the malic enzyme which catalyses the conversion of malate into pyruvate. Thus, the decrease of glucose and L-Gln uptake rates are implicated in the depletion of the intracellular pool in NADPH, a cofactor of iNOS enzyme.

Moreover, inhibition of iNOS activity alone resulted in similar effects on MSC-1 cell bioenergetic state since specific ATP and NADPH concentrations as well as the trends of nucleotide-derived biomarkers were practically similar to those measured in the iNOS and ARG1

-inhibited cultures (Figure 5-3). Nevertheless, ARG1 activity was stimulated and the resulting MSC-1 cells were still immunosuppressive. Therefore, ARG1 activity is not dependent on enhanced central carbon metabolism and high energetic state. This was confirmed in the L-Gln deprived culture where the cell specific ATP concentration progressively decreased at a rate of 0.022 ± 0.004 fmol.cell^{-1}.h^{-1} (Figure 5-1A) while NADPH concentration remained considerably low. This decreased bioenergetic state was accompanied by the inhibition of iNOS activity; whereas ARG1 activity was not affected and maintained the potential of MSC-1 cells to inhibit Jurkat cell proliferation.

5.2.5. Discussion

Co-induction of ARG1 and iNOS by bacterial lipopolysaccharide (LPS) in macrophages has been shown to modulate central carbon metabolism and respiration (Costa Rosa, et al., 1995; Murphy & Newsholme, 1998), and therefore to affect cell bioenergetic state. In this study, we characterized the MSC-1 cell nutritional profile and energetic states when iNOS and both iNOS and ARG1 activities are inhibited in order to highlight the immunosuppression-related energetic demands. Moreover, since L-Gln was shown to be responsible for the endogenous production of L-Arg, we investigated the effect of L-Gln deprivation on MSC-1 cell bioenergetic and immunosuppressive activity.

The characterization of the MSC-1 cell nutritional profile showed that these cells exhibit high glucose uptake rate (292.49 ± 18.22 fmol.cell^{-1}.h^{-1} for MSC-1 cells versus 168.9 fmol.cell^{-1}.h^{-1} for CHO cells (DeBerardinis, Lum, Hatzivassiliou, & Thompson, 2008)) most likely to maintain high biosynthetic fluxes that are required for rapid growth (specific growth rate of 0.047 ± 0.001 h^{-1} compared to 0.027 h^{-1} for CHO cells). Lactate was also found to be generated at a

high rate (510.75 ± 28.09 fmol.cell^{-1}.h^{-1} (DeBerardinis, et al., 2008)) when compared to CHO cells (308.1 fmol.cell^{-1}.h^{-1} (DeBerardinis, et al., 2008)). Interestingly, the lactate-to-glucose ratio was substantially high (1.78 ± 0.18) in the control culture. This suggests that MSC-1 cells re-direct most of the glucose-derived carbon as lactate, or that another source of carbon, such as L-Gln, contributes to the high lactate production rate. However, the lactate-to-glucose ratio in L-Gln deprived cultures was also high (1.88 ± 0.01), suggesting that MSC-1 cells modulate glucose metabolism to ensure high lactate levels when cells are immunosuppressive. In fact, the oxygen consumption rate in the control culture was lower than that observed in iNOS and both iNOS and ARG1 -inhibited cultures (Table 5-1). Therefore, despite the abundant availability of oxygen (*in vitro*), MSC-1 cells favour glycolytic metabolism rather than oxidative phosphorylation, which lead to higher energy production efficiency. Indeed, primary MDSCs were shown to express the hypoxia induction factor HIF-1α in parallel with up-regulation of iNOS and ARG1 activities to adapt to the low oxygen tension encountered in tumours *in vivo* (Corzo, et al., 2010; Raghunand, Gatenby, & Gillies, 2003). Therefore, MDSCs carry anaerobic metabolism that ensures the acidification of the tumoural microenvironment and support tumour invasion, neovascularisation, angiogenesis and metastasis (Gatenby & Gillies, 2004; Marin-Hernandez, Gallardo-Perez, Ralph, Rodriguez-Enriquez, & Moreno-Sanchez, 2009). MSC-1 *In vitro*, cells' behaviour observed in this work is thus similar to that of tumour cells, which also exhibit a glycolytic phenotype to ensure acute and chronic acidification of the tumour. Likewise, MSC-1 cells consumed L-Gln at high rates (85.83 ± 4.36 fmol.cell^{-1}.h^{-1} versus 49.40 fmol.cell^{-1}.h^{-1} for CHO cells) through anaplerotic pathways to produce energy and intermediates for macromolecules biosynthesis. The absence of L-Gln triggered a significant decrease of the glucose consumption rate (Table 5-1) and consequently a decrease of the specific ATP and NADPH concentrations (Figure 5-3A and B) as well as of the intermediates of the TCA cycle (Figure 5-2).

Inhibiting iNOS and ARG1 resulted in the decrease of nutrient uptake (Table 5-1). This decrease cannot be associated to direct effects of 1400W and BEC on the expression or the activity of glucose or glutamine transporters; the presence of these inhibitors in Jurkat cell culture did not trigger any noticeable effect at the nutritional level, although Jurkat cells and macrophages, as MSC-1 cells, express the same nutrient transporters (Ahmed & Berridge, 2000; Fernandes, Mattozo, Machado, Rosa, & Curi, 1996). Inhibition of L-Arg metabolizing enzymes resulted in the decrease of specific concentrations of TCA cycle substrates (Figure 5-2) as well as of NADPH and ATP (Figure 5-3A and B). In fact, the down-regulation of nutrients' consumption rates has decreased the production rates of TCA cycle intermediates and of energy-rich shuttles, which were continuously consumed to support cell growth. However, the specific growth rate in the 1400W and BEC -treated culture was similar to that in the control culture, suggesting that the anabolic-related consumption rates of TCA cycle substrates and energy were probably similar when iNOS and both iNOS and ARG1 activities are inhibited. Moreover, although the oxygen consumption rate was more that 2-fold higher in the iNOS and ARG1 -inhibited culture compared to the control culture, the ATP-to-ADP ratio indicated that the ATP consumption rate was higher than that of production either by respiration or by the TCA cycle. Also, the AMPK activity was lower than that reported in the control culture, suggesting that the AMPK sensor was not up-regulated to respond to an energy deficiency condition. Nevertheless, inhibition of iNOS alone showed similar cell specific nucleotide concentrations with culture time and consequently similar behavioural marker trends. Taken together, our results indicate that the immunosuppressive machinery particularly that related to iNOS activity is dependent on enhanced central carbon metabolism and high energetic states. Previous work by Albina and colleagues show that iNOS activity in freshly isolated peritoneal macrophages was associated to higher glucose uptake rate and a decrease of the glucose flux through the TCA cycle (Albina &

Mastrofrancesco, 1993). However, in our study, cell concentrations of α-ketoglutarate, fumarate and malate were higher for the control culture when compared to those for 1400W and/or BEC-treated cultures (Figure 5-2). This suggests that MSC-1 cells metabolize L-Gln to ensure high activity of the TCA cycle, which is used as part of the L-Arg endogenous production pathway. Also, TCA cycle may be stimulated to produce energy and compensate for the low energy yield of the glycolytic metabolism.

Interestingly, MSC-1 cells cultured in L-Gln deprived medium were characterized by reduced iNOS activity, as revealed by the decrease of nitrite and nitrate concentration from 18 h. Several studies have emphasized the regulation of NO production and iNOS mRNA expression by L-Gln but resulted in contradictory conclusions. Indeed, L-Gln was shown to attenuate NO production and down-regulate iNOS mRNA in IL-1β-activated hepatocytes (Lu, Wang, & Tang, 2009). In contrast, L-Gln did not trigger any significant effect on NO levels and iNOS gene expression in Caco-2 and HCT-8 cancer cells (Marion et al., 2003). Our results are in agreement with those reported for LPS-treated macrophages, where NO production was reduced in the presence of glutaminase inhibitor (Murphy & Newsholme, 1998). However, the absence of L-Gln did not affect ARG1 activity and the resulting MSC-1 cells were able to inhibit Jurkat cell proliferation without any noticeable effect on cell viability. In addition to the inhibition of the L-Gln-to-L-Arg pathway due to reduced TCA cycle substrates, the absence of L-Gln may have down-regulated the L-Arg recycling pathway since L-Gln was shown to regulate the gene expression of argininosuccinate synthetase, one of the enzymes implicated in endogenous production of L-Arg (Brasse-Lagnel, Fairand, Lavoinne, & Husson, 2003). Thus, ARG1 activity may have been attenuated in a prolonged culture. Moreover, *in vivo*, ARG1 only affects immune cell functions and proliferation, which can be recovered by several stimuli such as MTOR, INF-γ, etc (Steer, Lake, Nowak, & Robinson, 2010). Therefore, in addition to L-Gln role as a necessary

nutrient for cell growth, L-Gln metabolism supports iNOS-associated immunosuppressive function by producing energy-rich nucleotides that are directly or indirectly required by the immunosuppression-related processes, and also by ensuring L-Arg availability. Controlling L-Gln availability or specifically inhibiting L-Gln transporters or glutaminolysis enzymes may thus bear promise for treating NO-induced pathologies, such as myocardial infarction, inflammatory bowel disease, neurodegenerative disorders, etc (Mocellin, et al., 2007).

In conclusion, we have demonstrated that L-Arg metabolism by iNOS and ARG1 modulates MSC-1 cell nutritional behaviour to ensure the production of energy-rich nucleotide and TCA cycle substrates that support the immunosuppression-related processes and that L-Gln plays an important role in regulating iNOS activity and the endogenous synthesis of L-Arg.

5.2.6. Acknowledgements

This project was funded by the Natural Sciences and Engineering Research Council of Canada (NSERC), the “Ministère du développement économique, innovation et exportation” (MDEIE) of the Government of Québec, the Canada Research Chair program and the Québec-Italy Program.

5.2.7. References

1. Gabrilovich DI, Bronte V, Chen SH, Colombo MP, Ochoa A, Ostrand-Rosenberg S, Schreiber H (2007) The terminology issue for myeloid-derived suppressor cells. Cancer Res 67 (1):425; author reply 426. doi:67/1/425 [pii]
10.1158/0008-5472.CAN-06-3037 [doi]

2. Serafini, Borrello I, Bronte V (2006) Myeloid suppressor cells in cancer: Recruitment, phenotype, properties, and mechanisms of immune suppression. Seminars in Cancer Biology 16 (1):53-65

3. Morris SM (2007) Arginine metabolism: Boundaries of our knowledge. Journal of Nutrition 137 (6):1602S-1609S

4. Mori M (2007) Regulation of nitric oxide synthesis and apoptosis by arginase and arginine recycling. Journal of Nutrition 137 (6):1616S-1620S

5. Rodriguez PC, Ochoa AC (2008) Arginine regulation by myeloid derived suppressor cells and tolerance in cancer: mechanisms and therapeutic perspectives. Immunol Rev 222:180-191. doi:IMR608 [pii]

10.1111/j.1600-065X.2008.00608.x [doi]

6. Bronte V, Serafini P, Mazzoni A, Segal DM, Zanovello P (2003) L-arginine metabolism in myeloid cells controls T-lymphocyte functions. Trends in Immunology 24 (6):301-305

7. Demas GE, Chefer V, Talan MI, Nelson RJ (1997) Metabolic costs of mounting an antigen-stimulated immune response in adult and aged C57BL/6J mice. Am J Physiol 273 (5 Pt 2):R1631-1637

8. Fiorucci S, Mencarelli A, Distrutti E, Baldoni M, del Soldato P, Morelli A (2004) Nitric oxide regulates immune cell bioenergetic: a mechanism to understand immunomodulatory functions of nitric oxide-releasing anti-inflammatory drugs. J Immunol 173 (2):874-882

9. Long KZ, Nanthakumar N (2004) Energetic and nutritional regulation of the adaptive immune response and trade-offs in ecological immunology. Am J Hum Biol 16 (5):499-507. doi:10.1002/ajhb.20064 [doi]

10. Apolloni E, Bronte V, Mazzoni A, Serafini P, Cabrelle A, Segal DM, Young HA, zanovello P (2000) Immortalized myeloid suppressor cells trigger apoptosis in antigen-activated T lymphocytes. The Journal of Immunology 165:6723-6730

11. Mazzoni A, Bronte V, Visintin A, Spitzer JH, Apolloni E, serafini P, Zanovello P, Segal DM (2002) Myeloid suppressor lines inhibit T cell responses by an NO-dependant mechanism. The Journal of Immunology 168:689-695

12. Garvey EP, Oplinger JA, Furfine ES, Kiff RJ, Laszlo F, Whittle BJ, Knowles RG (1997) 1400W is a slow, tight binding, and highly selective inhibitor of inducible nitric-oxide synthase in vitro and in vivo. J Biol Chem 272 (8):4959-4963

13. Berkowitz DE, White R, Li D, Minhas KM, Cernetich A, Kim S, Burke S, Shoukas AA, Nyhan D, Champion HC, Hare JM (2003) Arginase reciprocally regulates nitric oxide synthase activity and contributes to endothelial dysfunction in aging blood vessels. Circulation 108 (16):2000-2006. doi:10.1161/01.CIR.0000092948.04444.C7 [doi]

01.CIR.0000092948.04444.C7 [pii]

14. Görgens JF, Van Zyl WH, Knoetze JH (2005) Reliability of methods for the determination of specific substrate consumption rates in batch culture. Biochemical Engineering Journal 25 (2):109-112

15. Munder M, Eichmann K, Moran JM, Centeno F, Soler G, Modolell M (1999) Th1/Th2-regulated expression of arginase isoforms in murine macrophages and dendritic cells. Journal of Immunology 163 (7):3771-3777

16. Leist M, Single B, Naumann H, Fava E, Simon B, Kuhnle S, Nicotera P (1999) Inhibition of mitochondrial ATP generation by nitric oxide switches apoptosis to necrosis. Exp Cell Res 249 (2):396-403. doi:10.1006/excr.1999.4514 [doi]

S0014-4827(99)94514-7 [pii]

17. Lamboursain L, St-Onge F, Jolicoeur M (2002) A lab-respirometer forplant and animal cell culture. Biotechnology Progress 18:1377-1386

18. Kimball E, Rabinowitz JD (2006) Identifying decomposition products in extracts of cellular metabolites. Anal Biochem 358 (2):273-280. doi:S0003-2697(06)00546-X [pii]
10.1016/j.ab.2006.07.038 [doi]

19. Kim N, Cox J, Baggio R, Emig F, Mistry S, Harper S, Speicher D, Morris SJ, Ash D, Traish A, Christianson D (2001) Probing erectile function: S-(2-bronoethyl)-L-cysteine binds to arginase as a transition state analogue and enhances smooth muscle relaxation in human penile corpus cavernosum. Biochemistry 40 (9):2678-2688

20. Farley KS, Wang LF, Law C, Mehta S (2008) Alveolar macrophage inducible nitric oxide synthase-dependent pulmonary microvascular endothelial cell septic barrier dysfunction. Microvasc Res 76 (3):208-216. doi:S0026-2862(08)00101-5 [pii]
10.1016/j.mvr.2008.07.004 [doi]

21. Cavicchi M, Whittle BJ (1999) Potentiation of cytokine induced iNOS expression in the human intestinal epithelial cell line, DLD-1, by cyclic AMP. Gut 45 (3):367-374

22. Toque HA, Tostes RC, Yao L, Xu Z, Webb RC, Caldwell RB, Caldwell RW (2010) Arginase II Deletion Increases Corpora Cavernosa Relaxation in Diabetic Mice. J Sex Med. doi:10.1111/j.1743-6109.2010.02098.x [doi]

23. Colleluori DM, Ash DE (2001) Classical and slow-binding inhibitors of human type II arginase. Biochemistry 40 (31):9356-9362. doi:bi010783g [pii]

24. Cidad P, Almeida A, Bolanos JP (2004) Inhibition of mitochondrial respiration by nitric oxide rapidly stimulates cytoprotective GLUT3-mediated glucose uptake through 5'-AMP-activated protein kinase. Biochem J 384 (Pt 3):629-636. doi:10.1042/BJ20040886 [doi]
BJ20040886 [pii]

25. Reich JG, Sel'Kov EE (1981) Energy metabolism of the cell - a theoritical treatise. London

26. Newsholme P, Costa Rosa LF, Newsholme EA, Curi R (1996) The importance of fuel metabolism to macrophage function. Cell Biochem Funct 14 (1):1-10

27. Murphy C, Newsholme P (1998) Importance of glutamine metabolism in murine macrophages and human monocytes to L-arginine biosynthesis and rates of nitrite or urea production. Clin Sci (Lond) 95 (4):397-407

28. Costa Rosa LF, Curi R, Murphy C, Newsholme P (1995) Effect of adrenaline and phorbol myristate acetate or bacterial lipopolysaccharide on stimulation of pathways of macrophage glucose, glutamine and O2 metabolism. Evidence for cyclic AMP-dependent protein kinase mediated inhibition of glucose-6-phosphate dehydrogenase and activation of NADP+-dependent 'malic' enzyme. Biochem J 310 (Pt 2):709-714

29. DeBerardinis RJ, Lum JJ, Hatzivassiliou G, Thompson CB (2008) The biology of cancer: metabolic reprogramming fuels cell growth and proliferation. Cell Metab 7 (1):11-20

30. Corzo CA, Condamine T, Lu L, Cotter MJ, Youn JI, Cheng P, Cho HI, Celis E, Quiceno DG, Padhya T, McCaffrey TV, McCaffrey JC, Gabrilovich DI (2010) HIF-1alpha regulates function and differentiation of myeloid-derived suppressor cells in the tumor microenvironment. J Exp Med 207 (11):2439-2453. doi:jem.20100587 [pii]

10.1084/jem.20100587 [doi]

31. Raghunand N, Gatenby RA, Gillies RJ (2003) Microenvironmental and cellular consequences of altered blood flow in tumours. Br J Radiol 76 Spec No 1:S11-22

32. Marin-Hernandez A, Gallardo-Perez JC, Ralph SJ, Rodriguez-Enriquez S, Moreno-Sanchez R (2009) HIF-1alpha modulates energy metabolism in cancer cells by inducing over-expression of specific glycolytic isoforms. Mini Rev Med Chem 9 (9):1084-1101

33. Gatenby RA, Gillies RJ (2004) Why do cancers have high aerobic glycolysis? Nat Rev Cancer 4 (11):891-899

34. Ahmed N, Berridge MV (2000) Ceramides that mediate apoptosis reduce glucose uptake and transporter affinity for glucose in human leukaemic cell lines but not in neutrophils. Pharmacol Toxicol 86 (3):114-121

35. Fernandes LC, Mattozo CA, Machado UF, Rosa LF, Curi R (1996) Insulin treatment can abolish changes in glucose and glutamine metabolism of lymphocytes and macrophages caused by the implantation of the Walker 256 tumour. Cell Biochem Funct 14 (3):187-192. doi:10.1002/(SICI)1099-0844(199609)14:3<187::AID-CBF679>3.0.CO;2-M [pii]
10.1002/cbf.679 [doi]

36. Albina JE, Mastrofrancesco B (1993) Modulation of glucose metabolism in macrophages by products of nitric oxide synthase. Am J Physiol 264 (6 Pt 1):C1594-1599

37. Lu J, Wang XY, Tang WH (2009) Glutamine attenuates nitric oxide synthase expression and mitochondria membrane potential decrease in interleukin-1beta-activated rat hepatocytes. Eur J Nutr 48 (6):333-339. doi:10.1007/s00394-009-0018-x [doi]

38. Marion R, Coeffier M, Leplingard A, Favennec L, Ducrotte P, Dechelotte P (2003) Cytokine-stimulated nitric oxide production and inducible NO-synthase mRNA level in human intestinal cells: lack of modulation by glutamine. Clin Nutr 22 (6):523-528. doi:S0261561403000542 [pii]

39. Brasse-Lagnel C, Fairand A, Lavoinne A, Husson A (2003) Glutamine stimulates argininosuccinate synthetase gene expression through cytosolic O-glycosylation of Sp1 in Caco-2 cells. J Biol Chem 278 (52):52504-52510

40. Steer HJ, Lake RA, Nowak AK, Robinson BW (2010) Harnessing the immune response to treat cancer. Oncogene 29 (48):6301-6313. doi:onc2010437 [pii]
10.1038/onc.2010.437 [doi]

41. Mocellin S, Bronte V, Nitti D (2007) Nitric oxide, a double edged sword in cancer biology: searching for therapeutic opporuinities. Medicinal Research reviews 27 (3):317-352

CHAPITRE 6. L'OXYDE NITRIQUE AFFECTE LA BIOÉNERGÉTIQUE DES CELLULES DU SYSTÈME IMMUNITAIRE : les effets de l'exposition prolongée aux dérivés de l'oxyde nitrique sur le métabolisme des cellules Jurkat leucémiques

---

6.1. Présentation de l'article

Cette section reprend l'article intitulé "**Nitric oxide affects immune cell bioenergetics : Long-term effects of nitric-oxide derivatives on leukemic Jurkat cell metabolism**". L'article a été soumis dans la revue "Immunology and Cell Biology" en 2011.

L'utilisation des donneurs de NO est controversée puisqu'en plus de leurs effets bénéfiques consistant en l'inhibition de la progression de la tumeur et l'accumulation des MDSC, le NO affecte considérablement la respiration des cellules effectrices du système immunitaire. Notre objectif était alors de caractériser l'effet du NO, pas l'intermédiaire d'un nouveau donneur de NO, AT38, sur le comportement métabolique des cellules Jurkat considérées comme modèle de cellules T stimulées. Cette étude a résulté en l'identification d'une approche thérapeutique permettant l'atténuation des effets néfastes du NO sur le système immunitaire.

6.2. Nitric oxide affects immune cells bioenergetics: Long-term effects of nitric-oxide derivatives on leukemic Jurkat cell metabolism

Ines Hammami[1], Marie Bertrand[1], Jingkui Chen[1], Vincenzo Bronte[2], Gregory De Crescenzo[1], Mario Jolicoeur[1*]

[1]Department of Chemical Engineering. École Polytechnique de Montréal. Montreal, Quebec, Canada.

[2]Department of Pathology. Immunology Section. Verona University. Verona, Veneto, Italy.

* Corresponding author:

Mario Jolicoeur

PO 6079 Station Centre-Ville

Montreal, Qc, Canada H3C 3A7

Tel: +1 514 340 4711 ext. 4525

Fax: +1 514 340 4159

e-mail: mario.jolicoeur@polymtl.ca

6.2.1. Abstract

Major advances in dissecting mechanisms of NO-induced down-regulation of the anti-tumour specific T-cell function have been accomplished during the last decade. In this work, we studied the effects of a NO donor (AT38) on leukemic Jurkat cell bioenergetics. Culturing Jurkat cells in the presence of AT38 triggered irreversible inhibition of cell respiration, led to the depletion of 50% of the intracellular ATP content and induced the arrest of cell proliferation and the loss of cell viability. Although a deterioration of the overall metabolic activity has been observed, glycolysis was stimulated, as revealed by the increase of glucose uptake and lactate accumulation rates as well as by the up-regulation of GLUT-1 and PFK-1 mRNA levels. In the presence of NO, cell ATP was rapidly consumed by energy-requiring apoptosis mechanisms; under a glucose concentration of about 12.7 mM, cell death was switched from apoptosis into necrosis. Exposure of Jurkat cells to DMSO (1% v/v), SA and AT55, the non-NO releasing moiety of AT38, failed to modulate neither cell proliferation nor bioenergetics. Thus, as for all NSAIDs, beneficial effects of AT38 on tumour regression are accompanied by the suppression of the immune system. We then showed that pre-treating Jurkat cells with low concentration of cyclosporine A, a blocker of the mitochondrial transition pore, attenuates AT38-induced inhibition of cell proliferation and suppresses cell death. Finally, we have studied and compared the effects of nitrite and nitrate on Jurkat cells to those of NO and we are providing evidence that nitrate, which is considered as a biologically inert anion, has a concentration and time-dependent immunosuppressive potential.

6.2.2. Introduction

The metabolic, energetic and biosynthetic demands of immune cells increase dramatically after their activation by antigens and mitogens. Mounting a functional immune response requires rapid and extensive cell growth, proliferation, activation and production of effector proteins (Maciver et al., 2008). Immunoregulatory functions are known to be ATP-dependant and sensitive to disturbances in intracellular nutrient levels (Buttgereit, et al., 2000). Co-stimulation of T-cells by TCR and CD28 was shown to lead in PI3K/Akt-dependent up-regulation of glucose transporter 1 (GLUT-1) gene expression, glucose uptake and oxygen metabolism (Frauwirth et al., 2002).

In aerobic organisms, energy is provided by glycolysis or respiration via oxidative phosphorylation, which has the higher energy production efficiency. However, the tumoural microenvironment is characterized by low concentrations of oxygen and glucose, as well as high levels of lactate and reductive and oxidative species (Raghunand, et al., 2003). Specifically, a myeloid-derived suppressor cell population ensures high output of NO via the enzymatic activity of inducible NO synthase (iNOS) (Serafini, et al., 2006). NO diffuses freely and reacts rapidly with various biomolecules and intracellular compounds (e.g. O_2^-, H_2O_2) within both NO-generating cells and also target cells to produce reactive nitrogen oxide species (Mocellin, et al., 2007). The primary decomposition product of NO in aerobic aqueous solution is nitrite (NO_2^-), which can be further oxidized to generate nitrate (NO_3^-) in the presence of additional oxidizing species such as oxyhemoproteins (Ignarro, Fukuto, Griscavage, Rogers, & Byrns, 1993). NO is known to be responsible for various physiological functions and is implicated in multiple pathologies (Mocellin, et al., 2007), but special attention is accorded to its role in cancer pathogenesis and tumour-related immunosuppression phenomena since effective anti-NO and

NO-based anti-cancer drugs showed contradictory findings. In fact, low/intermediate steady-state concentrations (nano/picomolar) promote cancer progression, whereas higher levels (micromolar) lead to tumour regression. Moreover, short-term exposure of T-cells to physiologic concentrations of NO rapidly induces mitochondrial hyperpolarization and inhibits complex IV of the respiratory chain in a reversible manner, while prolonged exposure to NO results in a gradual and persistent inhibition of complex I (Clementi, Brown, Feelisch, & Moncada, 1998). NO also triggers the release of cytochrome *c* followed by the cleavage, and so the activation, of pro-apoptotic caspases, morphological changes, DNA fragmentation, and, ultimately, cell death (Kuida et al., 1998; Li, et al., 1997). Concomitant release and activation of cell death signals and the availability of glycolytic ATP induce apoptosis; and the decrease of ATP turnover is known to switch cell death process into necrosis (Leist, et al., 1999a; Leist et al., 1999b).

NO-donating non-steroidal anti-inflammatory drugs (NO-NSAIDs), which represent a novel and promising class of cancer chemopreventive compounds (Nath, Labaze, Rigas, & Kashfi, 2005), were reported to modulate respiration and bioenergetics of immune cells and to induce their death (Fiorucci, et al., 2004). In this study, we investigated the long-term effects of AT38 on leukemic Jurkat cells. The AT38 used herein is a NSAID consisting of a salicylic acid (SA)-like moiety linked to a furoxan moiety (details for AT38 structure, formulation and release mechanisms will be fully described in another submitted manuscript). These furoxan based- NO donors are now emerging for the selective inhibition of cyclooxygenase, including their use for the treatment of certain cancer types and neurological disorders (Del Grosso et al., 2005). We also compared the effects of NO donors to nitrite and nitrate donors ($NaNO_2$ and $NaNO_3$, respectively) on Jurkat cell bioenergetics and showed a time- and concentration-dependent immunosuppressive potential of nitrate. As for all other NO-donors, AT38 inhibits Jurkat cell bioenergetics, and so, *in vivo*, the AT38-mediated tumour regression will be accompanied by the

dysfunction of immune system. Because cyclosporine A (CsA) at low doses (0.1 – 5 μM) is known to inhibit most of the mitochondrial changes caused by NO, such as the loss of mitochondrial transmembrane potential, the opening of the mitochondrial permeability transition pore (MPTP) and consequently the release of cytochrome *c* (Roy et al., 2006), we demonstrated that pre-treating Jurkat cells with CsA attenuate AT38 effects on cell growth and viability.

6.2.3. Materials and Methods

6.2.3.1. Materials

RPMI1640, Foetal Bovine Serum, Penicillin/Streptomycin, Cyclosporine A, IL-2 ELISA kit, hemoglobin and Jurkat cells (Clone E6-1) were purchased from Cedarlane (Ontario, Canada). AT38 and AT55 were synthesized in Prof. Bronte's laboratory (manuscript under submission). Dimethyl Sulfoxide (DMSO), Sodium Nitrate and Sodium Nitrate, Salicylic Acid (SA), Perchloric Acid, Potassium Bicarbonate, Concanavalin A (ConA), nucleotides standards and all other reagents were from Sigma-Aldrich (St. Louis, MO).

6.2.3.2. Cell culture and treatment

Jurkat cells were cultured at an initial density of 0.2×10^6 cells/mL in RPMI1640 culture medium supplemented with 10% (v/v) of FBS, 100 U/mL Penicillin and 150 U/mL Streptomycin in 75-cm^2 untreated T-flasks (VWR, Ontario, Canada). Cells were incubated at 37ºC under a humidified 5% CO_2 atmosphere for 2 days.

When required, Jurkat cells were cultured for 36 hours in complete culture medium containing $NaNO_2$, $NaNO_3$ and AT38 at final concentrations of 25 µM, 50 µM and 25 µM, respectively. AT38, AT55 and SA are dissolved in DMSO (1% v/v of final volume) prior to addition to cell suspension.

CsA dissolved in 0.1% Eth (1mM) was used for cell treatment. In specific experiments, Jurkat cells were pre-treated for 30 min with 5 µM of CsA.

6.2.3.3. Respirometry and oxygen uptake rate

20×10^6 cells were cultured in a 250 mL glass baffled spinner flask containing 100 mL of complete culture medium in the presence of 25 µM of AT38 or 25 µM of $NaNO_2$ or 50 µM $NaNO_3$. To investigate whether NO-mediated inhibition of Jurkat cell respiration is reversible, 10 µM of hemoglobin (Hb) were added in the medium after 3 h of culture in the presence of AT38. Humidified gas mixture (400 mL/min, 95% air / 5% CO_2) was fed by surface aeration and medium was magnetically agitated at 60 RPM. Culture medium was circulated in an in-house 316 stainless steel chamber containing a dissolved oxygen (DO) probe (Ingold, Urdorf, Switzerland) and a pH probe (Fisher) by a peristaltic pump (Cole Parmer, Montreal, Quebec, Canada) at a constant flow rate of 3.0 mL/min. Data were recorded by an acquisition system (Virgo, Longueuil, Quebec, Canada) and a mass balance on oxygen was performed to calculate the oxygen uptake rate (OUR).

6.2.3.4. Assays

Glucose and lactate concentrations in supernatants were measured using a 2700 SELECT biochemistry analyser (YSI Inc, Ohio). IL-2 concentration was assessed according to manufacturer recommendations.

6.2.3.5. Nucleotides determinations

The extraction protocol was based on the method developed by Ryll and Wagner (Ryll & Wagner, 1991). Briefly, 4×10^6 viable cells were extracted twice with 0.5 mL (each) of 0.5 M Perchloric Acid solution and neutralized by 0.3 mL of a 2 M $KHCO_3$ solution. Nucleotides concentrations were then determined by high performance ion-pairing liquid chromatography-electrospray ionization mass spectrometry using a HPLC-MS (Waters, Milford, MA). Nucleotides were separated on a Symmetry C_{18} column (150*2.1 mm, 3.5 µm) (Waters) and a Security C_{18} guard-column (Phenomenex, Torrance, CA). Mobile phase consisted in Buffer A: 10 mM Ammonium acetate, 15 mM DMHA, pH 7.00 and Buffer B: 40% (v/v) Acetonitrile in water. Flow rate was set at 0.3 mL/min using the following gradient: 0-10 min at 15% B, 10-11 min linear gradient from 15 to 30% B, 11-30 min at 30% B, 30-35 min linear gradient from 30 to 70% B, 35-40 min at 70% B, 40-41 min linear gradient from 70 to 15% B and 41-50 min at 15% B.

6.2.3.6. Detection of apoptotic versus necrotic cells

The cell death process was distinguished using a PromoKine Apoptotic/Necrotic/Healthy Cells Detection Kit (PromoCell). Briefly, healthy, apoptotic and necrotic cells were stained with

Hoechst 33342, Fluorescein (FITC) and Ethidium Homodimer I, respectively. Fluorescence was detected by an inverted fluorescence microscope Axiovert S100TV (Carl Zeiss Canada, North York, Ontario, Canada) equipped with a mercury lamp and an adequate set of filters. Images were taken with a QICAM Fast 1394 camera (QImaging) and acquired with the NORTHERN ECLIPSE image acquisition software (Empix imaging).

6.2.3.7. GLUT-1 and PFK-1 mRNA assay

Total RNA was extracted and purified using the GenElute Mammalian Total RNA Miniprep Kit (Sigma) and quantified by a BioAnalyzer according to manufacturer's recommendations. First, 5 µg of RNA was denatured at 75 °C for 5 min, then 0.5 µg of oligodT and 10 ng of dNTP were added and the total volume was adjusted to 12 µL by ddH_2O and allowed to anneal to RNA for 3 min on ice. Reverse transcription was performed with 200 U of Moloney Murine Leukemia Virus Reverse Transcriptase, in the presence of 40 U RNAse inhibitor and 0.2 µmol DTT and the final volume was adjusted to 20 µl using the 5X buffer supplied with the enzyme (all from Invitrogen, Canada). The reaction proceeded for 1 h at 37 °C. Reverse transcriptase was then inhibited for 5 min at 95 °C and then for 1 min at 4 °C.

PCR reactions were performed in the Genomics core facility of the IRIC (Université de Montréal) for 384 well plate formats were performed using 2 µl of cDNA samples (5-25 ng), 5 µl of the Fast Universal qPCR MasterMix (Applied Biosystems), 2 µM of each primer and 1 µM of a UPL probe (probes 67 and 76 for GLUT-1 and PFK-1 genes, respectively) in a total volume of 10 µl. The ABI PRISM® 7900HT Sequence Detection System (Applied Biosystems) was used to detect the amplification level and was programmed with an initial step of 3 minutes at 95ºC, followed by 45 cycles of: 5 s at 95ºC and 30 s at 60ºC.

HPRT and TBP were used as housekeeping genes and the following primers for the target genes were used:

Glut-1 For: GGTTGTGCCATACTCATGACC

Gut-1 Rev: CAGATAGGACATCCAGGGTAGC

PFK1 For: TCAGACCCCCGGTATCTAAG

PFK1 Rev: AGCGAACAGCAGCATTCAT

6.2.3.8. Statistical analysis

Measurements from individual cultures were always performed in triplicate. The results are expressed as the mean ± standard error of the mean (SEM) for three different culture preparations.

6.2.4. Results

6.2.4.1. AT38, $NaNO_2$ and $NaNO_3$ cytotoxicity assays

Exposure of Jurkat cells to $NaNO_2$, $NaNO_3$ and AT38 resulted in a time- and concentration-dependent inhibition of cell proliferation and viability (Figure 6-1). Cell density was decreased at a rate of 0.075 ± 0.002 10^6cells.mL^{-1}.h^{-1} in the presence of 25 µM of $NaNO_2$ between 24 and 32 h; whereas the rates of decrease in the presence of 50 and 75 µM of $NaNO_2$ were practically similar (i.e. 0.117 ± 0.009 and 0.104 ± 0.007 10^6cells.mL^{-1}.h^{-1}, respectively). This suggests that a concentration of 50 µM of $NaNO_2$ is sufficient to inhibit cell proliferation.

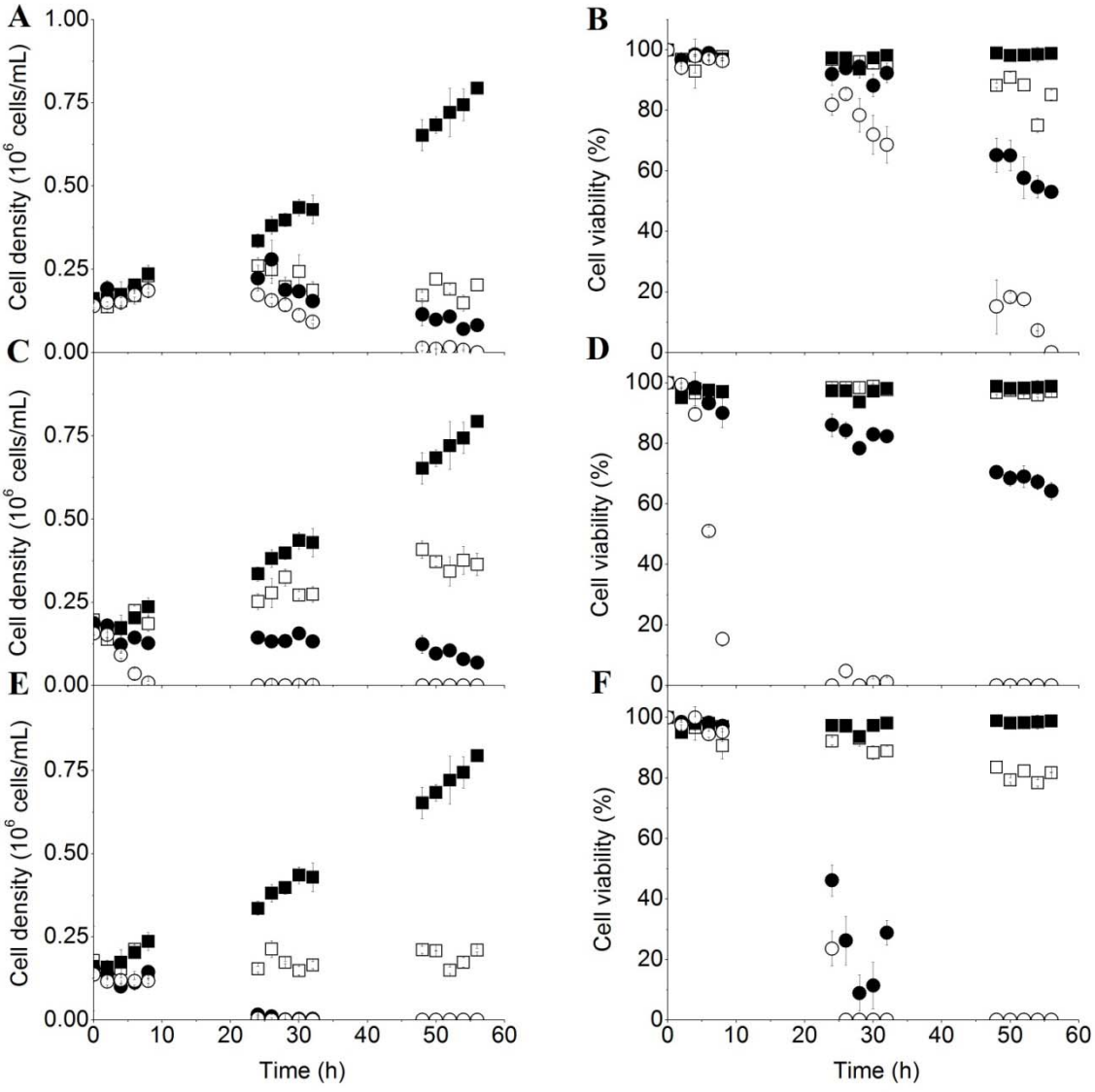

Figure 6-1: Dose and time -dependent effects of $NaNO_2$, $NaNO_3$ and AT38 on Jurkat cells.

Cell density (left panel) and viability (right panel) by the Trypan Blue assay compared to the control culture (■). Symbols (□), (●) and (○) correspond respectively to: A. and B. 25, 50 and 75 µM of $NaNO_2$; C. and D. 50, 100 and 200 µM of $NaNO_3$; E. and F. 25, 50 and 100 µM of AT38 dissolved in 1% v/v DMSO. A concentration of 25 µM of $NaNO_2$ and AT38 were sufficient to inhibit Jurkat cell proliferation within the first day of treatment while maintaining more than 80%

of cell viability; whereas a concentration of 50 μM of $NaNO_3$ was required to report similar effects.

However, cell viability was decreased at higher rate in the presence of 75 μM when compared to that measured in the presence of 25 or 50 μM of nitrite. Similarly, $NaNO_3$ and AT38 decreased the cell accumulation rate as the concentration of nitrate or NO donor is increased. Specifically, 50 μM of $NaNO_2$ or AT38 were sufficient to inhibit Jurkat cell proliferation within 10 hours and induce 50% of mortality, whereas concentrations higher than 100 μM of $NaNO_3$ were required to induce similar effects. We thus selected intermediate concentrations (25 μM of $NaNO_2$ and AT38 and 50 μM of $NaNO_3$) to enable studying long-term (36 hours) effects of NO and of its derivatives on Jurkat cells.

The inhibition of Jurkat cell proliferation (Figure 6-2A) and the induction of cell death (Figure 6- 2B) by NO, nitrite and nitrate donors were observed after 15 hours. This coincided with a decrease of the specific cell concentration in pyrimidines from 2.45 ± 0.24 fmol/cell in the control culture to 1.31 ± 0.09 fmol/cell in the treated groups (Figure 6- 2C). In fact, pyrimidines, which include CTP, UTP and UDP-N-Acetyl-glucosamine and galactosamine (UDPGNAc), are involved in different anabolic reactions and metabolic processes that are mostly growth-related such as membrane lipid synthesis, DNA strand break repair and protein glycosylation. Simultaneous decrease of the specific cell concentration in pyrimidines and the UTP-to-ATP ratio (Figure 6-2D), which is a marker of protein production (Chou, et al., 1984), confirmed the cytotoxic effects of NO, nitrite and nitrate donors on Jurkat cells.

In contrast to the use of AT38, DMSO (1% v/v), SA and AT55 do not induce NO formation and failed to modulate cell density and viability (data not shown). Moreover, effects of $NaNO_2$

and $NaNO_3$ on cells cannot be associated to the release of sodium at micromolecular levels since the initial medium contained already about 0.13 M of sodium-rich inorganic salts.

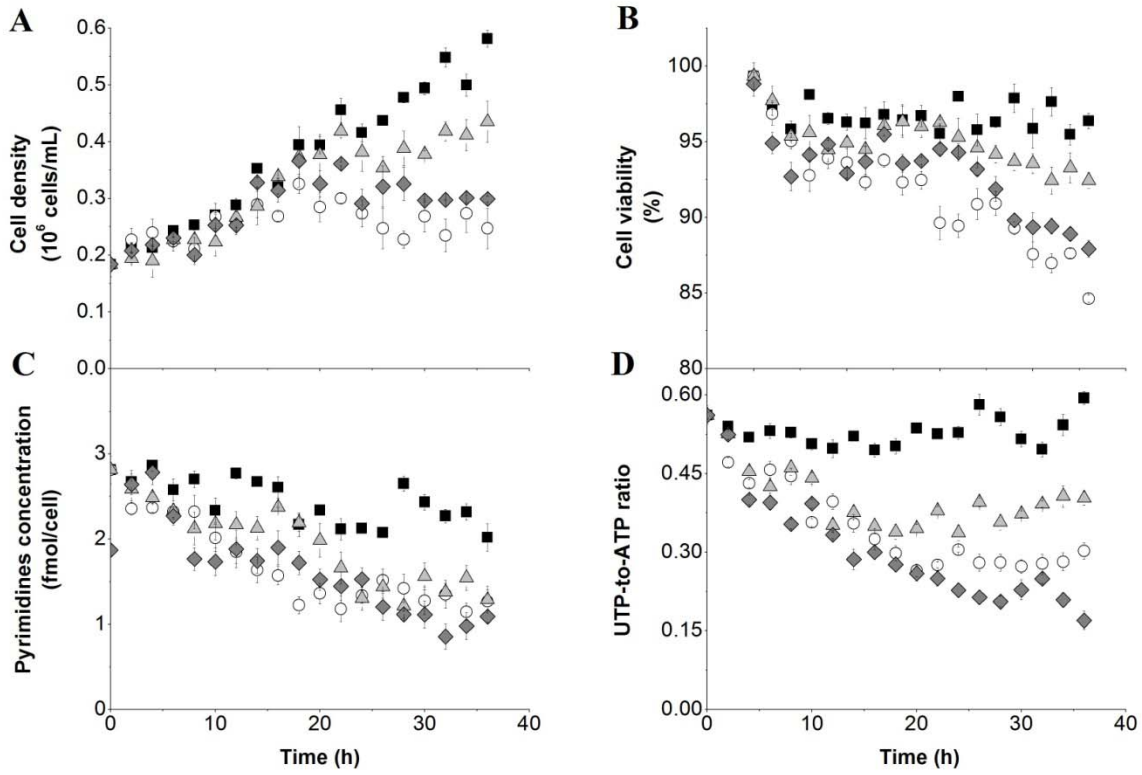

Figure 6-2: Effects of chosen concentrations on Jurkat cells.

25 µM $NaNO_2$ (○), 50 µM $NaNO_3$ (▲), 25 µM AT38 (♦) versus control culture (■). A. Cell density, B. cell viability, C. specific pyrimidines cell concentration, D. UTP-to-ATP ratio. 4 millions cells were extracted by 1 mL of 0.5 M PCA and neutralized by 0.3 mL of $KHCO_3$, and extracts were analyzed by HPLC-MS. AT38-induced inhibition of cell proliferation was accompanied by the decrease of pyrimidine concentration and the UTP-to-ATP ratio suggesting the arrest of growth-related processes.

6.2.4.2. Effects of AT38, $NaNO_2$ and $NaNO_3$ on Jurkat cell respiration and bioenergetics

On-line monitoring of dissolved oxygen (DO) concentration in Jurkat cell cultures treated with NO, nitrite and nitrate donors showed that AT38 and $NaNO_2$ inhibit cell respiration within the first 2 hours, whereas $NaNO_3$ induced similar effect only after 5 hours (Figure 6-3). Although the AT38- and $NaNO_2$-induced inhibition of cell proliferation has been observed after 15 hours of treatment, the DO concentration decreased rapidly during the first 2 hours until a stable value of about 65% due to the decrease of the specific oxygen uptake rate. Whereas, the DO concentration in the control culture decreased continuously due to the increase of cell density.

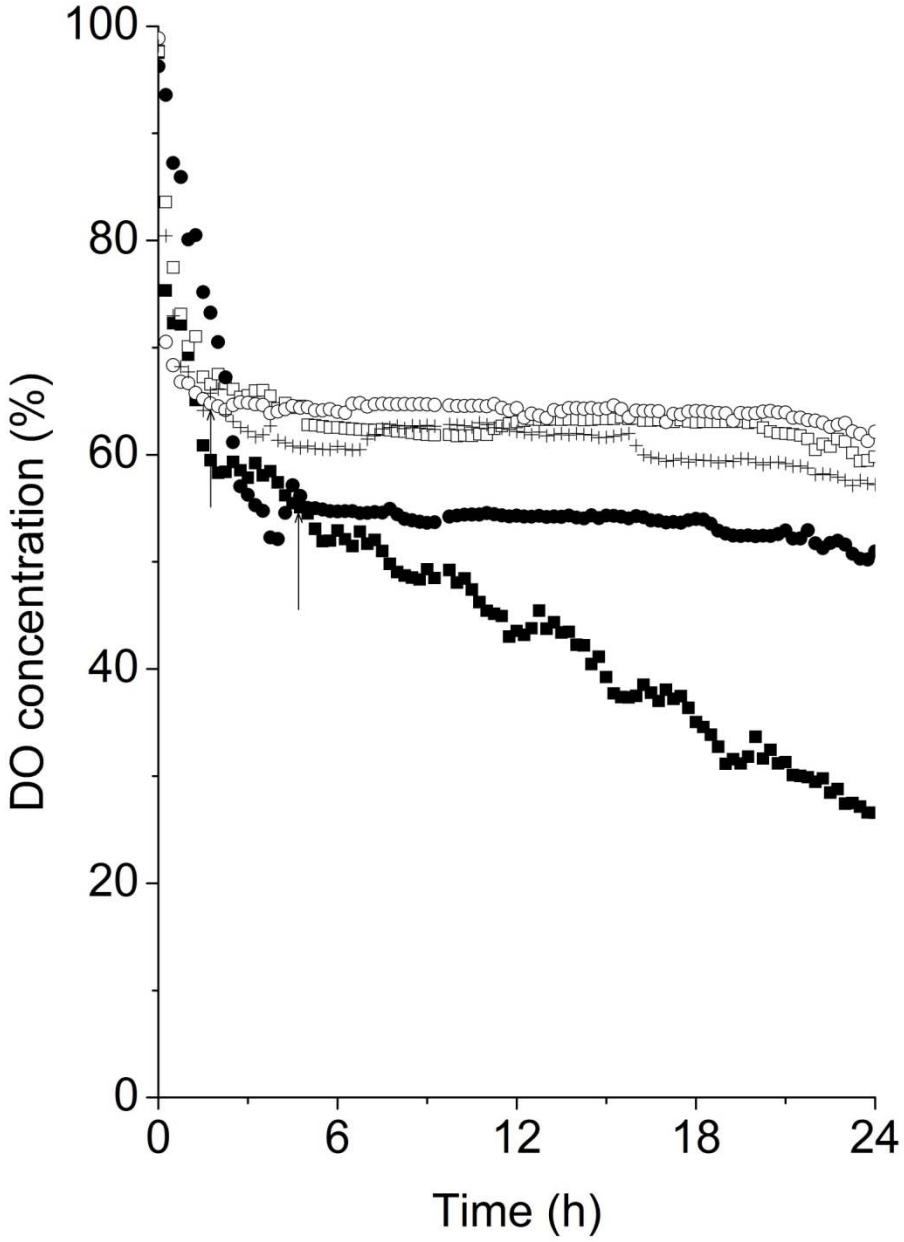

Figure 6-3 : Dissolved oxygen concentration in Jurkat cell cultures.

In the presence of 25 µM $NaNO_2$ (□), 50 µM $NaNO_3$ (●), 25 µM AT38 (○) versus control culture (■). Jurkat cells were cultured in a 250 mL spinner magnetically agitated at 60 RPM, 5% CO_2 / 95% air humidified gas mixture was fed by surface aeration and DO concentration was measured

by a polarographic DO probe. Cell respiration was inhibited irreversibly within 2 to 3 hours since Hb, a NO scavenger, failed to recover cell respiration in the presence of AT38 (+).

Inhibition of cell respiration was confirmed by the decrease of the ATP-to-ADP ratio, which is known as a marker of respiration (Reich & Sel'Kov, 1981). Indeed, ATP-to-ADP ratio in the control culture decreased within the first minutes following experiment initiation due to various stresses caused by cell manipulation and inoculation, and then increased progressively during the exponential growth phase until a maximal value of 3.79 ± 0.19. However, the treated groups were characterized by a continuous decrease of the ATP-to-ADP ratio until stabilization at 0.97 ± 0.10 (Figure 6-4A).

Inhibition of Jurkat cell respiration was accompanied by the decrease of specific ATP concentration from 3.73 ± 0.39 fmol/cell in the control culture to similar concentrations of 2.53 ± 0.25, 2.43 ± 0.20 and 2.63 ± 0.20 fmol/cell in AT38, $NaNO_2$ and $NaNO_3$ -treated groups, respectively (Figure 6-4B). Although the decrease of specific ATP and pyrimidine concentrations, NO, NO_2 an NO_3 donors triggered an increase of the NTP ratio ((ATP+GTP)/(UTP+CTP)), which represents the energy-related nucleotides-to-the anabolism-related nucleotides ratio (Figure 6-4C) (Ryll & Wagner, 1992). Indeed, NTP ratio for the control culture decreased progressively during the exponential phase, suggesting the activation of the metabolic activity. However, this ratio started to increase after 10 hours of treatment to reach a maximal value of 4.70 ± 0.12 for AT38 and $NaNO_2$ treated groups, and 3.47 ± 0.16 in the presence of $NaNO_3$ after 20 hours; thus announcing the deterioration of the overall metabolic activity.

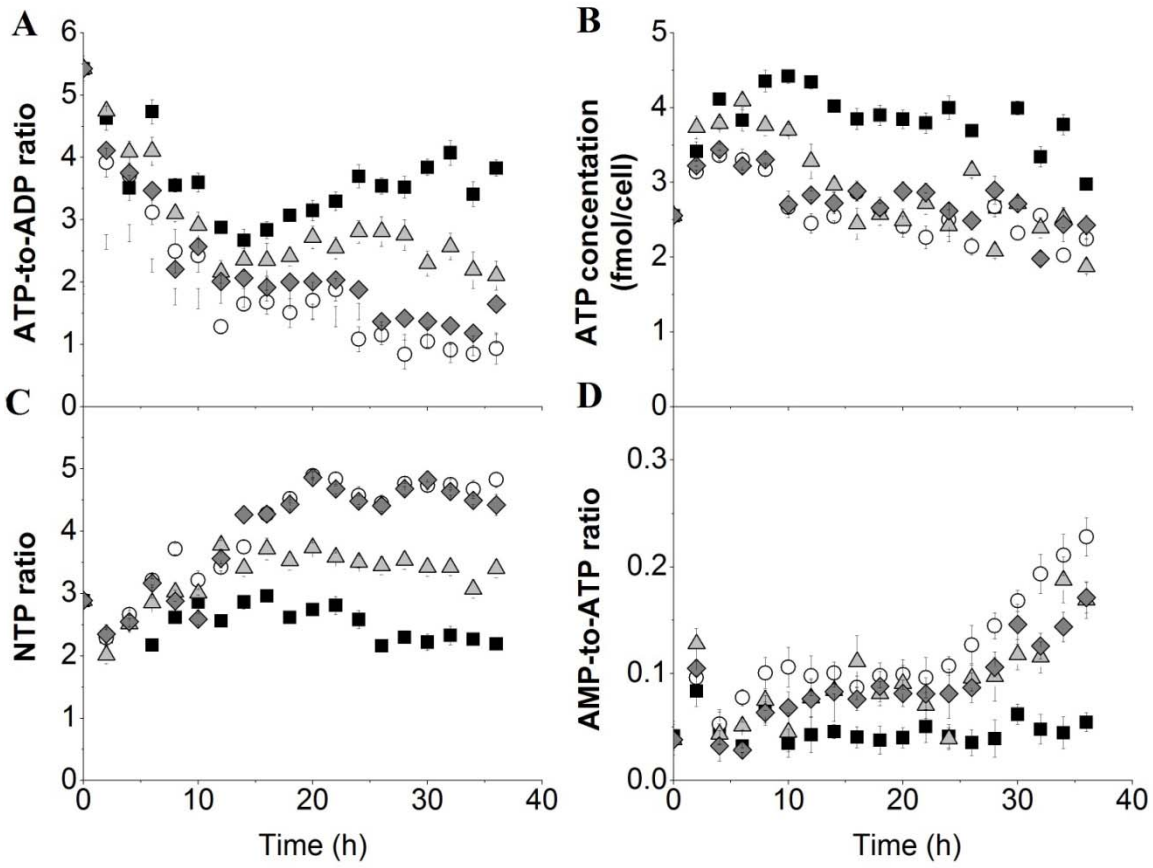

Figure 6-4 : Modulation of Jurkat cell bioenergetics by AT38, NaNO2 and NaNO3.

A. ATP-to-ADP ratio, B. specific ATP cell concentration, C. NTP ratio, D. AMP-to-ATP ratio. Presence of NO, nitrite and nitrate donors lead to a deterioration of the overall metabolic activity although a stimulation of glycolysis has been noticed. Inhibition of cell respiration is revealed by the decrease of the ATP-to-ADP ratio and the simultaneous decrease of the intracellular ATP content and the accumulation of ADP. Same symbols as in Figure 6-2.

6.2.4.3. NO and derivatives modulate Jurkat cell metabolic profile and death process

Although the addition of NO and its derivatives resulted in a decrease of cell specific concentration in ATP, glycolysis was stimulated in all treated groups, as revealed by the increase of the glucose consumption and lactate production rates (Table 6-1).

	Control culture	**$NaNO_2$-treated culture**	**$NaNO_3$-treated culture**	**AT38-treated culture**
Maximum growth rate	0.031±0.002	0.005±0.0002	0.025±0.004	0.013±0.002
Glucose consumption rate	0.507±0.021	10.498±0.493	0.825±0.058	2.920±0.030
Lactate production rate	0.538±0.055	6.405±0.288	0.990±0.086	2.770±0.071

Table 6-1 : Effects of $NaNO_2$, $NaNO_3$ and AT38 on Jurkat cell nutritional profile.

Maximum growth rate (μ, h^{-1}) and glucose consumption and lactate production rates ($nmol.cell^{-1}.h^{-1}$). Glucose uptake and lactate accumulation were up-regulated in the presence of NO and derivatives in Jurkat cell cultures.

In fact, glucose uptake was increased by 20 and 6 -fold increase in the presence of $NaNO_2$ and AT38, respectively, compared to the control culture. Furthermore, exposure of Jurkat cells to NO and nitrite donors resulted in a slight enhancement of GLUT-1 mRNA expression at different culture times until a maximal value of about 125% of that for the control culture (Figure 6-5A; n = 3). Similarly, the gene expression of PFK-1, which is known as a master regulator of glycolysis, was increased (115%) in the treated groups (Figure 6-5B, n = 3). This was accompanied by a 3 to 4 -fold increase of the AMP-to-ATP ratio (Figure 6-4D), which is considered as a marker of glycolysis stimulation (Cidad, et al., 2004). Thus, as ATP production

via oxidative phosphorylation was inhibited by NO and its derivatives, our results suggest that Jurkat cells have switched to glycolytic metabolism to support ATP-consuming reactions.

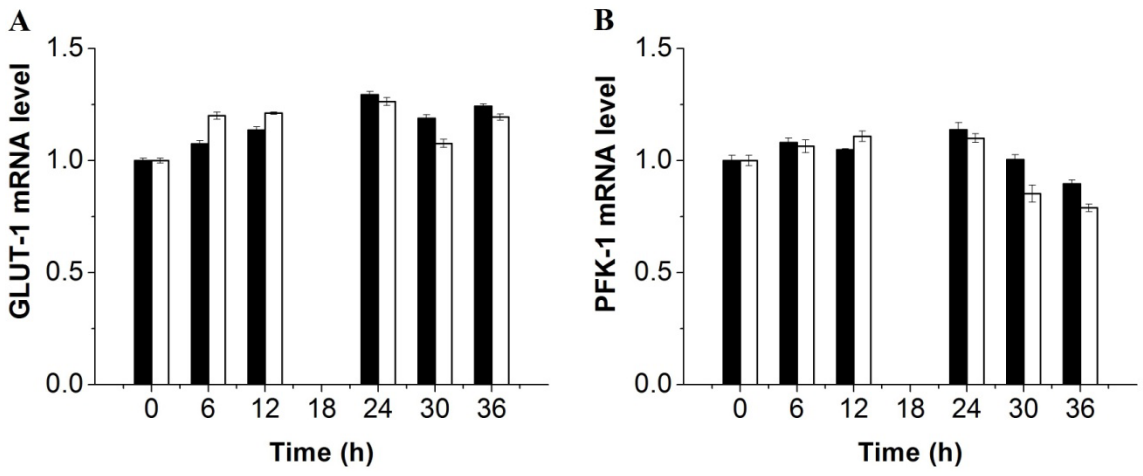

Figure 6-5 : qRT-PCR analysis of GLUT-1 (A) and PFK-1 (B) gene expression levels at different culture times.

In addition to the increase of glucose consumption and lactate production rates, GLUT-1 and PFK-1 gene expression was up-regulated in the presence of $NaNO_2$ (black bar) and AT38 (white bar).

Moreover, concomitant activation of apoptosis mechanisms (Li, et al., 1997) and the deterioration of overall metabolic activity induced cell death (Figure 6-2B). Investigation of cell death process by means of specific dyes (Hoechst 33342, Fluorescein and Ethidium Homodimer I) demonstrated that apoptosis was activated during the first 12 hours in the presence of $NaNO_2$ and AT38, and that death process switched from apoptosis to necrosis after 24 hours (Figure 6-6). The switch of cell death process coincided with the decrease of glucose consumption rate

from 0.386 ± 0.009 $mM.h^{-1}$ to 0.161 ± 0.011 $mM.h^{-1}$, and the stabilization of ATP concentration (Figure 6-4B).

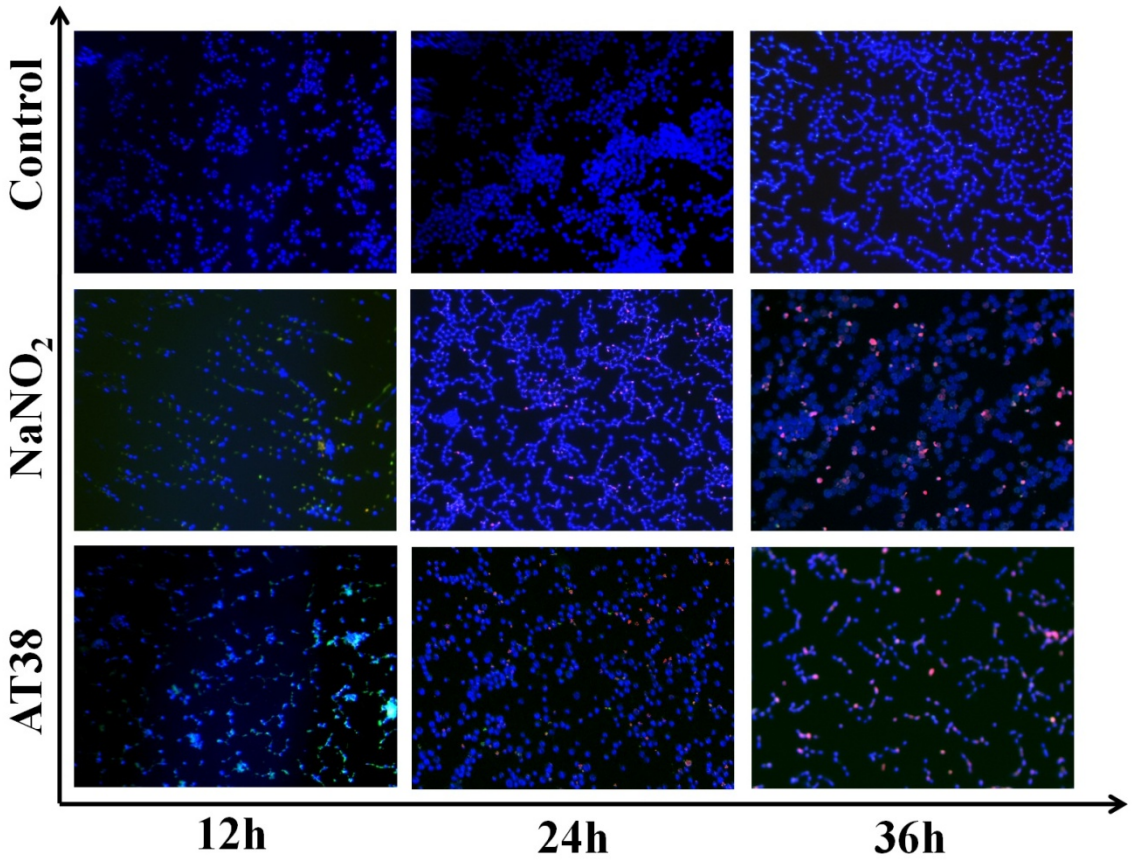

Figure 6-6 : NO switches cell death process from apoptosis into necrosis.

Viable (blue), apoptotic (green) and necrotic (red) cells were stained by specific dyes (see Materials and Methods section). In the $NaNO_2$ and AT38 -treated groups, dead cells were 90% apoptotic within the first 24 hours and then necrosis was promoted due to lack of energy supply.

6.2.4.4. AT38 effects on CsA pre-treated Jurkat cells

Incubation of Jurkat cells in a 5 µM CsA -enriched culture medium for 30 min showed to abrogate ConA-induced IL-2 production (data not shown) as previously reported by Takahashi and coworkers (Takahashi et al., 2009). Culturing Jurkat cells in the presence of CsA slightly decreased the specific growth rate (µ) from 0.036 ± 0.003 h^{-1} in the control culture to 0.032 ± 0.001 h^{-1} without any significant effect on cell viability (Figure 6-7). Whereas, pre-treating Jurkat cells by CsA prevented the AT38-induced inhibition of cell proliferation since µ increased from 0.012 ± 0.001 h^{-1} in the AT38-treated group to 0.024 ± 0.007 h^{-1}. Moreover, CsA showed to inhibit the AT38-induced cell death since cell viability in the presence of CsA after 34 hours was still 15% higher than that for the AT38-treated group.

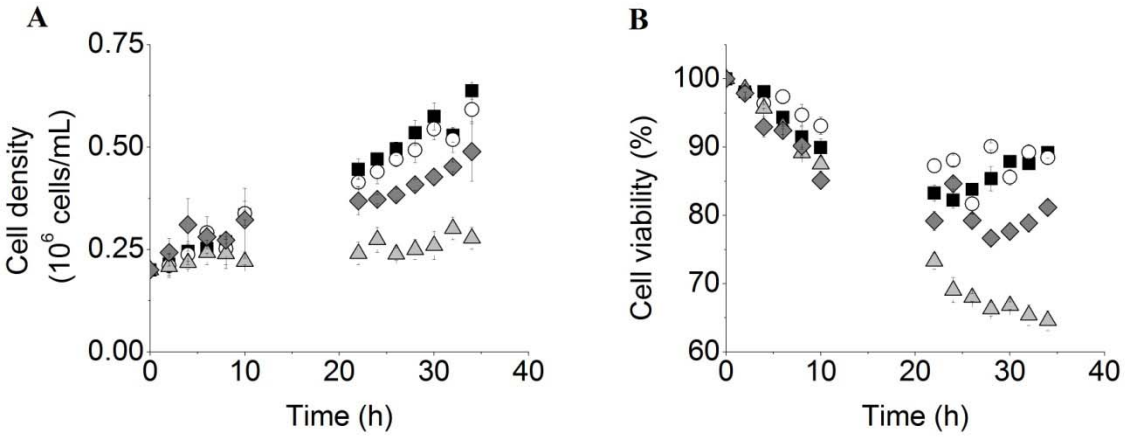

Figure 6-7 : Pre-treating Jurkat cells with low dose of CsA attenuates AT38 effects.

A. Cell density, B. cell viability. Ctrl (■) vs 5 µM CsA pre-treated Jurkat cells (○) vs 25 µM AT38 (▲) vs 5 µM pre-treated Jurkat cells in the presence of 25 µM AT38 (♦). Pre-treated Jurkat

cells with low dose of CsA (5 μM) within short exposition time (30 min) decreases AT38-induced inhibition of Jurkat proliferation and loss of cell viability.

6.2.5. Discussion

Nitrite coupled to hydrogen peroxide has been shown to be responsible for nitrosylating tyrosine residues of cytochrome *c*, and thus negatively affect the mitochondrial respiratory chain and induce apoptotic mechanisms (Castro, Eiserich, Sweeney, Radi, & Freeman, 2004); whereas nitrate has been usually considered as a biologically inert anion (Bruno, Parker, & Kiel, 1994). In this study, we showed that long-term exposure of Jurkat cells to high (≥ 50 μM) $NaNO_3$ concentrations induced similar effects triggered by $NaNO_2$ and AT38 (25 μM, both). First, these delayed effects can be probably due to different diffusion rates between NO, nitrite and nitrate. In fact, NO is characterized by its rapid, active and facilitated diffusion from its point of synthesis (a diffusion coefficient 1.4 times that of oxygen at 37ºC) as well as its ability to easily permeate cell membranes without the need for extracellular NO transporters (Mocellin, et al., 2007). In comparison, nitrite and nitrate anions cross the phospholipid membrane via anion exchanger proteins or by proton-facilitated diffusion of undissociated nitrous (HNO_2) and nitric (HNO_3) acid, respectively. Due to different acid dissociation constants, diffusion of HNO_2 across cell membrane at physiological pH is facilitated compared to that of HNO_3, which requires acidic pH for optimal diffusion and dissociation (Samouilov, Woldman, Zweier, & Khramtsov, 2007). However, it is important to note that, *in vivo*, the acidity of the tumoural microenvironment ensures rapid diffusion of both anions. Second, the delayed effects of nitrate are probably associated to the time and concentration -dependent nitrate to nitrite reduction (Jansson et al., 2008).

The central finding discussed herein is that AT38 rapidly inhibits Jurkat cell respiration in an irreversible manner resulting in 50% depletion of intracellular ATP content and modulates cell death process dependently on glycolytic ATP turnover capacity. Although AT38 has two pharmacologically active moieties, its effects on mitochondrial functions are strictly related to the release of NO, since DMSO (1% v/v), SA and AT55 failed to alter Jurkat cell bioenergetics. Moreover, NO scavenging by Hb has greatly prevented the inhibition of cell respiration and proliferation as well as the loss of cell viability.

Indeed, exposure of immune cells to low NO-donor concentrations (1-10 μM) triggered a reversible interaction with cytochrome *c* oxidase (complex IV) leading to a transitory inhibition of cell respiration and oxidative phosphorylation process; whereas higher concentrations (50-100 μM) induced an irreversible S-nitrosylation-dependent inhibition of complex I of the mitochondrial respiratory chain (Clementi, et al., 1998; Paxinou et al., 2001). In this study, we used an intermediate concentration (25 μM) of AT38 that generated low amount of NO comparable to levels endogenously produced by iNOS (~ 1 μM) (Mateo, Garcia-Lecea, Cadenas, Hernandez, & Moncada, 2003). These conditions led to a situation of metabolic hypoxia; the inhibition of Jurkat cell respiration was rapid (within 3 hours) and irreversible suggesting persistent alteration of complex I activity and a decrease of its affinity for oxygen, and this despite the presence of NO scavenger and oxygen availability.

Inhibition of cell respiration was accompanied by the stimulation of glycolysis, as measured by increased glucose uptake and lactate accumulation rates, and also by the rise of cell ADP and AMP concentrations, which resulted in the reduction of ATP-to-ADP ratio and about 5-fold increase of AMP-to-ATP ratio. Taken together, these biomarkers suggest that a Pasteur Effect (Rapoport, 1986) occurred in NO-treated Jurkat cells. In this work, we demonstrated that long-term exposure of Jurkat cells also leads to the up-regulation of PFK-1 gene expression level

to ensure the increase of glycolytic metabolism. In accordance with our results, NCX-4016, a NO-releasing derivative of acetylsalicylic acid, was shown to decrease TCA cycle intermediate concentrations and to increase the glycolytic rate via the enhancement of glucose uptake and PFK-1 activity, resulting in the conversion of about 70% of glucose into lactate (Fiorucci, et al., 2004). However, the stimulation of glycolysis was not sufficient to compensate for the decreased energy production caused by the inhibition of oxidative phosphorylation. Moreover, the NO-induced release and activation of pro-death caspases prevented the accumulation of glycolytic ATP because of the high energetic demand of apoptosis mechanisms (Elmore, 2007). Thus, the depletion of intracellular ATP under a glucose concentration of 12.65 ± 0.08 mM coincided with the switch from apoptosis into necrosis. This result is in agreement with previous work of Leist et al who showed that NO can inhibit apoptosis in Jurkat cells which are dependent on mitochondrial energy production and induce necrosis with delayed onset (Leist, et al., 1999b). *In vivo*, low glucose and oxygen concentration in the tumoural microenvironment will favour T-cell death by necrosis, whereas tumour cells can compensate for inefficient glycolysis and oxidative phosphorylation –related energy production by metabolizing other carbon sources such as lactate, amino acids ,etc. (Ganapathy, Thangaraju, & Prasad, 2009) . However, T-cell necrosis is always associated to an inflammatory response that can promote tumour progression and decrease the efficiency of anti-cancer therapies (Jin, DiPaola, Mathew, & White, 2007). These results might have clinical relevance; since high levels of ATP are required to sustain apoptosis, it seems likely that maintaining a high bioenergetic status of immune cells might help to reduce the inflammatory edge in the tumour microenvironment and so tumour invasion.

Moreover, it has been well described that the opening of the MPTP is a key event in apoptosis, and pore closure results in mitochondria repolarization and so the recovering of energy-linked functions. MTP opening can be potently inhibited by lowering intracellular pH

(between 6.5 and 7) and by CsA (Bernardi, 1996). In our study, we showed that pre-treating Jurkat cells with CsA (5 μM for 30 min) abrogated ConA-induced IL-2 production and attenuated AT38 toxicity. In fact, CsA has been reported to interfere with transcription of early T-cell activation genes thereby inhibiting the production of IL-2 as well as of other lymphokines and growth factors (Herold, Lancki, Moldwin, & Fitch, 1986; Jansson, et al., 2008). Sato et al have showed that CsA significantly increased the number of living cells in SNAP-treated RGC-5 cells in comparison to cell-permeable radical scavenger (TEMPOL) and general caspase inhibitor (Z-VAD-FMK) who partially protected RGC-5 cells against SNAP-mediated cell death (Sato et al., 2009). However, literature has reported several CsA-related side effects such as nephrotoxicity, gastrotoxicity, hypertension, heperlipidemia, neurophaties and diabetes type II (Erdmann et al.; Takahashi, et al., 2009). Therefore, there is a need for novel cytokine regulating – MPTP blockers with fewer adverse effects.

In conclusion, this study demonstrated that NO, nitrite and nitrate negatively affect Jurkat cells at different steps. The presence of NO and its derivatives triggers irreversible and rapid (within 2 h) inhibition of Jurkat cell respiration. This was followed by the arrest of anabolic processes, as revealed by the decrease of growth-related biomolecules, leading to the inhibition of Jurkat cell proliferation (after 15 h). Although the inhibition of oxidative phosphorylation was followed by glycolysis stimulation, glycolytic ATP was continuously depleted since it was devoted to apoptosis mechanisms. Under a glucose threshold, cell death was switched into necrosis around 24 h. To overcome the AT38 associated cytotoxicity on immune cells, we confirmed the ability of CsA to prevent NO-induced inhibition of Jurkat cell proliferation suggesting the potential of CsA+NSAIDs combination as a non invasive anti-cancer immune-based therapy.

6.2.6. Aknowledgements

Authors would like to thank the Canada Research Chair program and NSERC for funding, as well as Dr. Anis Klouz, for helpful discussion and advices on the use of CsA.

6.2.7. References

1. Maciver NJ, Jacobs SR, Wieman HL, Wofford JA, Coloff JL, Rathmell JC. Glucose metabolism in lymphocytes is a regulated process with significant effects on immune cell function and survival. *J Leukoc Biol* 2008; **84**(4)**:** 949-57.

2. Buttgereit F, Burmester GR, Brand MD. Bioenergetics of immune functions: fundamental and therapeutic aspects. *Immunol Today* 2000; **21**(4)**:** 192-9.

3. Frauwirth KA, Riley JL, Harris MH, Parry RV, Rathmell JC, Plas DR *et al.* The CD28 signaling pathway regulates glucose metabolism. *Immunity* 2002; **16**(6)**:** 769-77.

4. Raghunand N, Gatenby RA, Gillies RJ. Microenvironmental and cellular consequences of altered blood flow in tumours. *Br J Radiol* 2003; **76 Spec No 1:** S11-22.

5. Serafini, Borrello I, Bronte V. Myeloid suppressor cells in cancer: Recruitment, phenotype, properties, and mechanisms of immune suppression. *Semin Cancer Biol* 2006; **16**(1)**:** 53-65.

6. Mocellin S, Bronte V, Nitti D. Nitric oxide, a double edged sword in cancer biology: searching for therapeutic opporuinities. *Medicinal Research reviews* 2007; **27**(3)**:** 317-352.

7. Ignarro LJ, Fukuto JM, Griscavage JM, Rogers NE, Byrns RE. Oxidation of nitric oxide in aqueous solution to nitrite but not nitrate: comparison with enzymatically formed nitric oxide from L-arginine. *Proc Natl Acad Sci U S A* 1993; **90**(17)**:** 8103-7.

8. Clementi E, Brown GC, Feelisch M, Moncada S. Persistent inhibition of cell respiration by nitric oxide: crucial role of S-nitrosylation of mitochondrial complex I and protective action of glutathione. *Proc Natl Acad Sci U S A* 1998; **95**(13)**:** 7631-6.

9. Li P, Nijhawan D, Budihardjo I, Srinivasula SM, Ahmad M, Alnemri ES *et al.* Cytochrome c and dATP-dependent formation of Apaf-1/caspase-9 complex initiates an apoptotic protease cascade. *Cell* 1997; **91**(4)**:** 479-89.

10. Kuida K, Haydar TF, Kuan CY, Gu Y, Taya C, Karasuyama H *et al.* Reduced apoptosis and cytochrome c-mediated caspase activation in mice lacking caspase 9. *Cell* 1998; **94**(3)**:** 325-37.

11. Leist M, Single B, Naumann H, Fava E, Simon B, Kuhnle S *et al.* Nitric oxide inhibits execution of apoptosis at two distinct ATP-dependent steps upstream and downstream of mitochondrial cytochrome c release. *Biochem Biophys Res Commun* 1999; **258**(1)**:** 215-21.

12. Leist M, Single B, Naumann H, Fava E, Simon B, Kuhnle S *et al.* Inhibition of mitochondrial ATP generation by nitric oxide switches apoptosis to necrosis. *Exp Cell Res* 1999; **249**(2)**:** 396-403.

13. Nath N, Labaze G, Rigas B, Kashfi K. NO-donating aspirin inhibits the growth of leukemic Jurkat cells and modulates beta-catenin expression. *Biochem Biophys Res Commun* 2005; **326**(1)**:** 93-9.

14. Fiorucci S, Mencarelli A, Distrutti E, Baldoni M, del Soldato P, Morelli A. Nitric oxide regulates immune cell bioenergetic: a mechanism to understand immunomodulatory functions of nitric oxide-releasing anti-inflammatory drugs. *J Immunol* 2004; **173**(2)**:** 874-82.

15. Del Grosso E, Boschi D, Lazzarato L, Cena C, Di Stilo A, Fruttero R *et al.* The furoxan system: design of selective nitric oxide (NO) donor inhibitors of COX-2 endowed with anti-aggregatory and vasodilating activities. *Chem Biodivers* 2005; **2**(7)**:** 886-900.

16. Roy MK, Takenaka M, Kobori M, Nakahara K, Isobe S, Tsushida T. Apoptosis, necrosis and cell proliferation-inhibition by cyclosporine A in U937 cells (a human monocytic cell line). *Pharmacol Res* 2006; **53**(3)**:** 293-302.

17. Ryll T, Wagner R. Improved ion-pair high-performance liquid chromatographic method for the quantification of a wide variety of nucleotides and sugar-nucleotides in animal cells. *J Chromatogr* 1991; **570**(1)**:** 77-88.

18. Chou IN, Zeiger J, Rapaport E. Imbalance of total cellular nucleotide pools and mechanism of the colchicine-induced cell activation. *Proc Natl Acad Sci U S A* 1984; **81**(8)**:** 2401-5.

19. Reich JG, Sel'Kov EE. *Energy metabolism of the cell - a theoritical treatise*: London, 1981.

20. Ryll T, Wagner R. Intracellular ribonucleotide pools as a tool for monitoring the physiological state of in vitro cultivated mammalian cells during production processes. *Biotechnol Bioeng* 1992; **40**(8)**:** 934-46.

21. Cidad P, Almeida A, Bolanos JP. Inhibition of mitochondrial respiration by nitric oxide rapidly stimulates cytoprotective GLUT3-mediated glucose uptake through 5'-AMP-activated protein kinase. *Biochem J* 2004; **384**(Pt 3)**:** 629-36.

22. Takahashi K, Murakami M, Hosaka K, Kikuchi H, Oshima Y, Kubohara Y. Regulation of IL-2 production in Jurkat cells by Dictyostelium-derived factors. *Life Sci* 2009; **85**(11-12)**:** 438-43.

23. Castro L, Eiserich JP, Sweeney S, Radi R, Freeman BA. Cytochrome c: a catalyst and target of nitrite-hydrogen peroxide-dependent protein nitration. *Arch Biochem Biophys* 2004; **421**(1)**:** 99-107.

24. Bruno JG, Parker JE, Kiel JL. Plant nitrate reductase gene fragments enhance nitrite production in activated murine macrophage cell lines. *Biochem Biophys Res Commun* 1994; **201**(1)**:** 284-9.

25. Samouilov A, Woldman YY, Zweier JL, Khramtsov VV. Magnetic resonance study of the transmembrane nitrite diffusion. *Nitric Oxide* 2007; **16**(3)**:** 362-70.

26. Jansson EA, Huang L, Malkey R, Govoni M, Nihlen C, Olsson A *et al.* A mammalian functional nitrate reductase that regulates nitrite and nitric oxide homeostasis. *Nat Chem Biol* 2008; **4**(7)**:** 411-7.

27. Paxinou E, Weisse M, Chen Q, Souza JM, Hertkorn C, Selak M *et al.* Dynamic regulation of metabolism and respiration by endogenously produced nitric oxide protects against oxidative stress. *Proc Natl Acad Sci U S A* 2001; **98**(20)**:** 11575-80.

28. Mateo J, Garcia-Lecea M, Cadenas S, Hernandez C, Moncada S. Regulation of hypoxia-inducible factor-1alpha by nitric oxide through mitochondria-dependent and -independent pathways. *Biochem J* 2003; **376**(Pt 2)**:** 537-44.

29. Rapoport SM. *The reticulocyte*, CRC Press, 1986.

30. Elmore S. Apoptosis: a review of programmed cell death. *Toxicol Pathol* 2007; **35**(4)**:** 495-516.

31. Ganapathy V, Thangaraju M, Prasad PD. Nutrient transporters in cancer: relevance to Warburg hypothesis and beyond. *Pharmacol Ther* 2009; **121**(1)**:** 29-40.

32. Jin S, DiPaola RS, Mathew R, White E. Metabolic catastrophe as a means to cancer cell death. *J Cell Sci* 2007; **120**(Pt 3)**:** 379-83.

33. Bernardi P. The permeability transition pore. Control points of a cyclosporin A-sensitive mitochondrial channel involved in cell death. *Biochim Biophys Acta* 1996; **1275**(1-2)**:** 5-9.

34. Herold KC, Lancki DW, Moldwin RL, Fitch FW. Immunosuppressive effects of cyclosporin A on cloned T cells. *J Immunol* 1986; **136**(4)**:** 1315-21.

35. Sato T, Oku H, Tsuruma K, Katsumura K, Shimazawa M, Hara H *et al.* Hypoxia Makes RGC-5 Cells Susceptible to Nitric Oxide. *Invest Ophthalmol Vis Sci* 2009.

36. Erdmann F, Weiwad M, Kilka S, Karanik M, Patzel M, Baumgrass R *et al.* The novel calcineurin inhibitor CN585 has potent immunosuppressive properties in stimulated human T cells. *J Biol Chem*; **285**(3)**:** 1888-98.

CHAPITRE 7. DISCUSSION GÉNÉRALE

Comme il a été précisé antérieurement, les thérapies anti-MDSC conventionnelles ciblent majoritairement les voies de signalisation qui contrôlent leur maturation à partir de précurseurs myéloïdes, leur recrutement dans le microenvionnement tumoral et leurs fonctions immunosuppressives. Cependant, plusieurs voies et facteurs de signalisation, incluant les C/EBPβ, JAK/STAT3, MAPK et PI3-K, sont impliqués dans le processus de maturation des MDSC (Fleetwood, et al., 2005; Marigo, et al., 2010). Les demandes énergétiques associées à l'activation de ces voies de signalisation sont toutefois mal caractérisées. De plus, l'activité de iNOS, surexprimée chez les MDSC, requiert la NADPH comme cofacteur et la synthèse endogène du L-arg nécessite l'hydrolyse de l'ATP (S. M. Morris, Jr., 2004). Dans ce contexte, nous avons étudié, dans le cadre de cette thèse, l'évolution de l'état énergétique cellulaire lors de la maturation des MDSC et de l'acquisition de leur activité immunosuppressive. L'hypothèse ayant guidé ces travaux visait à évaluer le potentiel du contrôle de l'énergétique des MDSC en tant qu'approche immunothérapeutique innovante qui agirait à la fois en amont et en aval de leur maturation. Cette stratégie thérapeutique a déjà montré des résultats prometteurs dans le traitement de certains cas de psoriasis ou d'arythmie cardiaque ainsi que pour la malaria et le diabète, et ce en inhibant la production d'ATP, soit par l'inhibition de l'oxydation des nutriments ou par le découplage de la phosphorylation oxydative (Buttgereit, et al., 2000). Cependant, jusqu'à maintenant, cette approche a été peu exploitée dans le contexte du phénomène d'immunosuppression, nous en avons alors fait l'objectif principal de cette thèse pour élucider son potentiel dans le traitement du cancer.

7.1. Comportement métabolique des MDSC

Compte tenu du fait que l'inhibition de la maturation des MDSC représente une solution d'intérêt permettant de préserver la réponse immunitaire anti-tumorale, une étude exhaustive des besoins énergétiques requis pour le déclenchement des cascades de signalisation impliquées dans le processus de maturation a été effectuée. Pour ce faire, les profils nutritionnel et énergétique des MDSC ont été suivis durant leur maturation, *in vitro*, à partir de cellules de la moelle osseuse traitées par la combinaison de deux cytokines, le GM-CSF et l'IL-6. Cette approche est utilisée pour générer des MDSC semblables à celles qui s'infiltrent dans la tumeur (Marigo, et al., 2010). L'étude des MDSC associées à la tumeur est pertinente puisque ces dernières sont les plus immunosuppressives parmi les différentes sous-populations de MDSC (Dolcetti, et al., 2010), et aussi pour étudier leur influence sur le microenvironnement tumoral.

Nos travaux ont montré que le processus de maturation des MDSC est accompagné par une augmentation des taux de consommation du glucose et de la L-gln. Néanmoins, le glucose internalisé est majoritairement métabolisé à travers la glycolyse et non la PPP. En fait, la phase non-oxydative de la PPP, qui est reliée aux processus anaboliques, n'est pas particulièrement active au vu du faible taux spécifique de croissance observé. Ainsi, la faible quantité de glucose-6-phosphate acheminée à la PPP était principalement métabolisée à travers les réactions oxydatives permettant ainsi la production de NADPH et le réacheminement des intermédiaires vers les dernières réactions de la glycolyse. Ces résultats corroborent ceux retrouvés dans la littérature où il a été montré que l'IL-6 stimule l'activité de l'hexokinase et de la phosphofructokinase via la voie du STAT3, alors que le GM-CSF provoque une augmentation de l'affinité du transporteur du glucose via la voie du PI3-K (Ando, et al., 2010; Dhar-Mascareno, et al., 2003). De plus, malgré la présence abondante d'oxygène dissous dans les conditions *in vitro*, la respiration des MDSC a diminué et la glycolyse anaérobique a été favorisée. En fait, *in vivo*,

les MDSC tumorales expriment le facteur d'induction de l'hypoxie (HIF-1α pour "Hypoxia Induction Factor-1α") parallèlement à l'expression des enzymes iNOS et ARG1 (Corzo, et al., 2010), suggérant ainsi que les MDSC adaptent leur métabolisme aux conditions quasi-hypoxiques rencontrées dans la tumeur. Ce comportement s'avère similaire à l'effet Warburg observé chez les cellules tumorales qui accumulent le lactate dans le microenvironnement tumoral pour promouvoir la progression de la tumeur ainsi que la métastase, la néovascularisation et l'angiogenèse (Gatenby & Gillies, 2004). La glutaminolyse s'est avérée également très impliquée dans la production de lactate via l'activité de l'enzyme malique qui produit conjointement le NADPH et le pyruvate à partir du malate.

La stimulation de la glycolyse permet donc de fournir deux substrats du cycle de l'urée, et ce en métabolisant le pyruvate en acétyl coenzyme A (AcoA pour "Acetyl Coenzyme A") et en oxaloacétate via la déshydrogénase et la carboxylase du pyruvate, respectivement. De même, la régulation à la hausse de la glutaminolyse supplémente la cellule en α-kétoglutarate, un autre substrat du cycle de l'urée. L'activation de ce cycle permet alors de recycler le L-arg et de compenser le faible rendement énergétique du métabolisme anaérobique en produisant de l'énergie. En fait, la stimulation du cycle de l'urée est probablement régulée par l'AMPK dont l'activé a été fortement augmentée en présence de GM-CSF et de l'IL-6 afin de réagir au déficit énergétique cellulaire en accélérant la production d'énergie par les processus cataboliques.

Ces travaux, présentés au chapitre 3 de cette thèse, ont permis de confirmer l'hypothèse que la maturation des MDSC est fonction de l'état énergétique cellulaire. Aussi, nos résultats suggèrent que le NADPH est principalement produit par l'enzyme malique et que l'AMPK est responsable de la stimulation des processus qui produisent l'ATP, principalement le cycle de l'urée qui assure, entre autres, la synthèse endogène du L-arg.

Par la suite, nous avons investigué conjointement les besoins énergétiques associés au métabolisme du L-arg ainsi que le rôle de la L-gln dans le maintien du potentiel immunosuppressif des MDSC. Pour ce faire, les cellules MSC-1, une lignée immortalisée dérivée de MDSC murines, ont été utilisées comme système modèle pour étudier le comportement des MDSC *in vitro*. Le suivi de l'état énergétique des cellules MSC-1 par la résonance magnétique nucléaire du ^{31}P (^{31}P-NMR) et par des mesures de concentration de nucléotides dans des extraits cellulaires ont permis de caractériser la ligne de base de l'état énergétique des cellules MSC-1 en culture *in vitro*. Particulièrement, deux états énergétiques stationnaires qui correspondaient aux phases de croissance exponentielle et stationnaire ont été identifiés. Il a été entre autre observé que les cellules MSC-1 sont métaboliquement actives durant la phase de croissance exponentielle. Cependant, la phase stationnaire est caractérisée par une détérioration globale de l'état métabolique des cellules MSC-1 indiquant l'amorce de la phase de déclin. Cette ligne de base a servi à titre de contrôle pour l'étude du comportement des cellules MSC-1 lors de l'inhibition des activités enzymatiques de iNOS et ARG1. Ces travaux ont montré que la machinerie immunosuppressive associée à iNOS représente une demande élevée en énergie, alors que les cellules MSC-1 dont seule ARG1 est maintenue active suite à l'inhibition d'iNOS, sont immunosuppressives malgré la détérioration de l'état énergétique global des cellules. En fait, l'inhibition du métabolisme du L-arg a résulté en la diminution de l'oxydation des substrats, i.e. le glucose et la L-gln, et conséquemment en la diminution des concentrations spécifiques en nucléotides énergétiques et en substrats du cycle de l'urée, bien que le taux spécifique de consommation de l'oxygène ait été augmenté. Ceci suggère que la glycolyse et la respiration cellulaire sont découplées permettant ainsi la consommation de l'oxygène sans la production de substrats du cycle de l'urée. Cependant, l'étude des marqueurs comportementaux ATP/ADP et AMP/ATP a montré que le taux de production de l'ATP demeure inférieur à la demande. En fait,

l'inhibition du métabolisme du L-arg n'affecte pas la croissance cellulaire; ainsi les besoins en énergie et en substrats du cycle de l'urée associés aux processus anaboliques sont similaires à ceux observés chez les MDSC dont iNOS et ARG1 sont actives. Le rétablissement de la capacité respiratoire des cellules MSC-1 suite à l'inhibition de l'activité de l'enzyme iNOS suggère également que cette dernière régule probablement l'expression du facteur HIF-1α. Ces résultats sont en accord avec d'autres études où l'expression de iNOS s'est avérée être associée à la stimulation de la glycolyse, la PPP et la glutaminolyse (Albina & Mastrofrancesco, 1993; Murphy & Newsholme, 1998).

Ainsi, malgré le faible rendement énergétique du métabolisme glycolytique, une accumulation des nucléotides énergétiques a été observée chez les cellules MSC-1 non traitées par les inhibiteurs de iNOS et ARG1. Cette accumulation est probablement due à un taux de production de l'énergie largement supérieur à celui de la demande, bien que nous avons montré que l'activité de iNOS et la machinerie immunosuppressive qui y est associée est dépendant de l'énergie. Le turnover énergétique des cellules MSC-1 est probablement régulé par la suractivité de l'AMPK qui vraisemblablement stimule, à son tour, le cycle de l'urée pour produire l'énergie nécessaire pour le processus d'immunosuppression et également pourvsynthétiser les intermédiaires requis pour la production endogène du L-arg. Nos résultats complémentent alors ceux qui proposent que les enzymes iNOS et ASS, une enzyme impliquée dans les voies de recyclage du L-arg, sont co-induites (Mori, 2007) selon un nouveau mécanisme de régulation par lequel l'activité de iNOS assure indirectement la production des intermédiaires requis pour la synthèse endogène du L-arg.

De plus, l'activité de l'enzyme iNOS, mais non celle de l'ARG1, s'est avérée régulée par la glutaminolyse. L'inhibition de la glutaminolyse a diminué drastiquement l'activité du cycle TCA. Conséquemment, ce phénomène compromet la synthèse endogène du L-arg et réduit

l'accumulation du lactate ainsi que la production de l'énergie nécessaire pour l'activité de l'enzyme iNOS et les processus énergivores qui s'y rattachent. Plusieurs études ont investigué l'effet de la L-gln sur l'expression génique de iNOS; ces travaux ont mené à des conclusions contradictoires dépendamment des systèmes cellulaires utilisées. La L-gln régule à la baisse l'expression de l'ARNm de iNOS chez les hépatocytes, mais n'exerce aucun effet sur l'expression du gène de iNOS chez les cellules cancéreuses Caco-2 et HCT-8 (Lu, et al., 2009; Marion, et al., 2003). Les résultats de ces travaux, présentés au chapitre 4, montrent ainsi que la L-gln régule indirectement l'activité de iNOS en modulant ses besoins énergétiques. En fait, le glucose est majoritairement métabolisé via la glycolyse anaérobique, malgré une légère augmentation du taux spécifique de consommation de l'oxygène, diminuant ainsi l'activité du cycle de l'urée. L'inhibition de la glutaminolyse s'avère alors une cible potentielle pour le traitement des pathologies associées au NO, comme le cancer, les désordres neurodégénératifs, ainsi que d'autres maladies métaboliques.

7.2. L'effet du NO sur l'énergétique du système immunitaire

Malgré son rôle important dans l'inhibition du processus d'immunosurveillance, le NO a été utilisé, par l'entremise de donneurs de NO, pour ralentir et même abolir la progression de la tumeur, et par conséquence inhiber l'accumulation des MDSC chez les patients présentant une tumeur (Mocellin, et al., 2007). Cependant, le NO inhibe drastiquement la capacité respiratoire des cellules effectrices du système immunitaire en plus de déclencher leur mort (Clementi, et al., 1998; Li, et al., 1997). L'effet d'AT38, un nouveau NO-NSAID constitué d'un groupement furoxane attaché à une molécule d'acide salicylique, sur le comportement des cellules Jurkat, considérées comme un système modèle pour des cellules du système immunitaire stimulées, a été

investigué. Une concentration similaire à celle utilisée pour corriger, *in vivo*, le processus d'immunosurveillance a été utilisée pour simuler *in vitro* les interactions entre ce médicament et le système immunitaire. L'exposition des cellules Jurkat à l'AT38 inhibe leur prolifération, en plus d'inhiber irréversiblement leur respiration, ce qui détériore leur état énergétique global. Contrairement à la diminution du taux de production de l'ATP émanant de la phosphorylation oxydative, l'activation de l'AMPK et l'augmentation de l'expression des gènes de GLUT-1 et PFK-1 démontrent que la glycolyse, et donc la production de l'ATP glycolytique, a été stimulée. Il s'est avéré, cependant, que cet ATP est consommé par les mécanismes énergivores de l'apoptose initiée par le relargage du cytochrome *c*. À partir d'une concentration "seuil" en glucose, la nécrose, processus de mort indépendant de l'ATP, est déclenchée. Toutefois, *in vivo*, la nécrose est souvent associée à l'inflammation qui à son tour réduit l'efficacité des thérapies anticancéreuses (Jin, et al., 2007). Ainsi, la faible concentration en glucose dans le microenvironnement tumoral et sa forte consommation par les cellules tumorales et les MDSC favorisent l'émergence de la nécrose et par la suite la progression de la tumeur. Ces résultats corroborent ceux de Fiorucci et de ses collaborateurs qui ont montré que NCX-4016, un NO-NSAID, favorise un métabolisme glycolytique en régulant à la hausse la consommation du glucose et l'activité de la PFK-1, résultant en la conversion de 70% du glucose en lactate (Fiorucci, et al., 2004). De même, il a été démontré que le NO module le processus de mort cellulaire dépendamment de la disponibilité de l'ATP (Leist, et al., 1999b). En plus, les effets d'AT38 sur le métabolisme des cellules Jurkat ont été comparés à ceux des donneurs de nitrite et de nitrate ($NaNO_2$ et $NaNO_3$, respectivement) afin d'investiguer le rôle spécifique de ces deux dérivés de NO. Contrairement au nitrite qui engendre les mêmes effets sur les cellules Jurkat qu'AT38 à la même concentration, les effets de $NaNO_3$ sur la prolifération et l'énergétique des cellules Jurkat ont été observés à une concentration plus élevée que pour le $NaNO_2$, et avec un

délai qui pourrait être dû à la dissociation du nitrate dans le milieu de culture et à sa faible capacité de diffusion dans la cellule. Nos résultats suggèrent ainsi que le nitrate, qui a toujours été considéré comme un anion biologiquement inerte (Bruno, et al., 1994), a un potentiel immunosuppressif dépendant à la fois de la concentration et du temps.

Pour atténuer les effets néfastes d'AT38 sur les cellules effectrices du système immunitaire, une stratégie consistant à bloquer l'ouverture du pore de transition de perméabilité mitochondrial (MPTP pour "Mitochondrial Permeability Transition Pore") par la cyclosporine A est proposée. En fait, l'ouverture du MPTP résulte en la libération du cytochrome *c*, ce qui déclenche différentes cascades pro-apoptotiques. De plus, la CsA permet de repolariser la mitochondrie et de corriger les fonctions énergétiques qui y sont associées (Bernardi, 1996). Il s'est avéré alors que le prétraitement des cellules Jurkat avec la CsA inhibe les effets d'AT38 sur leur prolifération et leur viabilité. Cependant, la CsA est associée à des problèmes de toxicité néphrologique et gastrique, etc. (Erdmann, et al.; Takahashi, et al., 2009) et le développement de bloqueurs de MPTP sans effets secondaires majeurs s'avère indispensable pour bénéficier des retombées thérapeutiques de cette stratégie. Ces résultats sont confirmés par plusieurs études ayant rapporté le potentiel de la CsA à inhiber les effets du NO sur la mitochondrie et sa capacité à préserver les cellules effectrices du système immunitaire qui pourraient être ultérieurement stimulées pour activer leurs fonctions immunomodulatoires (Herold, et al., 1986; Sato, et al., 2009).

La principale innovation de cette thèse réside dans la caractérisation des évènements métaboliques qui régulent la suppression de la fonction anti-tumorale spécifique aux cellules T par les MDSC. Les trois étapes majeures du phénomène d'immunosuppression ont été considérées, soient la maturation des MDSC, leurs fonctions et leurs effets sur les cellules T.

Tout d'abord, nous avons pu démontrer que la maturation des MDSC et de leur potentiel immunosuppressif sont des processus énergivores (Figure 7-1).

Figure 7-1 : Figure récapitulative du comportement métabolique des MDSC et de son effet sur les cellules T.

Les flèches en gras montrent les flux régulés à la hausse durant la maturation des MDSC et le métabolisme du L-arg. Le symbole ┤ en rouge indique l'inhibition par un agent thérapeutique.

Particulièrement, l'AMPK et l'enzyme malique régulent les processus cataboliques pour assurer la production permanente d'énergie et d'intermédiaires requis pour la synthèse endogène du L-arg ainsi que l'accumulation du lactate qui est favorable à la progression de la tumeur. Ensuite, une stratégie permettant d'atténuer les effets néfastes du NO sur le système immunitaire a été proposée. Notre approche s'inscrit alors dans la volonté de mieux comprendre le phénomène d'immunosuppression au niveau métabolique dans l'ultime but d'identifier de nouvelles cibles d'immunothérapie.

CHAPITRE 8. CONCLUSION ET RECOMMENDATIONS

L'immunothérapie représente une alternative de grand intérêt pour le traitement du cancer vu son caractère non-invasif. Cette stratégie consiste à corriger la capacité du système immunitaire à reconnaître les tumeurs et à inhiber leur progression. Cependant, les MDSC qui s'infiltrent dans la tumeur inhibent ce processus d'immunosurveillance en plus de diminuer l'efficacité des approches conventionnelles telles que la chimiothérapie. La majorité des stratégies thérapeutiques anti-MDSC développées jusqu'à présent ciblent des marqueurs de surface spécifiques, des enzymes clées et des voies de signalisation pour inhiber la maturation des MDSC ainsi que leurs activités immunosuppressives. Dans le cadre de cette thèse, le phénomène d'immunosuppression a été abordé d'un point de vue métabolique afin d'obtenir une meilleure compréhension des réactions mises en jeu dans ce processus, et ce, dans l'ultime but de définir de nouvelles cibles d'immunothérapie.

8.1. Conclusion

La maturation des MDSC à partir de précurseurs myéloïdes débute dans la moelle osseuse, se poursuit dans les organes lymphoïdes et la rate pour finalement générer des MDSC complètement immunosuppressives dans la tumeur. La combinaison des cytokines GM-CSF et IL-6, utilisées *in vitro* pour simuler la maturation des MDSC, montre que ce processus mobilise les ressources nutritives au profit de la machinerie immunosuppressive des MDSC. La caractérisation du profil nutritionnel des MDSC montre que ces dernières métabolisent le glucose via un mode glycolytique. Particulièrement, la maturation des MDSC et le métabolisme du L-arg

régulent à la baisse la respiration cellulaire. En fait, les MDSC expriment le facteur d'initiation à l'hypoxie HIF-1α conjointement aux enzymes iNOS et ARG1 (Corzo, et al., 2010). Ainsi, les MDSC favorisent la conversion du glucose en lactate par rapport au haut rendement énergétique de la respiration. La L-gln joue aussi un rôle indirect très important dans l'accumulation du lactate en assurant une forte activité du cycle de l'urée qui génère le malate à des taux plus élevés que celui du PEP. Les MDSC supportent alors les cellules tumorales en leur assurant, par l'acidification du microenvironnement tumoral, des conditions propices à leur croissance ainsi qu'à la néovascularisation, l'angiogenèse et la métastase (Gatenby & Gillies, 2004).

Cependant, la L-gln n'est pas principalement dirigée vers la voie de production de lactate. En fait, l'activité de l'AMPK est stimulée durant le processus de maturation des MDSC et lors du métabolisme du L-arg, en réponse au déficit énergétique causé par le faible rendement énergétique du mode anaérobique. La L-gln est ainsi métabolisée pour fournir les intermédiaires du cycle de l'urée, et ainsi combler les besoins cellulaires en énergie. La stimulation du cycle de l'urée supporte également la synthèse endogène du L-arg et la conversion du malate en pyruvate via l'enzyme malique qui coproduit la NADPH. Toutefois, cette régulation croisée entre la glycolyse et la glutaminolyse durant le processus de maturation est particulièrement associée à l'activation de l'enzyme iNOS, vu que l'activité de l'ARG1 n'est pas affectée par la détérioration globale de l'état métabolique des cellules MSC-1 et que leur potentiel immunosuppressif est maintenu. De plus, la L-gln régule indirectement l'activité de iNOS, et cet effet peut être à la fois associé à la diminution du taux de production de la NADPH par l'enzyme malique et à la régulation à la baisse de la production, par le cycle de l'urée, des intermédiaires requis pour la synthèse endogène du L-arg.

Dans un autre ordre d'idée, il a été démontré que les MDSC modulent indirectement l'énergétique des cellules effectrices du système immunitaire en secrétant le NO et ses dérivés.

Le donneur de NO utilisé dans le cadre de cette thèse pour simuler l'interaction entre les MDSC et le système immunitaire, soit l'AT38, inhibe irréversiblement la respiration des cellules Jurkat. Aussi, les niveaux d'expression des l'ARNm du transporteur de glucose et de la phosphofructokinase sont augmentés, de même que l'activité sensorielle de l'enzyme AMPK, le tout stimulant la production glycolytique de l'ATP. À partir d'une concentration "seuil" en glucose, l'ATP n'est plus suffisamment synthétisée à un taux permettant de combler la demande énergétique des mécanismes de l'apoptose, dont les cascades sont déclenchées par le NO (Li, et al., 1997), et les cellules Jurkat meurent alors par nécrose. Il a été démontré que la mort des cellules effectrices du système immunitaire peut toutefois être évitée en bloquant l'ouverture du MPTP, par la cyclosporine A, ce qui inhibe le relargage du cytochrome *c* et l'activation des signaux de la mort cellulaire.

D'un point de vue fondamental, la compréhension du comportement des MDSC au niveau métabolique est extrêmement pertinente et peut, tel que démontré dans nos travaux, donner naissance à une nouvelle génération d'immunothérapie anticancéreuse basée sur la modulation de l'énergétique et de la nutrition des MDSC. En effet, nos résultats permettent de suggérer deux pistes d'intérêt pour la correction de la réponse immunitaire anti-tumorale : i) l'inhibition de l'AMPK pour abolir son potentiel de régulation de l'état énergétique des MDSC, et ii) le contrôle des flux à travers la glutaminolyse pour altérer le métabolisme du L-arg et sa synthèse endogène.

8.2. Recommandations

Cette thèse met en évidence les besoins énergétiques et nutritionnels nécessaires au processus de maturation des MDSC ainsi que pour l'acquisition et le maintien de leur potentiel immunosuppressif. Cependant, certains aspects doivent être clarifiés. Premièrement,

l'accumulation des nucléotides énergétiques et des intermédiaires de la glycolyse, de la PPP et du cycle de l'urée doit être investiguée et les flux attribués à chaque voie doivent être déterminés avec précision. Pour ce faire, un modèle métabolique doit être développé et calibré avec les données expérimentales provenant de la culture des cellules myéloïdes en présence de GM-CSF et IL-6. Ce modèle pourra alors améliorer la compréhension des phénomènes nutritionnels et énergétiques en jeu et fournir des pistes permettant la modulation de l'activité des enzymes directement impliquées dans la production de l'énergie et des substrats requis par le processus de maturation. De plus, des mesures des activités de ces enzymes pourraient permettre de valider ou d'invalider les hypothèses émises à l'aide du modèle métabolique. Cependant, étant donné que toutes les cellules expriment plus ou moins les mêmes enzymes impliquées dans le métabolisme central du carbone, il est important que des systèmes de livraison des inhibiteurs soient utilisés afin de cibler spécifiquement les MDSC et éviter l'altération de fonctions physiologiques essentielles lorsque la stratégie est appliquée *in vivo*.

Il serait également important de vérifier si les MDSC pourraient s'adapter à une régulation à la baisse de la glycolyse et de la glutaminolyse, par exemple en métabolisant des phopholipides ou des protéines, pour s'approvisionner en précurseurs et intermédiaires métaboliques et en énergie requis pour leur maturation et fonctions immunosuppressives.

Ensuite, pour complémenter cette étude métabolique, le profil génétique des MDSC doit être caractérisé, par puces à ARN, afin de déterminer les gènes qui doivent être ciblés pour l'inhibition de la maturation des MDSC ou le blocage du métabolisme du L-arg. Plusieurs alternatives pourraient être exploitées à cette fin, dont les petits ARN interférents (siRNA pour "Small Interfering RNA") qui assurent une haute spécificité face à une cible (Shim & Kwon, 2010).

De plus, lors de futures études, il serait pertinent d'investiguer plus en détails le rôle de la L-gln dans le processus de maturation des MDSC et dans le maintien de leur activité immunosuppressive. Il serait tout d'abord judicieux de vérifier si l'effet de l'absence de la L-gln sur l'activité de iNOS est dû à la régulation à la baisse de l'expression du gène ou de la production de la protéine active puisque les deux cas pourraient expliquer l'arrêt de la production des dérivés du NO. De même, l'utilisation de la L-gln marquée aux isotopes C^{13} ou C^{14} pourrait aider à élucider l'implication de cet acide aminé dans la stimulation du métabolisme central du carbone.

Finalement, étant donné le caractère énergivore du phénomène d'immunosuppression, il serait pertinent de vérifier, tant *in vitro* que *in vivo*, en utilisant des animaux normaux ou knock-out (par invalidation génique) porteurs de tumeurs, si des composés thérapeutiques qui affectent négativement l'état énergétique des cellules, tels que les glucorticoïdes, des bloqueurs de canaux potassique, la cyclosporine (Buttgereit, et al., 2000), peuvent inhiber la maturation des MDSC et leur capacité à abroger la réponse anti-tumorale spécifique aux cellules T. Particulièrement, l'administration des bloqueurs du MPTP dans la tumeur peut avoir un double effet, soit la détérioration de l'état énergétique des cellules tumorales et des MDSC et la prévention de la mort des cellules T en présence de NO-NSAIDs. Le développement de bloqueurs de MPTP sans effets secondaires majeurs pourrait alors représenter une approche à privilégier pour le rétablissement du processus d'immunosurveillance et l'éradication de la tumeur.

RÉFÉRENCES

Abbas, A. K., & Lichtman, A. H. (2006). *Basic Immunology: Functions and Disorders of the Immune System*.

Ahmed, N., & Berridge, M. V. (2000). Ceramides that mediate apoptosis reduce glucose uptake and transporter affinity for glucose in human leukaemic cell lines but not in neutrophils. *Pharmacol Toxicol, 86*(3), 114-121.

Albina, J. E., & Mastrofrancesco, B. (1993). Modulation of glucose metabolism in macrophages by products of nitric oxide synthase. *Am J Physiol, 264*(6 Pt 1), C1594-1599.

Ando, M., Uehara, I., Kogure, K., Asano, Y., Nakajima, W., Abe, Y., et al. (2010). Interleukin 6 enhances glycolysis through expression of the glycolytic enzymes hexokinase 2 and 6-phosphofructo-2-kinase/fructose-2,6-bisphosphatase-3. *J Nippon Med Sch, 77*(2), 97-105.

Apolloni, E., Bronte, V., Mazzoni, A., Serafini, P., Cabrelle, A., Segal, D. M., et al. (2000). Immortalized myeloid suppressor cells trigger apoptosis in antigen-activated T lymphocytes. *J of Immunol, 165*, 6723-6730.

Atkinson, D. E. (1977). *Cellular Energy Metabolism and its Regulation*. USA.

Berkowitz, D. E., White, R., Li, D., Minhas, K. M., Cernetich, A., Kim, S., et al. (2003). Arginase reciprocally regulates nitric oxide synthase activity and contributes to endothelial dysfunction in aging blood vessels. *Circulation, 108*(16), 2000-2006.

Bernardi, P. (1996). The permeability transition pore. Control points of a cyclosporin A-sensitive mitochondrial channel involved in cell death. *Biochim Biophys Acta, 1275*(1-2), 5-9.

Bernstein, C., Bernstein, H., Payne, C. M., & Garewal, H. (2002). DNA repair/pro-apoptotic dual-role proteins in five major DNA repair pathways: fail-safe protection against carcinogenesis. *Mutat Res, 511*(2), 145-178.

Bingisser, R. M., Tilbrook, P. A., Holt, P. G., & Kees, U. R. (1998). Macrophage dervied Nitric Oxide regulates T cell activation via reversible disruption of the Jak3/STAT5 sinaling pathway *The Journal of Immunology, 160*, 5729-5734.

Boulland, M. L., Marquet, J., Molinier-Frenkel, V., Moller, P., Guiter, C., Lasoudris, F., et al. (2007). Human IL4I1 is a secreted L-phenylalanine oxidase expressed by mature dendritic cells that inhibits T-lymphocyte proliferation. *Blood, 110*(1), 220-227.

Brasse-Lagnel, C., Fairand, A., Lavoinne, A., & Husson, A. (2003). Glutamine stimulates argininosuccinate synthetase gene expression through cytosolic O-glycosylation of Sp1 in Caco-2 cells. *J Biol Chem, 278*(52), 52504-52510.

Bronte, & Zanovello. (2005). Regulation of immune reponses by L-arginine metabolism. *Nature Reviews | Immunology, 5*, 641-654.

Bronte, V., Chappell, D. B., Apolloni, E., Cabrelle, A., Wang, M., Hwu, P., et al. (1999). Unopposed production of granulocyte-macrophage colony-stimulating factor by tumors inhibits CD8+ T cell responses by dysregulating antigen-presenting cell maturation. *J Immunol, 162*(10), 5728-5737.

Bronte, V., Serafini, P., Mazzoni, A., Segal, D. M., & Zanovello, P. (2003). L-arginine metabolism in myeloid cells controls T-lymphocyte functions. *Trends in Immunology, 24*(6), 301-305.

Bruno, J. G., Parker, J. E., & Kiel, J. L. (1994). Plant nitrate reductase gene fragments enhance nitrite production in activated murine macrophage cell lines. *Biochem Biophys Res Commun, 201*(1), 284-289.

Buttgereit, F., Burmester, G. R., & Brand, M. D. (2000). Bioenergetics of immune functions: fundamental and therapeutic aspects. *Immunol Today, 21*(4), 192-199.

Cao, X. (2010). Regulatory T cells and immune tolerance to tumors. *Immunol Res, 46*(1-3), 79-93.

Cao, X., Shores, E. W., Hu-Li, J., Anver, M. R., Kelsall, B. L., Russell, S. M., et al. (1995). Defective lymphoid development in mice lacking expression of the common cytokine receptor gamma chain. *Immunity, 2*(3), 223-238.

Carvalhal, A. V., Marcelino, I., & Carrondo, M. J. (2003). Metabolic changes during cell growth inhibition by p27 overexpression. *Appl Microbiol Biotechnol, 63*(2), 164-173.

Castro, L., Eiserich, J. P., Sweeney, S., Radi, R., & Freeman, B. A. (2004). Cytochrome c: a catalyst and target of nitrite-hydrogen peroxide-dependent protein nitration. *Arch Biochem Biophys, 421*(1), 99-107.

Cavicchi, M., & Whittle, B. J. (1999). Potentiation of cytokine induced iNOS expression in the human intestinal epithelial cell line, DLD-1, by cyclic AMP. *Gut, 45*(3), 367-374.

Chou, I. N., Zeiger, J., & Rapaport, E. (1984). Imbalance of total cellular nucleotide pools and mechanism of the colchicine-induced cell activation. *Proc Natl Acad Sci U S A, 81*(8), 2401-2405.

Cidad, P., Almeida, A., & Bolanos, J. P. (2004). Inhibition of mitochondrial respiration by nitric oxide rapidly stimulates cytoprotective GLUT3-mediated glucose uptake through 5'-AMP-activated protein kinase. *Biochem J, 384*(Pt 3), 629-636.

Clementi, E., Brown, G. C., Feelisch, M., & Moncada, S. (1998). Persistent inhibition of cell respiration by nitric oxide: crucial role of S-nitrosylation of mitochondrial complex I and protective action of glutathione. *Proc Natl Acad Sci U S A, 95*(13), 7631-7636.

Coleman, D. R. t., Ren, Z., Mandal, P. K., Cameron, A. G., Dyer, G. A., Muranjan, S., et al. (2005). Investigation of the binding determinants of phosphopeptides targeted to the SRC homology 2 domain of the signal transducer and activator of transcription 3. Development of a high-affinity peptide inhibitor. *J Med Chem, 48*(21), 6661-6670.

Colleluori, D. M., & Ash, D. E. (2001). Classical and slow-binding inhibitors of human type II arginase. *Biochemistry, 40*(31), 9356-9362.

Continenza, M. A., Vicentini, C., Paradiso-Galatioto, G., Fileni, A., & Tchokogoue, E. (2003). In vitro study of Human Dermal Fibroblasts seeded on two kinds of surgical meshes: monofilamented Polypropylene and multifilamented Polyestere. *Ital J Anat Embryol, 108*(4), 231-239.

Corzo, C. A., Condamine, T., Lu, L., Cotter, M. J., Youn, J. I., Cheng, P., et al. (2010). HIF-1alpha regulates function and differentiation of myeloid-derived suppressor cells in the tumor microenvironment. *J Exp Med, 207*(11), 2439-2453.

Costa Rosa, L. F., Curi, R., Murphy, C., & Newsholme, P. (1995). Effect of adrenaline and phorbol myristate acetate or bacterial lipopolysaccharide on stimulation of pathways of macrophage glucose, glutamine and O2 metabolism. Evidence for cyclic AMP-dependent protein kinase mediated inhibition of glucose-6-phosphate dehydrogenase and activation of NADP+-dependent 'malic' enzyme. *Biochem J, 310 (Pt 2)*, 709-714.

Costello, R. T., Gastaut, J. A., & Olive, D. (1999). Tumor escape from immune surveillance. *Arch Immunol Ther Exp (Warsz), 47*(2), 83-88.

Daly, P. F., Lyon, R. C., Straka, E. J., & Cohen, J. S. (1988). 31P-NMR spectroscopy of human cancer cells proliferating in a basement membrane gel. *FASEB J, 2*(10), 2596-2604.

DeBerardinis, R. J., Lum, J. J., Hatzivassiliou, G., & Thompson, C. B. (2008). The biology of cancer: metabolic reprogramming fuels cell growth and proliferation. *Cell Metab, 7*(1), 11-20.

Del Grosso, E., Boschi, D., Lazzarato, L., Cena, C., Di Stilo, A., Fruttero, R., et al. (2005). The furoxan system: design of selective nitric oxide (NO) donor inhibitors of COX-2 endowed with anti-aggregatory and vasodilating activities. *Chem Biodivers, 2*(7), 886-900.

Demas, G. E., Chefer, V., Talan, M. I., & Nelson, R. J. (1997). Metabolic costs of mounting an antigen-stimulated immune response in adult and aged C57BL/6J mice. *Am J Physiol, 273*(5 Pt 2), R1631-1637.

Dhar-Mascareno, M., Chen, J., Zhang, R. H., Carcamo, J. M., & Golde, D. W. (2003). Granulocyte-macrophage colony-stimulating factor signals for increased glucose transport via phosphatidylinositol 3-kinase- and hydrogen peroxide-dependent mechanisms. *J Biol Chem, 278*(13), 11107-11114.

Dolcetti, L., Marigo, I., Mantelli, B., Peranzoni, E., Zanovello, P., & Bronte, V. (2008). Myeloid-derived suppressor cell role in tumor-related inflammation. *Cancer Lett, 267*(2), 216-225.

Dolcetti, L., Peranzoni, E., Ugel, S., Marigo, I., Fernandez Gomez, A., Mesa, C., et al. (2010). Hierarchy of immunosuppressive strength among myeloid-derived suppressor cell subsets is determined by GM-CSF. *Eur J Immunol, 40*(1), 22-35.

El-Gayar, S., Thuring-Nahler, H., Pfeilschifter, J., Rollinghoff, M., & Bogdan, C. (2003). Translational control of inducible nitric oxide synthase by IL-13 and arginine availability in inflammatory macrophages. *J Immunol, 171*(9), 4561-4568.

Elmore, S. (2007). Apoptosis: a review of programmed cell death. *Toxicol Pathol, 35*(4), 495-516.

Engedal, N., Gjevik, T., Blomhoff, R., & Blomhoff, H. K. (2006). All-trans retinoic acid stimulates IL-2-mediated proliferation of human T lymphocytes: early induction of cyclin D3. *J Immunol, 177*(5), 2851-2861.

Erdmann, F., Weiwad, M., Kilka, S., Karanik, M., Patzel, M., Baumgrass, R., et al. The novel calcineurin inhibitor CN585 has potent immunosuppressive properties in stimulated human T cells. *J Biol Chem, 285*(3), 1888-1898.

Fallarino, F., Grohmann, U., You, S., McGrath, B. C., Cavener, D. R., Vacca, C., et al. (2006). The combined effects of tryptophan starvation and tryptophan catabolites down-regulate T cell receptor zeta-chain and induce a regulatory phenotype in naive T cells. *J Immunol, 176*(11), 6752-6761.

Farley, K. S., Wang, L. F., Law, C., & Mehta, S. (2008). Alveolar macrophage inducible nitric oxide synthase-dependent pulmonary microvascular endothelial cell septic barrier dysfunction. *Microvasc Res, 76*(3), 208-216.

Fernandes, L. C., Mattozo, C. A., Machado, U. F., Rosa, L. F., & Curi, R. (1996). Insulin treatment can abolish changes in glucose and glutamine metabolism of lymphocytes and macrophages caused by the implantation of the Walker 256 tumour. *Cell Biochem Funct, 14*(3), 187-192.

Fiorucci, S., Mencarelli, A., Distrutti, E., Baldoni, M., del Soldato, P., & Morelli, A. (2004). Nitric oxide regulates immune cell bioenergetic: a mechanism to understand immunomodulatory functions of nitric oxide-releasing anti-inflammatory drugs. *J Immunol, 173*(2), 874-882.

Fleetwood, A. J., Cook, A. D., & Hamilton, J. A. (2005). Functions of granulocyte-macrophage colony-stimulating factor. *Crit Rev Immunol, 25*(5), 405-428.

Frauwirth, K. A., Riley, J. L., Harris, M. H., Parry, R. V., Rathmell, J. C., Plas, D. R., et al. (2002). The CD28 signaling pathway regulates glucose metabolism. *Immunity, 16*(6), 769-777.

Gabrilovich, D. (2004). Mechanisms and functional significance of tumour-induced dendritic-cell defects. *Nat Rev Immunol, 4*(12), 941-952.

Gabrilovich, D. I., Bronte, V., Chen, S. H., Colombo, M. P., Ochoa, A., Ostrand-Rosenberg, S., et al. (2007). The terminology issue for myeloid-derived suppressor cells. *Cancer Res, 67*(1), 425; author reply 426.

Gabrilovich, D. I., & Nagaraj, S. (2009). Myeloid-derived suppressor cells as regulators of the immune system. *Nat Rev Immunol, 9*(3), 162-174.

Gabrilovich, D. I., Velders, M. P., Sotomayor, E. M., & Kast, W. M. (2001). Mechanism of immune dysfunction in cancer mediated by immature Gr-1(+) myeloid cells. *Journal of Immunology, 166*(9), 5398-5406.

Ganapathy, V., Thangaraju, M., & Prasad, P. D. (2009). Nutrient transporters in cancer: relevance to Warburg hypothesis and beyond. *Pharmacol Ther, 121*(1), 29-40.

Garvey, E. P., Oplinger, J. A., Furfine, E. S., Kiff, R. J., Laszlo, F., Whittle, B. J., et al. (1997). 1400W is a slow, tight binding, and highly selective inhibitor of inducible nitric-oxide synthase in vitro and in vivo. *J Biol Chem, 272*(8), 4959-4963.

Gatenby, R. A., & Gillies, R. J. (2004). Why do cancers have high aerobic glycolysis? *Nat Rev Cancer, 4*(11), 891-899.

Gmati, D., Chen, J., & Jolicoeur, M. (2004). Development of a small-scale bioreactor: application to in vivo NMR measurement. *Biotechnology and Bioengineering, 89*, 138-147.

Görgens, J. F., Van Zyl, W. H., & Knoetze, J. H. (2005). Reliability of methods for the determination of specific substrate consumption rates in batch culture. *Biochemical Engineering Journal, 25*(2), 109-112.

Hammami, I., Chen, J., Bronte, V., Decrescenzo, G., & Jolicoeur, M. (2011). Immunosuppression mediated by myeloid-derived suppressor cells is energetically costly. *Submitted Paper*.

Hammermann, R., Dreissig, M. D., Mossner, J., Fuhrmann, M., Berrino, L., Gothert, M., et al. (2000). Nuclear factor-kappaB mediates simultaneous induction of inducible nitric-oxide synthase and Up-regulation of the cationic amino acid transporter CAT-2B in rat alveolar macrophages. *Mol Pharmacol, 58*(6), 1294-1302.

Hardie, D. G. (2011). AMP-activated protein kinase: a cellular energy sensor with a key role in metabolic disorders and in cancer. *Biochem Soc Trans, 39*(1), 1-13.

Hattori, Y., Campbell, E. B., & Gross, S. S. (1994). Argininosuccinate synthetase mRNA and activity are induced by immunostimulants in vascular smooth muscle. Role in the regeneration or arginine for nitric oxide synthesis. *J Biol Chem, 269*(13), 9405-9408.

Heissig, B., Hattori, K., Dias, S., Friedrich, M., Ferris, B., Hackett, N. R., et al. (2002). Recruitment of stem and progenitor cells from the bone marrow niche requires MMP-9 mediated release of kit-ligand. *Cell, 109*(5), 625-637.

Herold, K. C., Lancki, D. W., Moldwin, R. L., & Fitch, F. W. (1986). Immunosuppressive effects of cyclosporin A on cloned T cells. *J Immunol, 136*(4), 1315-1321.

Hoemann, C. D., Sun, J., Chrzanowski, V., & Buschmann, M. D. (2002). A multivalent assay to detect glycosaminoglycan, protein, collagen, RNA, and DNA content in milligram samples of cartilage or hydrogel-based repair cartilage. *Anal Biochem, 300*(1), 1-10.

Ignarro, L. J., Fukuto, J. M., Griscavage, J. M., Rogers, N. E., & Byrns, R. E. (1993). Oxidation of nitric oxide in aqueous solution to nitrite but not nitrate: comparison with enzymatically formed nitric oxide from L-arginine. *Proc Natl Acad Sci U S A, 90*(17), 8103-8107.

Jaiswal, M., LaRusso, N. F., Burgart, L. J., & Gores, G. J. (2000). Inflammatory cytokines induce DNA damage and inhibit DNA repair in cholangiocarcinoma cells by a nitric oxide-dependent mechanism. *Cancer Res, 60*(1), 184-190.

Jansson, E. A., Huang, L., Malkey, R., Govoni, M., Nihlen, C., Olsson, A., et al. (2008). A mammalian functional nitrate reductase that regulates nitrite and nitric oxide homeostasis. *Nat Chem Biol, 4*(7), 411-417.

Jin, S., DiPaola, R. S., Mathew, R., & White, E. (2007). Metabolic catastrophe as a means to cancer cell death. *J Cell Sci, 120*(Pt 3), 379-383.

Johnson, B. F., Clay, T. M., Hobeika, A. C., Lyerly, H. K., & Morse, M. A. (2007). Vascular endothelial growth factor and immunosuppression in cancer: current knowledge and potential for new therapy. *Expert Opin Biol Ther, 7*(4), 449-460.

Kao, J., Ko, E. C., Eisenstein, S., Sikora, A. G., Fu, S., & Chen, S. H. (2010). Targeting immune suppressing myeloid-derived suppressor cells in oncology. *Crit Rev Oncol Hematol*.

Keeble, J. E., & Moore, P. K. (2002). Pharmacology and potential therapeutic applications of nitric oxide-releasing non-steroidal anti-inflammatory and related nitric oxide-donating drugs. *Br J Pharmacol, 137*(3), 295-310.

Kelly, M., Gauthier, M. S., Saha, A. K., & Ruderman, N. B. (2009). Activation of AMP-activated protein kinase by interleukin-6 in rat skeletal muscle: association with changes in cAMP, energy state, and endogenous fuel mobilization. *Diabetes, 58*(9), 1953-1960.

Kim, N., Cox, J., Baggio, R., Emig, F., Mistry, S., Harper, S., et al. (2001). Probing erectile function: S-(2-bronoethyl)-L-cysteine binds to arginase as a transition state analogue and enhances smooth muscle relaxation in human penile corpus cavernosum. *Biochemistry, 40*(9), 2678-2688.

Kimball, E., & Rabinowitz, J. D. (2006). Identifying decomposition products in extracts of cellular metabolites. *Anal Biochem, 358*(2), 273-280.

Kortylewski, M., Kujawski, M., Wang, T., Wei, S., Zhang, S., Pilon-Thomas, S., et al. (2005). Inhibiting Stat3 signaling in the hematopoietic system elicits multicomponent antitumor immunity. *Nat Med, 11*(12), 1314-1321.

Kroncke, K. D., Fehsel, K., Suschek, C., & Kolb-Bachofen, V. (2001). Inducible nitric oxide synthase-derived nitric oxide in gene regulation, cell death and cell survival. *International Immunopharmacology, 1*(8), 1407-1420.

Kuida, K., Haydar, T. F., Kuan, C. Y., Gu, Y., Taya, C., Karasuyama, H., et al. (1998). Reduced apoptosis and cytochrome c-mediated caspase activation in mice lacking caspase 9. *Cell, 94*(3), 325-337.

Kusmartsev, S., Cheng, F., Yu, B., Nefedova, Y., Sotomayor, E., Lush, R., et al. (2003). All-trans-retinoic acid eliminates immature myeloid cells from tumor-bearing mice and improves the effect of vaccination. *Cancer Res, 63*(15), 4441-4449.

Kusmartsev, S., Eruslanov, E., Kubler, H., Tseng, T., Sakai, Y., Su, Z., et al. (2008). Oxidative stress regulates expression of VEGFR1 in myeloid cells: link to tumor-induced immune suppression in renal cell carcinoma. *J Immunol, 181*(1), 346-353.

Lamboursain, L., St-Onge, F., & Jolicoeur, M. (2002). A lab-respirometer forplant and animal cell culture. *Biotechnol Progr, 18*, 1377-1386.

Lathers, D. M., Clark, J. I., Achille, N. J., & Young, M. R. (2004). Phase 1B study to improve immune responses in head and neck cancer patients using escalating doses of 25-hydroxyvitamin D3. *Cancer Immunol Immunother, 53*(5), 422-430.

Lee, J., Ryu, H., Ferrante, R. J., Morris, S. M., Jr., & Ratan, R. R. (2003). Translational control of inducible nitric oxide synthase expression by arginine can explain the arginine paradox. *Proc Natl Acad Sci U S A, 100*(8), 4843-4848.

Leist, M., Single, B., Naumann, H., Fava, E., Simon, B., Kuhnle, S., et al. (1999a). Inhibition of mitochondrial ATP generation by nitric oxide switches apoptosis to necrosis. *Exp Cell Res, 249*(2), 396-403.

Leist, M., Single, B., Naumann, H., Fava, E., Simon, B., Kuhnle, S., et al. (1999b). Nitric oxide inhibits execution of apoptosis at two distinct ATP-dependent steps upstream and downstream of mitochondrial cytochrome c release. *Biochem Biophys Res Commun, 258*(1), 215-221.

Li, P., Nijhawan, D., Budihardjo, I., Srinivasula, S. M., Ahmad, M., Alnemri, E. S., et al. (1997). Cytochrome c and dATP-dependent formation of Apaf-1/caspase-9 complex initiates an apoptotic protease cascade. *Cell, 91*(4), 479-489.

Lind, D. S. (2004). Arginine and cancer. *Journal of Nutrition, 134*(10), 2837S-2841S.

Long, K. Z., & Nanthakumar, N. (2004). Energetic and nutritional regulation of the adaptive immune response and trade-offs in ecological immunology. *Am J Hum Biol, 16*(5), 499-507.

Losser, M. R., & Payen, D. (1996). Mechanisms of liver damage. *Semin Liver Dis, 16*(4), 357-367.

Lu, J., Wang, X. Y., & Tang, W. H. (2009). Glutamine attenuates nitric oxide synthase expression and mitochondria membrane potential decrease in interleukin-1beta-activated rat hepatocytes. *Eur J Nutr, 48*(6), 333-339.

Maciver, N. J., Jacobs, S. R., Wieman, H. L., Wofford, J. A., Coloff, J. L., & Rathmell, J. C. (2008). Glucose metabolism in lymphocytes is a regulated process with significant effects on immune cell function and survival. *J Leukoc Biol, 84*(4), 949-957.

Macphail, S. E., Gibney, C. A., Brooks, B. M., Booth, C. G., Flanagan, B. F., & Coleman, J. W. (2003). Nitric oxide regulation of human peripheral blood mononuclear cells: critical time dependence and selectivity for cytokine versus chemokine expression. *J Immunol, 171*(9), 4809-4815.

Marigo, I., Bosio, E., Solito, S., Mesa, C., Fernandez, A., Dolcetti, L., et al. (2010). Tumor-induced tolerance and immune suppression depend on the C/EBPbeta transcription factor. *Immunity, 32*(6), 790-802.

Marigo, I., Dolcetti, L., Serafini, P., Zanovello, P., & Bronte, V. (2008). Tumor-induced tolerance and immune suppression by myeloid derived suppressor cells. *Immunol Rev, 222*, 162-179.

Marin-Hernandez, A., Gallardo-Perez, J. C., Ralph, S. J., Rodriguez-Enriquez, S., & Moreno-Sanchez, R. (2009). HIF-1alpha modulates energy metabolism in cancer cells by inducing over-expression of specific glycolytic isoforms. *Mini Rev Med Chem, 9*(9), 1084-1101.

Marion, R., Coeffier, M., Leplingard, A., Favennec, L., Ducrotte, P., & Dechelotte, P. (2003). Cytokine-stimulated nitric oxide production and inducible NO-synthase mRNA level in human intestinal cells: lack of modulation by glutamine. *Clin Nutr, 22*(6), 523-528.

Marnett, L. J., Riggins, J. N., & West, J. D. (2003). Endogenous generation of reactive oxidants and electrophiles and their reactions with DNA and protein. *J Clin Invest, 111*(5), 583-593.

Mateo, J., Garcia-Lecea, M., Cadenas, S., Hernandez, C., & Moncada, S. (2003). Regulation of hypoxia-inducible factor-1alpha by nitric oxide through mitochondria-dependent and -independent pathways. *Biochem J, 376*(Pt 2), 537-544.

Mazzoni, A., Bronte, V., Visintin, A., Spitzer, J. H., Apolloni, E., serafini, P., et al. (2002). Myeloid suppressor lines inhibit T cell responses by an NO-dependant mechanism. *The Journal of Immunology, 168*, 689-695.

McMurray-Beaulieu, V., Hisiger, S., Durand, C., Perrier, M., & Jolicoeur, M. (2009). Na-butyrate sustains energetic states of metabolism and t-PA productivity of CHO cells. *J Biosci Bioeng, 108*(2), 160-167.

Melani, C., Chiodoni, C., Forni, G., & Colombo, M. P. (2003). Myeloid cell expansion elicited by the progression of spontaneous mammary carcinomas in c-erbB-2 transgenic BALB/c mice suppresses immune reactivity. *Blood, 102*(6), 2138-2145.

Melani, C., Sangaletti, S., Barazzetta, F. M., Werb, Z., & Colombo, M. P. (2007). Amino-biphosphonate-mediated MMP-9 inhibition breaks the tumor-bone marrow axis responsible for myeloid-derived suppressor cell expansion and macrophage infiltration in tumor stroma. *Cancer Res, 67*(23), 11438-11446.

Menetrier-Caux, C., Montmain, G., Dieu, M. C., Bain, C., Favrot, M. C., Caux, C., et al. (1998). Inhibition of the differentiation of dendritic cells from CD34(+) progenitors by tumor cells: role of interleukin-6 and macrophage colony-stimulating factor. *Blood, 92*(12), 4778-4791.

Messmer, U. K., Reed, U. K., & Brune, B. (1996). Bcl-2 protects macrophages from nitric oxide-induced apoptosis. *J Biol Chem, 271*(33), 20192-20197.

Mirza, N., Fishman, M., Fricke, I., Dunn, M., Neuger, A. M., Frost, T. J., et al. (2006). All-trans-retinoic acid improves differentiation of myeloid cells and immune response in cancer patients. *Cancer Res, 66*(18), 9299-9307.

Mocellin, S., Bronte, V., & Nitti, D. (2007). Nitric oxide, a double edged sword in cancer biology: searching for therapeutic opporuinities. *Medicinal Research reviews, 27*(3), 317-352.

Moncada, S., & Erusalimsky, J. D. (2002). Does nitric oxide modulate mitochondrial energy generation and apoptosis? *Nat Rev Mol Cell Biol, 3*(3), 214-220.

Mori, M. (2007). Regulation of nitric oxide synthesis and apoptosis by arginase and arginine recycling. *Journal of Nutrition, 137*(6), 1616S-1620S.

Morris, S. M. (2007). Arginine metabolism: Boundaries of our knowledge. *Journal of Nutrition, 137*(6), 1602S-1609S.

Morris, S. M., Jr. (2004). Enzymes of arginine metabolism. *J Nutr, 134*(10 Suppl), 2743S-2747S; discussion 2765S-2767S.

Munder, M., Eichmann, K., & Modolell, M. (1998). Alternative metabolic states in murine macrophages reflected by the nitric oxide synthase arginase balance: Competitive regulation by CD4(+) T cells correlates with Th1/Th2 phenotype. *Journal of Immunology, 160*(11), 5347-5354.

Munder, M., Eichmann, K., Moran, J. M., Centeno, F., Soler, G., & Modolell, M. (1999). Th1/Th2-regulated expression of arginase isoforms in murine macrophages and dendritic cells. *J Immunol, 163*(7), 3771-3777.

Munder, M., Schneider, H., Luckner, C., Giese, T., Langhans, C. D., Fuentes, J. M., et al. (2006). Suppression of T-cell functions by human granulocyte arginase. *Blood, 108*(5), 1627-1634.

Murphy, C., & Newsholme, P. (1998). Importance of glutamine metabolism in murine macrophages and human monocytes to L-arginine biosynthesis and rates of nitrite or urea production. *Clin Sci (Lond), 95*(4), 397-407.

Nath, N., Labaze, G., Rigas, B., & Kashfi, K. (2005). NO-donating aspirin inhibits the growth of leukemic Jurkat cells and modulates beta-catenin expression. *Biochem Biophys Res Commun, 326*(1), 93-99.

Nefedova, Y., Fishman, M., Sherman, S., Wang, X., Beg, A. A., & Gabrilovich, D. I. (2007). Mechanism of all-trans retinoic acid effect on tumor-associated myeloid-derived suppressor cells. *Cancer Res, 67*(22), 11021-11028.

Nefedova, Y., Nagaraj, S., Rosenbauer, A., Muro-Cacho, C., Sebti, S. M., & Gabrilovich, D. I. (2005). Regulation of dendritic cell differentiation and antitumor immune response in cancer by pharmacologic-selective inhibition of the janus-activated kinase 2/signal transducers and activators of transcription 3 pathway. *Cancer Res, 65*(20), 9525-9535.

Nelson, E. A., Walker, S. R., Kepich, A., Gashin, L. B., Hideshima, T., Ikeda, H., et al. (2008). Nifuroxazide inhibits survival of multiple myeloma cells by directly inhibiting STAT3. *Blood, 112*(13), 5095-5102.

Newsholme, P., Costa Rosa, L. F., Newsholme, E. A., & Curi, R. (1996). The importance of fuel metabolism to macrophage function. *Cell Biochem Funct, 14*(1), 1-10.

Nicolescu, A. C., Zavorin, S. I., Turro, N. J., Reynolds, J. N., & Thatcher, G. R. (2002). Inhibition of lipid peroxidation in synaptosomes and liposomes by nitrates and nitrites. *Chem Res Toxicol, 15*(7), 985-998.

Obermueller, E., Vosseler, S., Fusenig, N. E., & Mueller, M. M. (2004). Cooperative autocrine and paracrine functions of granulocyte colony-stimulating factor and granulocyte-macrophage colony-stimulating factor in the progression of skin carcinoma cells. *Cancer Res, 64*(21), 7801-7812.

Park, S. J., Nakagawa, T., Kitamura, H., Atsumi, T., Kamon, H., Sawa, S., et al. (2004). IL-6 regulates in vivo dendritic cell differentiation through STAT3 activation. *J Immunol, 173*(6), 3844-3854.

Paxinou, E., Weisse, M., Chen, Q., Souza, J. M., Hertkorn, C., Selak, M., et al. (2001). Dynamic regulation of metabolism and respiration by endogenously produced nitric oxide protects against oxidative stress. *Proc Natl Acad Sci U S A, 98*(20), 11575-11580.

Peng, T., Golub, T. R., & Sabatini, D. M. (2002). The immunosuppressant rapamycin mimics a starvation-like signal distinct from amino acid and glucose deprivation. *Mol Cell Biol, 22*(15), 5575-5584.

Peranzoni, E., Marigo, I., Dolcetti, L., Ugel, S., Sonda, N., Taschin, E., et al. (2007). Role of arginine metabolism in immunity and immunopathology. *Immunobiology, 212*(9-10), 795-812.

Peranzoni, E., Zilio, S., Marigo, I., Dolcetti, L., Zanovello, P., Mandruzzato, S., et al. (2010). Myeloid-derived suppressor cell heterogeneity and subset definition. *Curr Opin Immunol, 22*(2), 238-244.

Perez, G. M., Melo, M., Keegan, A. D., & Zamorano, J. (2002). Aspirin and salicylates inhibit the IL-4- and IL-13-induced activation of STAT6. *J Immunol, 168*(3), 1428-1434.

Pilz, R. B., & Casteel, D. E. (2003). Regulation of gene expression by cyclic GMP. *Circ Res, 93*(11), 1034-1046.

Popovic, P. J., Zeh, H. J., & Ochoa, J. B. (2007). Arginine and immunity. *Journal of Nutrition, 137*(6), 1681S-1686S.

Rabinovich, G. A., Gabrilovich, D., & Sotomayor, E. M. (2007). Immunosuppressive strategies that are mediated by tumor cells. *Annu Rev Immunol, 25*, 267-296.

Radi, R. (2004). Nitric oxide, oxidants, and protein tyrosine nitration. *Proc Natl Acad Sci U S A, 101*(12), 4003-4008.

Raghunand, N., Gatenby, R. A., & Gillies, R. J. (2003). Microenvironmental and cellular consequences of altered blood flow in tumours. *Br J Radiol, 76 Spec No 1*, S11-22.

Ramires, P. A., Mirenghi, L., Romano, A. R., Palumbo, F., & Nicolardi, G. (2000). Plasma-treated PET surfaces improve the biocompatibility of human endothelial cells. *J Biomed Mater Res, 51*(3), 535-539.

Rapoport, S. M. (1986). *The reticulocyte*: CRC Press.

Reich, J. G., & Sel'Kov, E. E. (1981). *Energy metabolism of the cell - a theoritical treatise*. London.

Restifo, N. P., Kawakami, Y., Marincola, F., Shamamian, P., Taggarse, A., Esquivel, F., et al. (1993). Molecular mechanisms used by tumors to escape immune recognition:

immunogenetherapy and the cell biology of major histocompatibility complex class I. *J Immunother Emphasis Tumor Immunol, 14*(3), 182-190.

Rodriguez, P. C., & Ochoa, A. C. (2006). T cell dysfunction in cancer: Role of myeloid cells and tumor cells regulating amino acid availability and oxidative stress. *Seminars in Cancer Biology, 16*(1), 66-72.

Rodriguez, P. C., & Ochoa, A. C. (2008). Arginine regulation by myeloid derived suppressor cells and tolerance in cancer: mechanisms and therapeutic perspectives. *Immunol Rev, 222*, 180-191.

Rodriguez, P. C., Quiceno, D. G., & Ochoa, A. C. (2007). L-arginine availability regulates T-lymphocyte cell-cycle progression. *Blood, 109*(4), 1568-1573.

Rodriguez, P. C., Zea, A. H., DeSalvo, J., Culotta, K. S., Zabaleta, J., Quiceno, D. G., et al. (2003). L-arginine consumption by macrophages modulates the expression of CD3 xi chain in T lymphocytes. *Journal of Immunology, 171*(3), 1232-1239.

Rosch, R., Junge, K., Schachtrupp, A., Klinge, U., Klosterhalfen, B., & Schumpelick, V. (2003). Mesh implants in hernia repair. Inflammatory cell response in a rat model. *Eur Surg Res, 35*(3), 161-166.

Rossner, S., Voigtlander, C., Wiethe, C., Hanig, J., Seifarth, C., & Lutz, M. B. (2005). Myeloid dendritic cell precursors generated from bone marrow suppress T cell responses via cell contact and nitric oxide production in vitro. *Eur J Immunol, 35*(12), 3533-3544.

Rotella, D. P. (2002). Phosphodiesterase 5 inhibitors: current status and potential applications. *Nat Rev Drug Discov, 1*(9), 674-682.

Roy, M. K., Takenaka, M., Kobori, M., Nakahara, K., Isobe, S., & Tsushida, T. (2006). Apoptosis, necrosis and cell proliferation-inhibition by cyclosporine A in U937 cells (a human monocytic cell line). *Pharmacol Res, 53*(3), 293-302.

Rutella, S., Zavala, F., Danese, S., Kared, H., & Leone, G. (2005). Granulocyte colony-stimulating factor: a novel mediator of T cell tolerance. *J Immunol, 175*(11), 7085-7091.

Ryll, T., & Wagner, R. (1991). Improved ion-pair high-performance liquid chromatographic method for the quantification of a wide variety of nucleotides and sugar-nucleotides in animal cells. *J Chromatogr, 570*(1), 77-88.

Ryll, T., & Wagner, R. (1992). Intracellular ribonucleotide pools as a tool for monitoring the physiological state of in vitro cultivated mammalian cells during production processes. *Biotechnol Bioeng, 40*(8), 934-946.

Saavedra, J. E., Shami, P. J., Wang, L. Y., Davies, K. M., Booth, M. N., Citro, M. L., et al. (2000). Esterase-sensitive nitric oxide donors of the diazeniumdiolate family: in vitro antileukemic activity. *J Med Chem, 43*(2), 261-269.

Salvadori, S., Martinelli, G., & Zier, K. (2000). Resection of solid tumors reverses T cell defects and restores protective immunity. *J Immunol, 164*(4), 2214-2220.

Samouilov, A., Woldman, Y. Y., Zweier, J. L., & Khramtsov, V. V. (2007). Magnetic resonance study of the transmembrane nitrite diffusion. *Nitric Oxide, 16*(3), 362-370.

Sancar, A., Lindsey-Boltz, L. A., Unsal-Kacmaz, K., & Linn, S. (2004). Molecular mechanisms of mammalian DNA repair and the DNA damage checkpoints. *Annu Rev Biochem, 73*, 39-85.

Sarti, P., Giuffre, A., Barone, M. C., Forte, E., Mastronicola, D., & Brunori, M. (2003). Nitric oxide and cytochrome oxidase: reaction mechanisms from the enzyme to the cell. *Free Radic Biol Med, 34*(5), 509-520.

Sato, T., Oku, H., Tsuruma, K., Katsumura, K., Shimazawa, M., Hara, H., et al. (2009). Hypoxia Makes RGC-5 Cells Susceptible to Nitric Oxide. *Invest Ophthalmol Vis Sci*.

Sebollela, A., Cagliari, T. C., Limaverde, G. S., Chapeaurouge, A., Sorgine, M. H., Coelho-Sampaio, T., et al. (2005). Heparin-binding sites in granulocyte-macrophage colony-stimulating factor. Localization and regulation by histidine ionization. *J Biol Chem, 280*(36), 31949-31956.

Segerstrom, S. C. (2007). Stress, Energy, and Immunity: An Ecological View. *Curr Dir Psychol Sci, 16*(6), 326-330.

Seliger, B., Harders, C., Lohmann, S., Momburg, F., Urlinger, S., Tampe, R., et al. (1998). Down-regulation of the MHC class I antigen-processing machinery after oncogenic transformation of murine fibroblasts. *Eur J Immunol, 28*(1), 122-133.

Serafini, Borrello, I., & Bronte, V. (2006). Myeloid suppressor cells in cancer: Recruitment, phenotype, properties, and mechanisms of immune suppression. *Semin Cancer Biol, 16*(1), 53-65.

Serafini, P., Carbley, R., Noonan, K. A., Tan, G., Bronte, V., & Borrello, I. (2004). High-dose granulocyte-macrophage colony-stimulating factor-producing vaccines impair the immune response through the recruitment of myeloid suppressor cells. *Cancer Research, 64*(17), 6337-6343.

Serafini, P., Meckel, K., Kelso, M., Noonan, K., Califano, J., Koch, W., et al. (2006). Phosphodiesterase-5 inhibition augments endogenous antitumor immunity by reducing myeloid-derived suppressor cell function. *Journal of Experimental Medicine, 203*(12), 2691-2702.

Serafini, P., Mgebroff, S., Noonan, K., & Borrello, I. (2008). Myeloid-derived suppressor cells promote cross-tolerance in B-cell lymphoma by expanding regulatory T cells. *Cancer Res, 68*(13), 5439-5449.

Shim, M. S., & Kwon, Y. J. (2010). Efficient and targeted delivery of siRNA in vivo. *Febs J, 277*(23), 4814-4827.

Sica, A., & Bronte, V. (2007). Altered macrophage differentiation and immune dysfunction in tumor development. *Journal of Clinical Investigation, 117*(5), 1155-1166.

Sinha, P., Clements, V. K., & Ostrand-Rosenberg, S. (2005). Reduction of myeloid-derived suppressor cells and induction of M1 macrophages facilitate the rejection of established metastatic disease. *Journal of Immunology, 174*(2), 636-645.

Song, H., Wang, R., Wang, S., & Lin, J. (2005). A low-molecular-weight compound discovered through virtual database screening inhibits Stat3 function in breast cancer cells. *Proc Natl Acad Sci U S A, 102*(13), 4700-4705.

Steer, H. J., Lake, R. A., Nowak, A. K., & Robinson, B. W. (2010). Harnessing the immune response to treat cancer. *Oncogene, 29*(48), 6301-6313.

Suzuki, E., Kapoor, V., Jassar, A. S., Kaiser, L. R., & Albelda, S. M. (2005). Gemcitabine selectively eliminates splenic Gr-1+/CD11b+ myeloid suppressor cells in tumor-bearing animals and enhances antitumor immune activity. *Clin Cancer Res, 11*(18), 6713-6721.

Takahashi, K., Murakami, M., Hosaka, K., Kikuchi, H., Oshima, Y., & Kubohara, Y. (2009). Regulation of IL-2 production in Jurkat cells by Dictyostelium-derived factors. *Life Sci, 85*(11-12), 438-443.

Talmadge, J. E., Hood, K. C., Zobel, L. C., Shafer, L. R., Coles, M., & Toth, B. (2007). Chemoprevention by cyclooxygenase-2 inhibition reduces immature myeloid suppressor cell expansion. *Int Immunopharmacol, 7*(2), 140-151.

Terabe, M., Matsui, S., Park, J. M., Mamura, M., Noben-Trauth, N., Donaldson, D. D., et al. (2003). Transforming growth factor-beta production and myeloid cells are an effector mechanism through which CD1d-restricted T cells block cytotoxic T lymphocyte-mediated tumor immunosurveillance: abrogation prevents tumor recurrence. *J Exp Med, 198*(11), 1741-1752.

Toque, H. A., Tostes, R. C., Yao, L., Xu, Z., Webb, R. C., Caldwell, R. B., et al. (2010). Arginase II Deletion Increases Corpora Cavernosa Relaxation in Diabetic Mice. *J Sex Med*.

Trikha, M., Corringham, R., Klein, B., & Rossi, J. F. (2003). Targeted anti-interleukin-6 monoclonal antibody therapy for cancer: a review of the rationale and clinical evidence. *Clin Cancer Res, 9*(13), 4653-4665.

Ugel, S., Delpozzo, F., Desantis, G., Papalini, F., Simonato, F., Sonda, N., et al. (2009). Therapeutic targeting of myeloid-derived suppressor cells. *Curr Opin Pharmacol, 9*(4), 470-481.

Velazquez, C., Praveen Rao, P. N., & Knaus, E. E. (2005). Novel nonsteroidal antiinflammatory drugs possessing a nitric oxide donor diazen-1-ium-1,2-diolate moiety: design, synthesis, biological evaluation, and nitric oxide release studies. *J Med Chem, 48*(12), 4061-4067.

Vellenga, E., Dokter, W., & Halie, R. M. (1993). Interleukin-4 and its receptor; modulating effects on immature and mature hematopoietic cells. *Leukemia, 7*(8), 1131-1141.

Wada, H. G., Indelicato, S. R., Meyer, L., Kitamura, T., Miyajima, A., Kirk, G., et al. (1993). GM-CSF triggers a rapid, glucose dependent extracellular acidification by TF-1 cells: evidence for sodium/proton antiporter and PKC mediated activation of acid production. *J Cell Physiol, 154*(1), 129-138.

Wegrzyn, J., Potla, R., Chwae, Y. J., Sepuri, N. B., Zhang, Q., Koeck, T., et al. (2009). Function of mitochondrial Stat3 in cellular respiration. *Science, 323*(5915), 793-797.

Yang, L., DeBusk, L. M., Fukuda, K., Fingleton, B., Green-Jarvis, B., Shyr, Y., et al. (2004). Expansion of myeloid immune suppressor Gr+CD11b+ cells in tumor-bearing host directly promotes tumor angiogenesis. *Cancer Cell, 6*(4), 409-421.

Yang, L., Huang, J., Ren, X., Gorska, A. E., Chytil, A., Aakre, M., et al. (2008). Abrogation of TGF beta signaling in mammary carcinomas recruits Gr-1+CD11b+ myeloid cells that promote metastasis. *Cancer Cell, 13*(1), 23-35.

Yu, H., Kortylewski, M., & Pardoll, D. (2007). Crosstalk between cancer and immune cells: role of STAT3 in the tumour microenvironment. *Nat Rev Immunol, 7*(1), 41-51.

Zou, H., Li, Y., Liu, X., & Wang, X. (1999). An APAF-1.cytochrome c multimeric complex is a functional apoptosome that activates procaspase-9. *J Biol Chem, 274*(17), 11549-11556.